To the Graduate Council:

I am submitting herewith a thesis written by Michael Gordon Browman entitled "Role of Silica Polymerization in the Treatment of Iron Bearing Groundwaters by the Addition of Sodium Silicate and Sodium Hypochlorite." I have examined the final copy of this thesis for form and content and recommend that it be accepted in partial fulfillment of the requirements for the degree of Master of Science, with a major in Environmental Engineering.

R. Bruce Robinson, Major Professor

We have read this thesis
and recommend its acceptance:

Accepted for the Council:

Vice Provost
and Dean of the Graduate School

STATEMENT OF PERMISSION TO USE

In presenting this thesis in partial fulfillment of the requirements for a Master's degree at The University of Tennessee, Knoxville, I agree that the Library shall make it available to borrowers under the rules of the Library. Brief quotations from this thesis are allowable without special permission, provided that accurate acknowledgement of the source is made.

Permission for extensive quotation from or reproduction of this thesis may be granted by my major professor, or in his absence, by the Head of the Interlibrary Services when, in the opinion of either, the proposed use of the material is for scholarly purposes. Any copying or use of the material in this thesis for financial gain shall not be allowed without my written permission.

Signature Michael G. Brosmer

Date August 3rd 1988

ROLE OF SILICA POLYMERIZATION IN THE TREATMENT OF IRON BEARING GROUNDWATERS BY THE ADDITION OF SODIUM SILICATE AND SODIUM HYPOCHLORITE

A Thesis

Presented for the

Master of Science

Degree

The University of Tennessee, Knoxville

Michael Gordon Browman

August 1986

DEDICATION

This thesis is dedicated to my parents Joseph S. Browman (deceased) and Lilian A. Browman who impressed upon me the value of a good education, and furthermore at much personal sacrifice made sure that the appropriate opportunities were available for me.

ACKNOWLEDGEMENTS

I wish to thank Professor Bruce Robinson for his guidance and support in the direction of my research and for his demonstrated confidence in my capabilities. My gratitude goes also to Professors Gregory Reed and Dennis Weeter for serving on my committee and for the critical examination of my thesis. Funding for the research as provided by the United States Environmental Protection Agency and the American Water Works Association Research Foundation, and for my graduate studies as provided for in part by a GPOP Fellowship is also much appreciated. Thanks also go to the PQ Corporation of Valley Forge, Pennsylvania for providing gratis the sodium silicate solutions used in this research.

ABSTRACT

Conventional treatment for problems associated with iron in groundwater supplies involves the physical removal of the iron from these waters. For this process, the unit operations of sedimentation and filtration are utilized. However, while this technique has been proven reliable, the associated capital, operating, and maintenance costs can be prohibitive for small low tax-based communities. Treatment by the addition of sodium silicate and sodium hypochlorite/chlorine to these iron bearing waters provides a recently exploited and relatively inexpensive alternative to conventional treatment. This technique does not remove the iron from the water but sequesters or stabilizes it such that it does not settle out in the distribution system and without the usual attendant "red water" problems. However, this method has been developed largely on an empirical basis. The objective of this investigation was to establish the chemical basis for success of the silicate hypochlorite treatment and to provide associated information that would allow optimization of treatment conditions.

In this investigation, a model groundwater at pH 7.0 containing 2 mg Fe^{2+}/L, 0 mg/L dissolved oxygen, and an alkalinity of 150 mg/L as $CaCO_3$ added as $NaHCO_3$, was dosed under anoxic conditions with a variety of sodium silicate solutions and sufficient 0.1% sodium hypochlorite (added separately) to oxidize all of the ferrous iron present. Where pH control was necessary, all sampling was done under a blanket of ultrapure nitrogen with the inclusion of sufficient carbon dioxide

admixed to provide a pH of 7.0. The major criterion for treatment success was % iron filterability, i.e., the fraction of total iron passing a 0.1 μm membrane filter. Total iron, pH, and turbidity were also measured routinely on a set schedule of 0,1,3,5,7, and 10 days post treatment. In one experiment, filterability was based also on ultrafiltration, and samples were taken also for particulate characterization and identification by transmission electron microscope (TEM). A variety of sodium silicate types (m-ratios 3.75, 3.22, 2.5, and 1.8) and dilutions (undiluted, 1/10,1/50,1/100, and 1/500 aged 24 hours) were used for dosing (8 to 15 mg SiO_2/L). Some of these silicate solutions were characterized by reactivity coefficients, K_1 and P_0, based on the rate of reaction of the solutions with molybdic acid as determined from changes in optical density measured at 400 nm. Theoretically, K_1 and P_0 are inversely and directly related, respectively, to the level of silica polymerization in the silicate solutions.

In the preliminary phases of the investigation, the optimal sequence of chemical application was found to be silicate applied 15 to 150 seconds ahead of the hypochlorite oxidant. Also, pH control was an important experimental condition. Thus, a given silicate dosage was less effective at the lower controlled pH(7.0) than at the higher pH levels (8 to 8.3) attained in the system for which the pH was uncontrolled.

Analysis of the data generated from treatments based on varying m-ratios and dilutions of the dosed silicate solutions showed that for typical treatment conditions (1) higher m-ratio silicates provided

more effective iron stablization and (2) higher silica concentrations in the feed solution produced better levels of iron stabilization. Thus, the t_{50}'s, times elapsed to 50% filterability, for undiluted silicates of m-ratios 3.75, 3.22, 2.5, and 1.8 were 9.8,6.7,5.8, and 2.4 days, respectively, and the the t_{50}'s for undiluted, 1/10,1/50,1/100, and 1/500, 3.75 ratio silicate were 9.8,8.7,6.2,5.5, and 2.1 days, respectively, for doses of 13-15 mg SiO_2/L.

The unifying interpretation of these results was that feed silicate solutions with higher levels of silica polymerization were more effective at stabilizing aqueous ferric iron. This conclusion was verified in large part by statistical analyses applied to models representing either treatment effectiveness (t_{50}) or % iron filterability as the dependent variable in terms of the measured parameters, including the reaction coefficients P_0 and to a lesser extent K_1. The critical importance of time elapsed since treatment, and silicate dose was also substantiated. Detailed analysis by ultrafiltration for various treatments supported the premise that the role of the silicate in effecting iron stabilization was to disperse the "iron" particles limiting their coalescence, growth, and subsequent sedimentation. Examination of treatment particulates did not provide any consistent trends with regard to the development of crystallinity with time or silicate dilution. Where some mineral identification was possible, the best characterizations were as an unnamed iron oxide hydroxide.

The treatment mechanism was readily explained in terms of classical colloidal double layer theory. It was assumed that the treatment

silicate combined with the iron particulates to produce a pH_{pzc} lower than for the iron particulate alone, favoring the production of a net negative surface charge at treatment pH and, as a consequence, particle dispersion. This last process disfavors coagulation and sedimentation.

TABLE OF CONTENTS

SECTION		PAGE
I.	INTRODUCTION	1
II.	LITERATURE REVIEW	4
	Aqueous Iron Chemistry	4
	Ferrous Iron Oxidation	4
	Iron Precipitates	11
	Iron Precipitate Solubility	14
	Aqueous Silicate Chemistry	18
	Silicate Solubility	19
	Concentrated Sodium Silicate Solutions	22
	Effects of Dilution	24
	Characterization of Silicate Solutions	27
	Interaction of Silica with Iron and Other Metal Ion Systems	30
	True Solutions of Silicate	31
	Colloidal Interactions	37
	Iron Treatment by Sodium Silicate and Chlorine	42
III.	METHODS AND MATERIALS	54
	Kinetic Characterization of Silicate Solutions	54
	Silicate Dilutions	56
	Iron Filterability (<0.1μm)	58
	Iron Filterability (Ultrafiltration)	60
	Transmission Electron Microscopy	61
	Routine Chemical Analyses	62
	Statistical Analysis	63
IV.	RESULTS AND DISCUSSION	65
	Silicate Characterization	65
	Iron Filterability	79
	Lag-time effects	82
	pH Control/No Control Effects with Silicate Dilutions	89
	Silica Dose Optimization	104
	Effect of Silicate Dilution on Treatment Performance	111
	Statistical Analysis	136
	Ultrafiltration	146
	Characterization of Iron Particulates	156

TABLE OF CONTENTS (continued)

SECTION	PAGE
V. GENERAL DISCUSSION	162
VI. CONCLUSIONS	172
VII. RECOMMENDATIONS FOR FURTHER WORK	175
BIBLIOGRAPHY	176
APPENDIX	182
VITA	193

LIST OF TABLES

TABLE		PAGE
1.	Chemical Composition and Critical Treatment Parameters for Successfully Field-Treated Water Systems (Dart and Foley (5))	46
2.	Properties of Liquid Silicates Used in Investigations (26).	57
3.	Reaction Coefficients Derived from the Reaction of Undiluted Sodium Silicates with Molybdic Acid with Time at 400 nm and 25-26°C	71
4.	Reaction Coefficients for Dilutions of 3.22 Ratio Sodium Silicate at ~21°C, and ~14 mg SiO_2/L	75
5.	Fraction of Total Iron Present as Ferrous Iron at the Start of Individual Treatments within Various Experiments	80
6.	Data on Lag-Time Effects for 3.22 Ratio Sodium Silicate at 9-10 mg SiO_2/L with No pH Control	87
7.	Data on Dilution Effects for 3.22 Ratio Sodium Silicate at ~10.5 mg SiO_2/L with No pH Control	95
8.	Data on Dilution Effects for 3.22 Ratio Sodium Silicate at ~9 mg SiO_2/L, pH Controlled and Uncontrolled	97
9.	Data on Silica Dose Effects for Undiluted and 1/100 Dilution of 3.22 Ratio Sodium Silicate with pH Controlled	110
10.	Data on Dilution Effects for 3.22 and 3.75 Ratio Sodium Silicates at ~13 mg SiO_2/L with pH Controlled	116
11.	Data on Dilution Effects for 2.5 and 3.75 Ratio Sodium Silicates at 13-14 mg SiO_2/L with pH Controlled	122
12.	Data on Dilution Effects for 1.8 and 2.5 Ratio Sodium Silicates at 13-15 mg SiO_2/L with pH Controlled	132

13. Comparative Effectiveness of Various Dilutions of Selected Sodium Silicates at Maintaining Iron Filterability 134

14. Statistical Models Applied to Dilutions of 3.22 Ratio Sodium Silicate with t_{50}, the Time to 50% Filterability, as Dependent Variable 138

15. Probability Significance of Individual Independent Variables in Models Applied to Dilutions of 3.22 Ratio Sodium Silicate with t_{50}, the Time Elapsed to 50% Filterability, as Dependent Variable 139

16. Statistical Models Applied to Undiluted 3.75, 3.22, 2.5, and 1.8 Ratio Sodium Silicates with % Iron Filterability as Dependent Variable 141

17. Probability Significance of Individual Independent Variables in Models Applied to Undiluted 3.75, 3.22, 2.5, and 1.8 Ratio Sodium Silicates with % Iron Filterability as Dependent Variable 142

18. Statistical Models Applied to Dilutions of 3.22 Ratio Sodium Silicate with % Iron Filterability as Dependent Variable 144

19. Probability Significance of Individual Independent Variables in Models Applied to Dilutions of 3.22 Ratio Sodium Silicate with % Iron Filterability as Dependent Variable 145

20. Data on Dilution Effects for 3.22 and 3.75 Ratio Sodium Silicates at 12-14 mg SiO_2/L with pH Controlled and Detail on Filterability by Ultrafiltration 154

21. Selected Area Diffraction Data for Particulate from the 1/100 Dilution of the 3.22 Ratio Sodium Silicate--Day 10 (Sample A-10) 160

A1. Raw and Converted Optical Density Data for the Reaction of Undiluted 3.75 Ratio Sodium Silicate with Molybdic Acid with Time at 400 nm and 25-26°C 183

A2. Raw and Converted Optical Density Data for the Reaction of Undiluted 3.22 Ratio Sodium Silicate with Molybdic Acid with Time at 400 nm and 25-26°C 184

A3. Raw and Converted Optical Density Data for the Reaction of Undiluted 2.5 Ratio Sodium Silicate with Molybdic Acid with Time at 400 nm and 25-26°C 185

A4. Raw and Converted Optical Density Data for the Reaction of Undiluted 1.8 Ratio Sodium Silicate with Molybdic Acid with Time at 400 nm and 25-26°C 186

A5. Raw and Converted Optical Density Data for the Reaction of Undiluted 2.50 Ratio Sodium Silicate with Molybdic Acid with Time at 400 nm and 20-21°C 187

A6. Raw and Converted Optical Density Data for the Reaction of Undiluted 3.22 Ratio Sodium Silicate with Molybdic Acid with Time at 400 nm and 20-21°C 188

A7. Raw and Converted Optical Density Data for the Reaction of 1/10 Dilution of 3.22 Ratio Sodium Silicate with Molybdic Acid with Time at 400 nm and 20-21°C 189

A8. Raw and Converted Optical Density Data for the Reaction of 1/50 Dilution of 3.22 Ratio Sodium Silicate with Molybdic Acid with Time at 400 nm and 20-21°C 190

A9. Raw and Converted Optical Density Data for the Reaction of 1/100 Dilution of 3.22 Ratio Sodium Silicate with Molybdic Acid with Time at 400 nm and 20-21°C 191

A10. Raw and Converted Optical Density Data for the Reaction of 1/500 Dilution of 3.22 Ratio Sodium Silicate with Molybdic Acid with Time at 400 nm and 20-21°C 192

LIST OF FIGURES

FIGURE		PAGE
1.	Solubility Diagram for Amorphous Ferrihydrite, (am.)$Fe(OH)_3$(S) (10)	17
2.	Solubility Diagram for Silica, SiO_2 (10)	21
3.	Optical Density vs. Time for the Reaction of Molybdic Acid with Undiluted 1.8, 2.5, 3.22, and 3.75 Ratio Sodium Silicates at 25-26°C	67
4.	Percent Unreacted Silica vs. Time for the Reaction of Molybdic Acid with Undiluted 1.8, 2.5, 3.22, and 3.75 Ratio Sodium Silicates at 25-26°C and 2.5 Ratio at 21°C	69
5.	Percent Unreacted Silica vs. Time for the Reaction of Molybdic Acid with Undiluted, and 1/10, 1/50, 1/100, and 1/500 Dilutions of 3.22 Ratio Sodium Silicate at 20-21°C	74
6.	Silicate Reactivity Coefficients Derived from the Reaction of Molybdic Acid with Dilutions of 3.22 Ratio Sodium Silicate at 21°C	77
7.	Lag-Time Effects for Undiluted 3.22 Ratio Sodium Silicate: Iron Filterability	83
8.	Lag-Time Effects for Undiluted 3.22 Ratio Sodium Silicate: Turbidity	84
9.	Lag-Time Effects for Undiluted 3.22 Ratio Sodium Silicate: pH	85
10.	Lag-Time Effects for Undiluted 3.22 Ratio Sodium Silicate: Total Iron	86
11.	Dilution Effects for 3.22 Ratio Sodium Silicate at ~10.5 mg SiO_2/L--No pH Control: Iron Filterability	91
12.	Dilution Effects for 3.22 Ratio Sodium Silicate at ~10.5 mg SiO_2/L--No pH Control: pH	92
13.	Dilution Effects for 3.22 Ratio Sodium Silicate at ~10.5 mg SiO_2/L--No pH Control: Turbidity	93

14. Dilution Effects for 3.22 Ratio Sodium Silicate at ~10.5 mg SiO_2/L--No pH Control: Total Iron 94

15. Dilution Effects for 3.22 Ratio Sodium Silicate at ~9 mg SiO_2/L--pH Controlled vs. Uncontrolled: Iron Filterability, 0 to 10 days 98

16. Dilution Effects for 3.22 Ratio Sodium Silicate at ~9 mg SiO_2/L--pH Controlled vs. Uncontrolled: Iron Filterability, 0 to 164 days 99

17. Dilution Effects for 3.22 Ratio Sodium Silicate at ~9 mg SiO_2/L--pH Controlled vs. Uncontrolled: pH 100

18. Dilution Effects for 3.22 Ratio Sodium Silicate at ~9 mg SiO_2/L--pH Controlled vs. Uncontrolled: Turbidity 101

19. Dilution Effects for 3.22 Ratio Sodium Silicate at ~9 mg SiO_2/L--pH Controlled vs. Uncontrolled: Total Iron 102

20. Silica Dose Effects for Undiluted 3.22 Ratio Sodium Silicate--pH Controlled: Iron Filterability 105

21. Silica Dose Effects for 1/100 Dilutions of 3.22 Ratio Sodium Silicate--pH Controlled: Iron Filterability 106

22. Silica Dose Effects for Undiluted and 1/100 Dilutions of 3.22 Ratio Sodium Silicate--pH Controlled: Turbidity 107

23. Silica Dose Effects for Undiluted and 1/100 Dilutions of 3.22 Ratio Sodium Silicate--pH Controlled: pH 108

24. Silica Dose Effects for Undiluted and 1/100 Dilutions of 3.22 Ratio Sodium Silicate--pH Controlled: Total iron 109

25. Dilution Effects for 3.22 Ratio Sodium Silicate at ~13 mg SiO_2/L--pH Controlled: Iron Filterability 112

26. Dilution Effects for 3.22 Ratio Sodium Silicate at ~13 mg SiO_2/L--pH Controlled: Turbidity 113

27. Dilution Effects for 3.22 Ratio Sodium Silicate at ~13 mg SiO_2/L--pH Controlled: pH 114

28. Dilution Effects for 3.22 Ratio Sodium Silicate at ~13 mg SiO_2/L--pH Controlled: Total Iron 115

29. Dilution Effects for 3.75 Ratio Sodium Silicate at ~13 mg SiO_2/L--pH Controlled: Iron Filterability 118

30. Dilution Effects for 3.75 Ratio Sodium Silicate at ~13 mg SiO_2/L--pH Controlled: Turbidity 119

31. Dilution Effects for 3.75 Ratio Sodium Silicate at ~13 mg SiO_2/L--pH Controlled: pH 120

32. Dilution Effects for 3.75 Ratio Sodium Silicate at ~13 mg SiO_2/L--pH Controlled: Total Iron 121

33. Dilution Effects for 2.5 Ratio Sodium Silicate at 13-14 mg SiO_2/L--pH Controlled: Iron Filterability 124

34. Dilution Effects for 2.5 Ratio Sodium Silicate at 13-14 mg SiO_2/L--pH Controlled: Turbidity 125

35. Dilution Effects for 2.5 Ratio Sodium Silicate at 13-14 mg SiO_2/L--pH Controlled: pH 126

36. Dilution Effects for 2.5 Ratio Sodium Silicate at 13-14 mg SiO_2/L--pH Controlled: Total Iron 127

37. Dilution Effects for 1.8 Ratio Sodium Silicate at 13-15 mg SiO_2/L--pH Controlled: Iron Filterability 128

38. Dilution Effects for 1.8 Ratio Sodium Silicate at 13-15 mg SiO_2/L--pH Controlled: Turbidity 129

39. Dilution Effects for 1.8 Ratio Sodium Silicate at 13-15 mg SiO_2/L--pH Controlled: Total Iron 130

40. Dilution Effects for 1.8 Ratio Sodium Silicate at 13-15 mg SiO_2/L--pH Controlled: pH 131

41. Iron Filterability for an Undiluted 3.75 Ratio Sodium Silicate System at 12.5 mg SiO_2/L under Controlled pH Using Standard Filtration and Ultrafiltration 147

42. Iron Filterability for a 1/100 Dilution of 3.75 Ratio Sodium Silicate System at 14.1 mg SiO_2/L under Controlled pH Using Standard Filtration and Ultrafiltration 148

43. Iron Filterability for an Undiluted 3.22 Ratio Sodium Silicate System at 13.9 mg SiO_2/L under Controlled pH Using Standard Filtration and Ultrafiltration 149

44. Iron Filterability for a 1/100 Dilution of 3.22 Ratio Sodium Silicate System at 13.8 mg SiO_2/L Under Controlled pH Using Standard Filtration and Ultrafiltration 150

45. Dilution Effects for 3.22 and 3.75 Ratio Sodium Silicates at 12-14 mg SiO_2/L--pH Controlled: Turbidity 151

46. Dilution Effects for 3.22 and 3.75 Ratio Sodium Silicates at 12-14 mg SiO_2/L--pH Controlled: pH 152

47. Dilution Effects for 3.22 and 3.75 Ratio Sodium Silicates at 12-14 mg SiO_2/L--pH Controlled: Total Iron 153

48. Iron Particulate--Plate 158

49. Selected Area Diffraction Pattern--Sample A10 159

I. INTRODUCTION

In the USA, groundwater is the common source of water for smaller communities. However, despite quality usually superior the surface waters, nevertheless groundwaters do commonly contain dissolved inorganic material some of which must be removed prior to industrial or municipal use of the water (1). Accordingly, well waters are often treated to remove the major hardness cations, calcium and magnesium, as well as iron and manganese (1).

Iron in groundwaters occurs primarily in the reduced divalent ferrous state. This in itself presents no toxicity or aesthetic problems within the range of typically observed concentrations. However, deliberate or incidental aeration of these same waters oxidizes the ferrous iron to the trivalent ferric state which, at normal groundwater pH levels, reacts readily with water to form very insoluble precipitates *in situ*. These red iron precipitates can present a problem in terms of both color and turbidity, although there is no associated toxicity. This "red water" presents primarily an aesthetic problem by being unappealing, and also by the staining of laundry and plumbing fixtures. In these instances, water treatment for iron removal has customarily been recommended.

The Maximum Contaminant Level for iron in U.S. drinking waters is 0.3 mg Fe/L (2), a concentration commonly exceeded in groundwaters. Thus, in the midwestern states of Iowa, Indiana, Illinois, and Michigan this iron concentration is exceeded in greater than 50% of the public groundwater supply systems (3). Moreover, in Tennessee, average iron

concentrations in excess of 0.3 mg Fe/L are common to all but one of the major aquifer types Zurawski (4).

Conventional water treatment for the removal of iron is usually an oxidation-flocculation/clarification-filtration or an oxidation-detention-filtration sequence depending on whether or not, respectively, water softening is to be accomplished also (1). Oxidation is effected typically by aeration, although the strong oxidants chlorine or permanganate are valid alternatives. The success of this conventional treatment has been well established. However, the construction and the operation and maintenance costs for such a system may be prohibitive for small low-tax-based communities.

Less expensive alternative treatment systems do exist. Notably, the Ontario (Canada) Ministry of the Environment has successfully reduced iron related problems for groundwaters by the application of commercial sodium silicate solutions and hypochlorite or chlorine gas to the groundwater at the well head (5,6). By this treatment iron is not removed from the water but is stabilized and prevented from percipitating while the water is in the distribution system. However, despite the general success of the treatment process, variability in various aspects of the process indicate uncertainty regarding the treatment mechanism and the need for further investigation.

The broad objective of the investigation reported herein is to provide a better understanding of the chemical mechanisms controlling the effectiveness of the treatment in the stabilization of the iron (sequestration) in water thus maintaining high level iron filterability. More specific objectives include 1. to establish the role of

pH in iron sequestration by silicate solutions; 2. to establish the role of silica polymerization in iron sequestration by silicate solutions; 3. characterization of particulates generated in iron filterability experiments in terms of size distribution as well as identification of mineral phases; 4. generation of a model equation relating iron filterability to readily measured experimental parameters such as time, silicate concentration, etc. 5. to determine the optimal silica dosage formula for iron sequestration in terms of pH and forms and amounts of silicate.

II. LITERATURE REVIEW

As a background for the presentation of the experimental procedures and results of this investigation, relevant iron and silica chemistry is discussed. Initially, the topics of iron and silica are treated separately, and then as these materials interact with each other. Finally, a detailed examination of the silicate-hypochlorite treatment for iron stabilization is presented.

Aqueous Iron Chemistry

The literature on iron chemistry is extensive. However, only those aspects of direct relevance to the understanding of the treatment procedure in question have been presented here.

Ferrous Iron Oxidation

Iron in groundwater is usually in the ferrous (Fe^{2+}) form. Upon oxidation to the ferric form the iron is subject to hydrolysis to hydrous ferric oxide at normal groundwater pH levels of 6 to 8. The rate of Fe^{2+} oxidation is affected by several factors as is the nature of the precipitate formed. The iron precipitate, which is very insoluble, may be formed and flocculated rapidly and then removed from the system, as in conventional water treatment. Alternatively, the precipitation/agglomeration rate may be inhibited by chemicals such as silicates and the iron allowed to remain in the delivered water, the subject of the current investigation.

The kinetics of oxidation of ferrous iron by molecular oxygen have been well established (7, 8, 9). The appropriate kinetic equation for pH > 5.5 is as follows (7):

$$\frac{-d[Fe^{2+}]}{dt} = K[Fe^{2+}]\,[OH^-]^2 P_{O_2} \qquad 1$$

where

$K = 8.0\ (\pm\ 2.5) \times 10^{13}\ min^{-1}\ atm^{-1}\ mol^{-2}$ at 20°C

$[Fe^{2+}]$ = ferrous iron concentration, M

t = time, minutes

$[OH^-]$ = hydroxyl ion concentration, M

P_{O_2} = partial pressure of oxygen, atm.

Significantly, the oxidation rate is dependent upon hydroxyl concentration squared, making the reaction rate particularly sensitive to pH, being substantially more rapid at alkaline pH levels than at acid or neutral ones. At pH < 3 the oxidation rate is independent of pH (8). Catalysts, especially Cu^{2+} and Co^{2+}, in trace quantities, as well as anions that form complexes with Fe(III), e.g., HPO_4^{2-}, increase the reaction rate markedly (10). Conversely, complexation of Fe^{2+} might be expected to inhibit the oxidation of Fe^{2+}. Nevertheless, perhaps because of Fe^{3+} complexes tend to be stronger than Fe^{2+} complexes, the net result is catalysis of Fe^{2+} oxidation by complexes.

For a fixed level of OH^- concentration and of P_{O_2}, conversion of equation (1) to the integral form followed by rearrangement yields:

$$t = \ln([Fe^{2+}]_o / [Fe^{2+}]_t) / (K[OH^-]^2 P_{O_2}) \qquad 2$$

where

t = time, min

$[Fe^{2+}]_o$ = initial concentration of Fe^{2+}, M

$[Fe^{2+}]_t$ = Fe^{2+} concentration at time t, M

At P_{O_2} = 0.21 atm, i.e. normal atmospheric oxygen levels, and pH = 8, $t_{0.9}$ -- time for 90% conversion, is 8 seconds. Changing the pH to 5.5 without altering the other conditions procedures $t_{0.9} \approx$ 10 hours.

At higher iron concentrations, 5-10 mg/L, in the presence of autocatalytic action by the colloidal precipitate formed, it was found that expanding equation 1 to account for this effect describes the process rate adequately, thus (11):

$$\frac{-d[Fe^{2+}]}{dt} = (K_o[OH^-] + K_{s,o} \frac{K[Fe_{ppt}]}{K_W}) [O_2][OH^-] [Fe^{2+}] \qquad 3$$

where

$K_o = 2.3 \times 10^{14}$ liter^3 mole^{-3} sec^{-1} at 25°C

$K_{s,o}$ = 73 liter mole^{-1} sec^{-1} at 25°C

$K = 2.5 \times 10^{10}$ liter mole^{-1} / mg of precipitate as Fe at 25°C

K_W = equilibrium product for water

$[O_2]$ = oxygen concentration, M

$[Fe_{ppt}]$ = concentration of iron precipitate in mg/L as Fe at time, t

Equation 3 was most applicable within the pH range 6-7 and inaccurate at pH > 9.

Schenk and Weber (12) observed that, within the tested concentration range, 0.1 to 1mM, silicic acid enhanced the oxidation of ferrous iron (< 5×10^{-5}M) by molecular oxygen. This augmented oxidation rate occurred in addition to the well-documented hydroxyl effect (7) and is presented in the following quation:

$$\frac{-d[Fe^{2+}]}{dt} = (KP_{O_2}[OH^-]^2 + K_{Si}\,[H_4SiO_4]^{0.5}[OH^-]^{0.5})[Fe^{2+}] \quad 4$$

where

K = 2.1 (± 0.5) x 10^{13} liter^2 mole^{-2} atm^{-1} min,

K_{Si} = 1.8 (± 0.3) x 10^3 liter mole^{-1}

$[OH^-]$ = hydroxyl concentration, M

$[H_4SiO_4]$ = silicic acid concentration, M

P_{O_2} = partial pressure of oxygen, atm

$[Fe^{2+}]$ = concentration of ferrous iron, M

It was suggested that the rate constant K_{Si} may have been a function of the P_{O_2} of the system. However, no mechanistic explanation regarding the role of silicic acid in the oxidation process was offered. The complexing ability of H_4SiO_4 for Fe(III) may well be involved also.

The rate of oxidation of ferrous iron by molecular oxygen in acid solution is very dependent upon the nature of the anions present. The rate increases as the complexing affinity for ferric iron increases. Thus, at a given pH, the rate decreases in the series pyrophosphate, phosphate, chloride, sulfate and perchlorate (13). Cher and Davidson 1955 (14) examined the oxidation of ferrous iron in phosphoric acid solutions within the pH range 1.1 to 1.7 and derived the following relationship:

$$\frac{d[Fe^{2+}]}{dt} = K_p[Fe^{2+}]P_{O_2}\,[H_2PO_4^-]^2 \qquad 5$$

where

$K_p = 4.5\ (\pm\ 0.3)\ atm^{-1}\ mole^{-2}\ hr^{-1}$ at 30°C

$[H_2PO_4^-]$ = concentration of dihydrogen phosphate, M

$[Fe^{2+}]$ and P_{O_2} are as given earlier

The pK_1 and pK_2 values for H_3PO_4, i.e., 2.2 and 7.2, respectively (10), dictate that $H_2PO_4^-$ ions provide a substantial proportion of phosphate species in the pH range of 1.2 to 8.2. However, calculations show that completion from the "hydroxyl" mechanism for ferrous iron

oxidation (7) would make the "dihydrogen phosphate" mechanism (14) virtually irrelevant at pH levels of neutral or above.

Huffman and Davidson (13) investigated the oxidation of ferrous iron by molecular oxygen in 1F H_2SO_4. It was found that the reaction proceeded by bimolecular and termolecular mechanisms at elevated temperatures (140-180°C) and by a termolecular mechanism at 30.5°C. The rate equation for the low temperature reaction was:

$$\frac{-d[Fe^{2+}]}{dt} = K_t[Fe^{2+}]^2 P_{O_2} \qquad 6$$

where

$K_t = 2.78 \times 10^{-6}$ M^{-1} sec^{-1},

$[Fe^{2+}]$, P_{O_2}, and t are as given earlier in the text.

The rate constant K_t was also given by:

$$K_t = \frac{K_u + K_s K[SO_4{}^{2-}]}{1 + K[SO_4{}^{2-}]^2} \qquad 7$$

where

K_u = rate constant for an uncatalyzed subreaction

K_s = rate constant for a sulfate catalyzed subreaction

K = formation constant $FeSO_4$ complex

$[SO_4{}^{2-}]$ = sulfate concentration, M

As for the phosphate dependent system, the sulfate system would be dominated by the hydroxyl system at pH levels of neutral or above.

Ferrous iron is also readily oxidized by aqueous chlorine. Crabtree and Schaefer (15) examined the production of Fe^{3+} from the Fe^{2+} at pH 1 following the addition of standardized aqueous chlorine. Levels of ferric ion were monitored via the measurement of absorbance at 335 nm. Experimental conditions included a temperature of 30°C and an ionic strength, $\mu = 1.0$. The rate equation for the oxidation of ferrous iron by chlorine is:

$$\frac{-d[Fe^{2+}]}{dt} = 2K[Fe^{2+}][\Sigma Cl_2] \qquad 8$$

where

$[\Sigma\ Cl_2] = [Cl_2] + [Cl_3^-]$

= total active chlorine species in solution

$K = 3.2 \times 10^{10}\ [(-11{,}200 \pm 100) / RT]\ \underline{M}$

$T = 278 - 303°K$

$[Cl^-] = 1\ \underline{M}$

R = universal gas constant

= 1.987 cal / °K. $\underline{M}$

= 0.0825 L atm / ° K $\underline{M}$

The reaction was considered to be independent of pH within the range tested, i.e., pH 1-2. Because the active agent in aqueous free chlorine systems is hypochlorous acid (1), HOCl, which has a $pK_a = 7.6$, it is anticipated that at neutral pH levels equation 8 would not be applicable unmodified, or at least not without a different rate constant value.

Iron Precipitates

Ferric iron, the oxidation product of ferrous iron, is readily hydrolyzed in aqueous systems at pH levels of neutral and above (10). The actual composition of the resultant precipitate would be a function of the composition of the solution in which the reactions occurs, in as much as this would control coprecipitation. Other conditions of precipitation, such as equilibration time and temperature, would also influence the nature of the isomorphs formed.

Information on iron compounds is voluminous. However, as previously stated, this discussion will not be comprehensive, but will be confined to those compounds of direct relevance to likely precipitates formed in water treatment plant (WTP) systems.

The iron precipitate in WTP's has been variously considered to be $Fe(OH)_3$ (ferric hydroxide), $FeCO_3$ (ferrous carbonate or siderite), and $FeCO_3$-$Fe(OH)_2$, depending on the level of oxidation in the system. While the last pair of compounds has been suggested, their actual occurrence in water treatment systems has not been verified ambiguously (16). Furthermore, in typical water treatment the level of oxidation,

whether produced by molecular oxygen (aeration) or by strong oxidants, along with the rapid mix conditions, would be sufficient to readily oxidize all ferrous forms to ferric precipitates.

The oxidation-hydrolysis product of ferrous iron is commonly referred to variously as ferric hydroxide or hydrous ferric oxide, "$Fe(OH)_3$". The compound ferric hydroxide does not exist as such. The material characterized as ferric hydroxide is likely a mixture of ferric oxide and hydrous ferric oxide gels (ferrihydrite). Stumm and Morgan (10) suggest that oxide hydroxides of Fe(III) precipitated in natural waters are often mixtures of amorphous material and goethite (α-FeOOH). However, the thermodynamic stability of these precipitates may be characterized by their solubility products given by ($[Fe^{3+}][OH^-]^3 = K_{so}$), implying some behavioral similarity to $Fe(OH)_3$.

The range of possible ferric iron oxides, oxyhdroxides, and hydroxides, as described in several sources, has been summarized by Robinson (16) as given below:

Fe_3O_4 (magnetite)

α-Fe_2O_3 (hematite)

Y-Fe_2O_3 (maghemite)

α-FeOOH (goethite)

β-FeOOH (akagenite)

Y-FeOOH (lepidocrocite)

δ-FeOOH

Ferrihydrite (amorphous ferric oxides and hydrous ferric oxide gels)

These iron compounds represent the range of compounds occurring in a variety of environments, and it is likely that only a few of these are possible in WTP systems because of the narrow range of precipitation conditions therein.

Schwertman and Taylor (17) examined the effects of pH, temperature, initial Fe(III) : Fe(II) ratio, total iron concentration, and rate of air flow and of oxygen transfer on the iron compound formed. They observed the following:

1. A rapid oxidation rate favored the formation of Y-FeOOH, while a slow rate favored Y-Fe_2O_3.
2. High initial Fe(III) : Fe(II) ratios favored formation of ferrihdrite, whereas ~ 10% Fe(III) yielded Y-Fe_2O_3, and 100% Fe(II) pure Y-FeOOH.
3. Higher temperatures favored Y-Fe_2O_3.
4. pH levels of 6-7 favored formation of Y-Fe_2O_3.

Applying these findings to water treatment systems suggests the predominance of Y-FeOOH, based on likely rapid oxidation rates and very low Fe^{3+} concentrations in groundwater. However, the natural pH levels around 6-7 suggest the formation of Y-Fe_2O_3.

Given enough time (100-500 hrs) Y-FeOOH will transform to α-FeOOH (goethite), but the process is retarded in the presence of silica. Again, the small detention time of water in WTP's and the customary presence of silica in groundwater favor Y-FeOOH over a-FeOOH. However, the presence of silica has a variable effect on the preferential formation of Y-FeOOH. Robinson (16) and Robinson et al. (18) identified the iron precipitates resulting from the aeration of a model groundwater (neutral pH, alkalinity = 400-500 mg/L as HCO_3^-, Fe^{2+} = 10 mg/L)

at 20-25°C with the inclusion of varying amounts of silica added as sodium metasilicate. Examination of the resultant precipitates by X-ray diffraction revealed that at silica concentration of $\leq$ 7 mg/L the product was crystalline lepidocrocite (Y-FeOOH) and at higher silica concentrations it was amorphous. Schwertman and Thalman (19) also examined the iron precipitate produced by the aeration of ferrous iron using higher concentrations of iron ($\geq$ 700 mg Fe/L) and observed that as the silica/iron ratio was increased less Y-FeOOH was formed. However, the resultant product rather than becoming gradually more amorphous, as found by Robinson et al. (18), instead included ferrihydrite in progressively larger amounts.

The discussion suggests that the aeration product in WTP's is likely to be Y-FeOOH or amorphous ferrihydrite. For either of these forms the mechanism by which silicates would stabilize ferric iron, the subject of this investigation, will likely remain the same.

Iron Precipitate Solubility

The success of aeration or any other alternative oxidation process, as a stage in iron removal, is dependent in large part on the solubility of the precipitate generated by the hydrolysis of the resultant ferric iron. Discussion in the previous section (10) suggests that the likely precipitates resulting from water treatment processes are some combination of Y-FeOOH and amorphous ferrihydrite. The solubility equation for either of these compounds can be expressed as for $Fe(OH)_3$. Thus, the solubility equilibrium for Y-FeOOH can be written as:

$$FeOOH(s) + 3H^+ = Fe^{3+} + 2H_2O \qquad 9$$

The solubility product is given by:

$$ {}^{c*}K_{so} = \frac{[Fe^{3+}]}{[H^+]^3} \text{ mol}^{-2} \text{ liter}^2 $$

$$ = [Fe^{3+}] \left(\frac{[OH^-]}{K_W}\right)^3 $$

$$ \therefore {}^{c}K_{so} = {}^{c*}K_{so} (K_W)^3 = [Fe^{3+}] [OH^-]^3 \qquad 10 $$

where

${}^{c}K_{so}$ = conventional solubility product

${}^{c*}K_{so}$ = solubility product for the solubility reaction written with H+ ion as a reactant

K_W = ion product for water

Equation (10) is the form used to represent the solubility of amorphous ferric hydroxide, also called amorphous ferrihydrite. Equations for the solubility equilibria between amorphous ferric hydroxide and each of several hydroxyl ferric complexes, and the corresponding solubility products are presented below for a 3M $NaClO_4$ solution at 25°C (10):

$$ (am)Fe(OH)_3(s) = Fe^{3+} + 3OH^- \quad K_{so} = 2.0 \times 10^{-39} \qquad 11 $$

$$ (am)Fe(OH)_3(s) = FeOH^{2+} + 2OH^- \quad K_{s1} = 3.2 \times 10^{-28} \qquad 12 $$

$$ (am)Fe(OH)_3(s) = Fe(OH)_2^+ + OH^- \quad K_{s2} = 2.5 \times 10^{-17} \qquad 13 $$

$$ (am)Fe(OH)_3(s) + OH^- = Fe(OH)_4^- \quad K_{s4} = 3.16 \times 10^{-5} \qquad 14 $$

Similar representations for FeOOH are given thus:

$$(am)FeOOH(s) + 3H^{+} = Fe^{3+} + 2H_2O \quad K_{so} = 3.5 \times 10^{3} \qquad 15$$

$$\alpha\text{-}FeOOH(s) + 3H^{+} = Fe^{3+} + 2H_2O \quad K_{so} = 4.0 \times 10^{1} \qquad 16$$

Equations 11 and 14 can be used to produce a solubility diagram (Figure 1) from which the concentration of any dissolved ferric or hydroxy-ferric species in equilibrium with amorphous ferric hydroxide can be determined for any given pH, within the range represented.

Based on Figure 1, for amorphous ferric hydroxide the highest solubility occurs at low pH levels -- $\leq$2.0, whereas the minimum solubility occurs at ~ pH 9 where the predominant dissolved iron species, $Fe(OH)_4^-$ and $Fe(OH)^{2+}$, are at ~ 10^{-10} M concentration. Amorphous ferric hydroxide ($(am.)Fe(OH)_3$) is virtually insoluble within the pH range 4-13. Based on equation 15, at pH 2 the concentration of Fe^{3+}, the likely predominant dissolved ferric species in equilibrium with amorphous FeOOH, would be 3.5 x 10^{-3}M, i.e., significantly less than the levels sustained by amorphous ferric hydroxide (Figure 1). Also, in the absence of the specific equilibrium expression values it can be assumed that at higher pH levels amorphous FeOOH would sustain Fe(III) concentrations broadly similar to those for amorphous ferric hydroxide. Thus, whether the ferric percipitate resulting from aeration be FeOOH or $(am)Fe(OH)_3$, within the pH range of natural wates, the equilibrium concentrations of ferric iron would be vanishingly small.

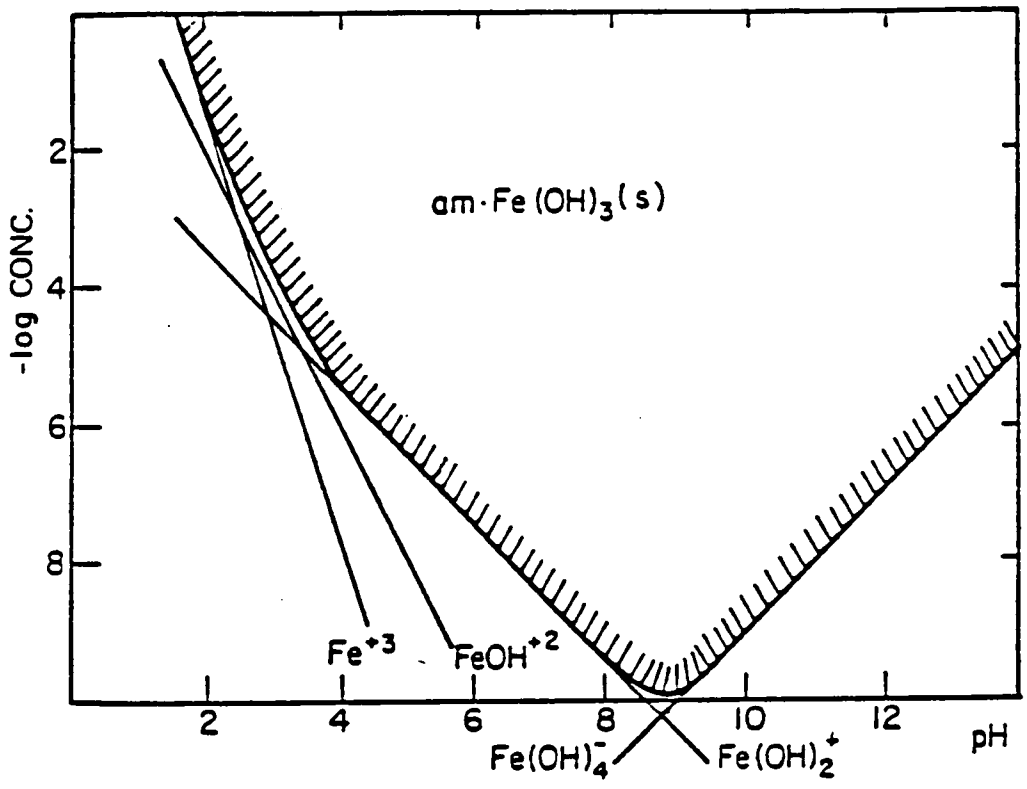


Figure 1. Solubility Diagram for Amorphous Ferrihydrite, (am.)$Fe(OH)_3$ (S) (10).

Aqueous Silicate Chemistry

Sodium silicate, used here in iron stabilization, is just one member of an extensive family of compounds, the silicates. Silicate minerals constitute greater than 90% of the earth's crust. The fundamental unit in all of these minerals is the regular silica tetrahedron consisting of a silicon ion surrounded by four oxygen ions subtended at equal solid angles. The Si-O bond is very strong (452 KJ/mol) and this stability allows a wide range of silicate structures, both natural and synthetic. No attempt will be made to cover the topic of silicates in depth. Such a treatment is already provided by Iler (20, 21). The coverage will be limited to aspects of silicate chemistry of direct relevance to the understanding of the silicate treatment mechanism for iron stabilzation. The terms "silica" and "solution" are each subject to a variety of interpretations. However, in the current discussion the terms will be used in the following sense: 1. The term silica will be used, unless otherwise designated, in its most general sense, i.e., to comprise all forms of silicon dioxide represented by the formula $(SiO_2 \cdot xH_2O)_n$ where x is from 0 to 2, and n is from 1 to infinity (22). 2. Also, although clear silicate liquids may contain colloids these will be described as solutions even though colloids may be present. In accordance with Anderson et al. (23) the term true solution will indicate the absence of colloids.

Silicate Solubility

Silicates have finite measurable aqueous solubilities. Thus, the abundance of silicates at the earth's surface and the consequent contact with rain water or other water in hydrologic transition results in the commonly observed natural dissolved silica concentrations of 5 to 35 mg/L SiO_2 is river water and 5 to 15 mg/L SiO_2 in sea water (21). Furthermore, Roy (24) reviewed the literature and concluded that the silica in natural waters was in true solution rather than colloidal as claimed by other researchers.

The commonly soluble form of silica is monomeric, i.e., each molecule contains only one silicon atom which is generally formulated as $Si(OH)_4$ and called monosilicic or orthosilicic acid (29). Silicic acid is often written as $Si(OH)_4$ rather than H_4SiO_4 to emphasize that metalloids (Si, B, Ge) similar to metal ions have a tendency to coordinate with hydroxo and oxo ligands (10). Monosilicic acid is essentially nonionic in neutral and weakly acidic solution, but is readily ionized in alkaline solution. However, it is not salted out of water nor can it be extracted by neutral organic solvents (21). Monosilicic acid remains in the monomeric state at concentrations of $< \sim 2 \times 10^{-3}$ M (~ 120 mg/L as SiO_2) at 25°C. But, like multivalent metal ions, metalloids like Si tend to form multinuclear species (10). This is evident when at concentrations in excess of 2×10^{-3}M monosilicic acid polymerizes, usually rapidly, at first forming polysilicic acids of low molecular weight and then larger polymeric species readily recognizable as colloidal particles (21).

The solubility of silica (SiO_2) is characterized by the following equilibria (10):

$$SiO_2(s, \text{quartz}) + 2H_2O \rightarrow Si(OH)_4 \qquad \log K_1 \ -3.7 \qquad 17$$

$$SiO_2\ (s, \text{amorphous}) + 2H_2O \rightarrow Si(OH)_4 \qquad \log K_2 = -2.7 \qquad 18$$

$$Si(OH)_4 \rightarrow SiO(OH)_3^- + H^+ \qquad \log K_3 = -9.46 \qquad 19$$

$$SiO(OH)_3^- \rightarrow SiO_2(OH)_2^{2-} + H^+ \qquad \log K_4 = -12.56 \qquad 20$$

$$4\ Si(OH)_4 \rightarrow Si_4O_6(OH)_6^{2-} + 2H^+ + 4H_2O \qquad \log K_4 = -12.56 \qquad 21$$

Alternative values for some of the solubility constants have been cited by Iler (21), viz., $\log K_3 = -9.8$ and $\log K_4 = -12.16$.

These equations, together with the appropriate equilibrium constants, can be used to generate ths solubility domains presented in Figure 2 (10). Although Figure 2 does not include individual equilibrium lines for all of the multinuclear Si-O-OH species postulated to exist (10), it is a sufficiently accurate representation for most purposes. Thus, as is congruent with past observations and evident from Figure 2, at pH $< \sim 9$ and SiO_2 concentration $< 2 \times 10^{-3}$ M, monosilicic acid remains in the monomeric form. Furthermore, $Si(OH)_4$ is the dominant soluble form under the conditions just stated. Under alkaline conditions the solubility of silica is enhanced by the ionization of silicic acid (25) as well as the formation of multimeric silicates (10). However, it should be recognized that Figure 2 is only an equilibrium diagram, and, as

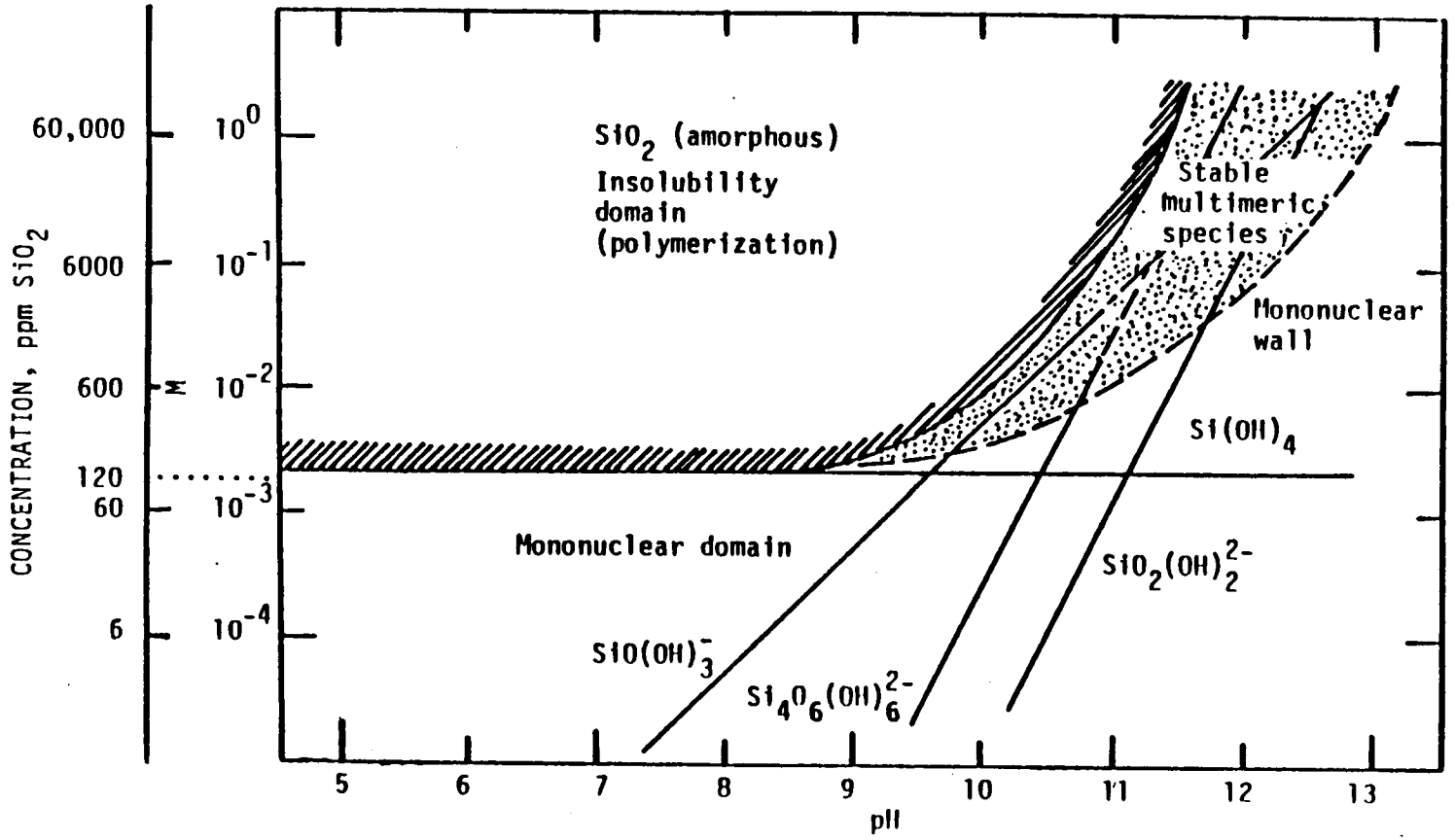


Figure 2. Solubility Diagram for Silica, SiO_2 (10).

such, it does not factor in kinetics which is commonly a major determinant of the distribution of species observed in natural or laboratory situations. Thus, the experimentally observed silicate speciation is typically and primarily a function of SiO_2 concentration, pH, equilibration time, and also sample history. Notably, the stippled portion of Figure 2 is the domain of stable multimeric silicate species. Commercially produced alkali metal silicate solutions such as the concentrated sodium silicate here used in iron stabilization treatments, fall within the multimeric domain (10).

Concentrated Sodium Silicate Solutions

The liquid sodium silicates are manufactured by fusing varying proportions of soda ash (Na_2CO_3) with specially selected silica sands (SiO_2) in furnaces at temperatures ranging from 1100 to > 1300°C (10, 26, 27). The relevant generalized reaction is:

$$Na_2CO_3 + nSiO_2 \rightarrow Na_2O \cdot nSiO_2 + CO_2 \qquad 22$$

The resulting soluble glass is dissolved in hot water under pressure and then filtered to remove any insoluble glass and unreacted sand (27). Although soluble sodium silicates with n values ranging from 0.5 to 4 are commonly produced (27), the sodium silicate with n = 3.22 is the most generally applied commercial silicate solution (28). Where the ratio, n, is 1.0 a distinct compound -- sodium metasilicate, $(Na_2SiO_3)_n$ is formed. At higher values of n (n > 1) distinct compounds have not been identified. The soluble silicates form clear or opalescent colloidal solutions in water which behave as non-Newtonian liquids

at all but the lowest concentrations. This is attributed to the formation of micelles from the polymeric anions especially at SiO_2/Na_2O ratios above 2.

Conceptions of the composition of the soluble silicate systems vary but are in basic agreement. Thus, Pearce (27) considered soluble silicate micelles to be constituted mainly by discrete SiO_4^-, orthosilicate ions, together with pyrosilicate $Si_2O_7^{6-}$, linear trisilicate $Si_3O_{10}^{8-}$, cyclic tetrasilicate $Si_4O_{12}^{8-}$ and polysilicate structures of higher complexity. Iler (29) suggested that concentrated solutions with molar SiO_2/M_2O ratios of 1/1 to 1/2 consist mainly of SiO_3^{2-} and $H_3Sio_3^-$ ions, but proposed that in solutions of higher ratios an increasing proportion of the silica forms extremely small 3-dimensional, internally condensed silicate polymer ions or charged particles. These charged particles are in solubility equilibrium with dissolved silica monomer, $Si(OH)_4$, which in turn is in equilibrium with monomeric silicate ions. Iler (21) elaborated further, suggested that particles as well as monomeric species both acquire negative charges by partial ionization of surface OH groups to SiO^- anionic sites thus:

$$Si(OH)_4 + OH^- \rightarrow (HO)_3SiO^- + H_2O \qquad 23$$

$$(HO)_3SiO^- + OH^- \rightarrow (HO)_2SiO_2^{2-} + H_2O \qquad 24$$

$$Si_nO_{(4n-nx)/2}(OH)_{nx} + zOH^- \rightarrow Si_nO_{(4n-nx)/2}(OH)_{nx-z}O_z^{z-} + zH_2O \qquad 25$$

where

z = the number of charges on a polymer containing n silicon atoms

Relatedly, Falcone (30) cited data indicating that the pKa's of these surface hydroxyl groups start at ~ 9.5 for the simple monomeric silicic acid and decrease continuously with increasing polymeric complexity to a value of about 6.5 for silica gel. This conception could be helpful in understanding the role of sodium silicates in iron stabilization.

Importantly, the polysilicate fraction of the soluble silicates at equilibrium is not comprised of a wide range of polyion or particle sizes because small particles are more soluble than the larger ones. This differential solubility causes rapid redistribution of silica until all of the charged particles are within a relatively uniform size range (21). Iler (29) concluded on the basis of ultrafiltration experiments that colloidal species are present in solutions of sodium silicates having SiO_2/Na_2O ratios > 2/1 and that a higher ratios a greater proportion of the silica is presented as polysilicic ions or particles generally > 30 nm in diameter. There appears to be a consensus among researchers that the lower limit ratio for the appearance of colloidal silica species is $SiO_2/Na_2O = 2$ (21).

Effects of Dilution

Dilution of the mixture of polymeric and monomeric silica species present in commercial liquid silicates produces varied results depending

on the manner of dilution with regard to aging, silica concentration, and pH. For optimal applications of these silicates in water treatment and corrosion prevention, understanding the role of dilution in silicate solution composition is important.

Iler (21) suggests that the reduction in hydroxyl ions and pH resulting from the dilution of these alkali metal silicates hydrolyzes the silicate ions and ultimately produces a disproportionation of the original system into one consisting of a higher polymeric species of colloid along with a residual silicate of lower SiO_2/Ha_2O ratio. This theory seems to conflict with the findings of O'Connor (31) who examined the effect of dilution on the level of polymerization and the proportion of silica in the polymeric form for 3.3 ratio SiO_2/Na_2O silicate in the range of 1 to 30% silica. The silica was characterized in terms of the reactivity of a given solution with molybdic acid as monitored colorimetrically with time for the development of the silicomolybdic acid color complex. The results showed that with increasing dilution, for the predominant silica forms, the level of polymerization and the proportion of total silica in that form both decreased.

Apparently, the dilution technique exerts significant control over the resultant silica speciation. McGarry and Hazel (32) diluted 3.45 SiO_2/K_2O ratio potassium silicate solutions from 10% to 0.03% SiO_2 in various ways, and examined the resultant particle size distributions by electron microscopy. Direct dilution from 10% to 0.03% SiO_2 yielded 89% of the observed particles being from 1 to 5 nm in diameter. Dilution from 10% to the intermediate concentration of 0.3% followed by

aging at that concentration before final dilution to 0.03% produces particles with a number average diameter of 8 nm. Because the 0.03% SiO_2 silica concentration falls within the monomeric domain, at the prevailing pH, it is evident that the presence of silica particles and differences between solutions prepared by the different techniques are both transient conditions. This view is supported, in part, by the investigations of Hazel (33) of the same dilutions used by McGarry and Hazel (32). He found, based on interaction between the silicates and the cationic dye pinacyanol chloride, that the 0.03% SiO_2 solution prepared from aged 0.3% SiO_2 solutions, with time, gave the same dye reaction color (blue) as the 0.03% SiO_2 solution prepared directly from the 10% SiO_2 solution. Because the dye is red when it is adsorbed, the above results indicate that with time both dilution systems produce similar distributions which are low anionic microparticles.

Lehman and Shuldener (34) found that undiluted 3.22 ratio sodium silicate (400,000 mg SiO_2/L) to 1400 and 700 mg SiO_2/L showed decreases of molybdate-reactive, presumably monomeric, silica to about 76 and 88%, respectively, within 24 hours, and down to 71 and 78%, respectively, within one week. In contrast, dilutions to 350 mg SiO_2/L and less were completely molybdate-reactive within a few hours. The combinations of pH (9 to 10.5) and silica concentrations, and the observed reactivity are consistent with the solubility domains presented in Figure 2 above. Sodium metasilicate solutions at ~ 1300, 65, and 13 mg SiO_2/L were 100% molybdate-reactive for the entire period of investigation -- 8 days (34). The pH of the 1300 mg SiO_2/L solutions was 12.1, placing it

within the domain of monomeric silica along with the 65 and 13 mg SiO_2/L solutions.

Thus, it is apparent that the domains presented in Figure 2 do hold in the long run, i.e., at equilibrium. However, the occurrence of alternate intermediate metastable states is common and is likely a function of pH, silica concentration, dilution history, and equilibration time at each change of solution conditions.

Characterization of Silicate Solutions

An old and rudimentary method for characterizing the composition of silicate solutions is on the basis of rates of reaction with molybdic acid. Molybdic acid reacts only with monomeric silica to form the yellow silicomolybdic acid (21). Because this reaction occurs at pH 1-2 where silicic acid polymerizes or depolymerizes least rapidly, samples taken from rapidly polymerizing or depolymerizing solutions are fixed at the moment they are mixed with the molybdic acid reagent (21). Moreover, because monomeric silica reacts with molybdic acid very rapidly (within 2 minutes), the polymerization/depolymerization of the silica is the rate limiting reaction. This last circumstance allows the polymeric silica distribution for a given system to be described by rate coefficients based on the rate of color development in the molybdate reagent.

Accordingly, the reaction of molybdic acid with silica constituents varies inversely with the degree of polymerization of the silica (35). Alexander (35) observed that with excess molybdic acid reagent the rate

of reaction with monosilic acid followed a first-order reaction rate law:

$$\frac{-dP_x}{dt} = K_x P_x \qquad 26$$

where

P_x = the concentration of monometer at time, t,

and K_x = the specific reaction rate constant

A similar representation with a smaller K_x was obtained for a silica dimer (P_x = concentration of dimer). Alexander (35) postulated that equation 26, above, would be generally applicable to any given silicic acid polymer, and that the rate constant would vary not only with the degree of polymerization (the number of silicon atoms in the molecule), but also with different isomers. However, plots of the logarithm of molybdic acid-reacted silica vs time were non-linear for silicates with SiO_2/Na_2O ratios of 3.25, 4.0, and 10.0, perhaps because the systems each included a mixture of polymers.

A more sophisticated equation, based on the same reactivity-rate principles, was developed by O'Connor (31):

$$\% \text{ color developed} = \left[\frac{0.435K_1}{K_o - K_1} - 0.565\right] P_o e^{-K_1 t} + 0.435 \left[100 - P_o\left(1 + \frac{K_1}{K_o - K_1}\right)\right] e^{-K_o t} + 56.5 \qquad 27$$

where

K_1 = the rate constant for the formation of β-silicomolybdate complex from depolymerization of polysilicate,

P_o = the initial level of polysilicate,

K_o = the rate constant for the spontaneous conversion of β-silicomolybdate to the less color absorbent α-silicomolybdate complex.

By this technique a silica solution is described by two coefficients: K_1, which is indicative of the complexity of major polymer fraction, and P_o, an indicator of the fraction of the total silica represented by this polymer.

In similar characterizations of silicate solutions by color development, Iler (21), rather than use a complicated expression (31), instead included a constant factor of 3.5%/hr to compensate for the conversion of β- to α-silicomolybdic acid as measured at 410 nm. Garrett and Walker (36) developed a procedure for measuring silicomolybdic acid at 329 nm, the isobiestic point for α- and β-silicomolybdic acids. Furthermore, the extinction coefficient at 329 nm is significantly greater than at 410 nm. However, presumably because the "color" development reaction takes 15 minutes to reach a maximum, this method has not been applied to the kinetic analysis of silicate solutions.

In further development of this molybdate-silicate reaction technique Iler (29), in addition to examination of whole solutions, also applied the method to selected fractions of silicate solutions. Specifically, silica sols were extracted with tetrahydrofuran (THF) for the selective removal of the colloidal fraction. The success of this extraction technique is due in large part to the immiscibility of THF with water, and to the stability of silica in the THF (as compared to

in water), in addition to the selectivity of THF for the silica colloids. The separated colloidal fraction was then reacted with molybdic acid and the pattern of color development at 410 nm analyzed, and compared with the color development pattern for the unextracted sols.

Ultrafiltration has also been used to characterize silicate solutions (21, 29). Commercial silicate solutions were diluted with an equal volume of water, aged for about a one week, filtered through fine filter paper to remove traces of suspended matter, and then ultrafiltered. For a 3.75 SiO_2/Na_2O ratio sodium silicate, membranes with nominal pore diameters of 18, 24, 33 and 52Å excluded 38, 25, 15, and 0%, respectively, of the silica present. In another series of tests using a single type of membrane with 18Å pores, solutions with molar SiO_2/Na_2O ratios of 2.4, 3.25, and 3.75 excluded 7, 14, and 25%, respectively, of the silica. The main conclusions, from these and other studies, were that colloidal species are present in sodium silicate solutions having SiO_2/Na_2O ratios of greater than 2/1, and that at higher ratios a greater proportion of the silica is present as polysilicate ions or particles generally greater than 30 nm. Ultrafiltration has been used also to investigate the polymerization of silicic acid at pH = 1.74 (22). Other techniques utilized to characterize silicate solutions include nuclear magnetic resonance (NMR) (37) and light scattering (38).

Interaction of Silica with Iron and Other Metal Ion Systems

Interactions between silica and metal ion systems exist on a continuum, ranging from reactions occurring in true solution all the

way to colloidal ones. For convenience, this discussion will deal initially with reactions (interactions) that appear to be occurring primarily in true solution, followed by those involving colloidal systems in any way.

True Solutions of Silicates

The majority of investigations in this area relate to the nature of iron-silicate complexes. In several of the instances discussed here, although the total experimental silica concentration fell within the domain of silica polymers at equilibrium, freshly prepared "solutions" were used in an attempt to examine reactions that occurred primarily in true solution prior to significant polymerization. Early conceptualization, without quantitation regarding formation or stability constants, was presented by Hazel et al. (39). These authors measured decreases in the pH of ferric (0.025 - 0.1M) and aluminum (0.01 - 0.2M) salt solutions upon combination with fresh silic acid solutions (2.5%). The observed final pH values in each instance was less than the corresponding individual initial pH of both the acid and the salt. This augmented acidic response could not be duplicated by substituting strong minearl acids for silicic acid. This was considered to be prima facie evidence of a special interaction between ferric ion (and aluminum ion to a lesser extent) and silicic acid. Initial pH values ranged from 2.21 to 3.27 for silicic acid, 1.77 to 2.12 for ferric chloride, and 3.07 to 3.42 for aluminum salts. Associated changes in H^+ concentration ranged from 7.2×10^{-4} to 3.0×10^{-3} M.

Similar experiments performed with silicic acid aged for 45 hours to 10 days produced smaller changes in pH than were observed with the fresh material. The reduction in pH decrease was attributed to polymerization of the silicic acid with aging, the suggested source of H^+ ions being the structure ≡SiOH. Relevant alternative chemical equations for the reaction were 1. for the unhydrated ferric iron:

$$n(\equiv SiOH) + Fe^{3+} \rightarrow [(\equiv SiO)_n - Fe]^{(3-n)+} + nH^+ \qquad 28$$

or 2. the two-step reaction:

$$Fe^{3+} + H_2O \rightarrow FeOH^{2+} + H^+ \qquad 29$$

followed by:

$$\equiv SiOH + FeOH^{2+} \rightarrow \equiv Si\text{-}O\text{-}FeOH^{2+} + H_2O \qquad 30$$

Presumably, the reaction presented in equation 30 drives equation 29 to the right producing H^+ ions beyond the equilibrium levels present in the ferric chloride solution prior to mixing the silicic acid. Equation 30 was offered, without follow up, by the authors as being consistent with the observation that silicates can discharge the color of iron from alkaline solution. This phenomenon may be due to the removal of the Fe^{3+} from further interaction with OH^- ions by the reaction presented in equation 30. Notably, the proposed reactions were not examined in terms of basic chemical parameters such as stability constants.

Aluminum salt solutions of pH and concentrations similar to the ferric solutions yielded smaller pH decreases than the latter indicating

a weaker interaction. Similar experiments with barium chloride, lanthanum chloride, copper sulfate, and chromic chloride indicated that there were no significant interactions for the first three salts, while the interaction of chromic chloride with silicic acid was slight.

More recently, several researchers (40, 41) have characterized the ferric-silica interaction in greater detail generating some of the previously mentioned chemical constants. Weber and Stumm (40) used UV absorbance measurements of dilute acidic solutions of ferric iron and silicic acid to demonstrate the existence of iron silicate complexes. Silicic acid solutions, freshly prepared in order to limit polymerization effects, ranging in concentration up to 5×10^{-2} M (300 mg SiO_2/L) were combined with ferric perchlorate ($[Fe^{3+}] \leq 10^{-4}$ M; $\leq$ 5.6 mg Fe/L) in dilute perchloric acid (pH < 3.5) and the absorbances monitored at 272 nm, the isobiestic point for the Fe^{3+} - $FeOH^{2+}$ equilibrium.

By combining equations for the equilibrium quotients for the first hydrolysis reaction of ferric ion with water (Q_H) and the hypothetical interaction of ferric iron with silicic acid (Q_1), with equations for the absorbances due to iron and iron-silicic acid species the following relationship was derived:

$$A = A_1 - \frac{(A-A_o)[H^+]^{4-n}[1 + Q_H/[H^+]]}{Q_1[Si(OH)_4]} \qquad 31$$

where

A = absorbance of a mixed silution of Fe(III) and Si)OH)$_4$

A_0 = absorbance for the Fe(III) in the absence of $Si(OH)_4$

A_1 = the hypothetical absorbance if all the Fe(III) were in the form of silicatoiron(III) complex

n = number of H's in the silicates-iron complex

No absorbance was expected from the silicic acid at this wavelength. For Fe(III) concentrations < 5×10^{-5} M (< 2.8 mg Fe/L) each plot of A vs $(A-A_o) / [Si(OH)_4]$ for a series of solutions of varying $Si(OH)_4$ concentration but the same formal concentration of Fe_T and H^+, yielded a straight line indicating the predominance of a single silicatoiron complex for the experimental conditions. Further, normalization by plotting $A/[Fe_T]$ vs $(A-A_o) / [Si(OH)_4] [Fe_T] \times 10^{-5}$ also yielded a straight line. The exponent of the concentration of $Si(OH)_4$ in this relationship was 1.0 and indicated that there was one mole ligand per mole metal ion. Inconsistent results at Fe(III) concentrations > 5×10^{-5} M were attributed to the formation of polynuclear complexes.

Data analysis produced an equilibrium quotient Q_1 for the complex in question:

$$Fe^{3+} + Si(OH)_4 \rightarrow FeOSi(OH)_3^{2+} + H^+ \qquad 32$$

$$Q_1 = 0.57$$

Combination of values from equation 32 with a literature value for the first dissociation constant for $Si(OH)_4$ yielded the concentration stability constant for the silicato-ferric complex thus:

$$K = Q_1/K_{Si(OH)_4} = [FeOSi(OH)_3^{2+}]/[Fe^{3+}[SiO(OH)_3^-] =$$

$$1.8 \times 10^9 \qquad 33$$

It should be emphasized that this reaction (equation 32) is most relevant at low pH values where free ferric ion and its first hydrolysis product are the significant iron species competing for the silicate. Olson and O'Melia (41), also examined the interaction of ferric iron with silicic acid using spectral measurements within the range 200 to 400 nm. They used freshly prepared monomeric silicic acid and in some instances exceeded the solubility of amorphous silica (2×10^{-3} M), but abandoned any system showing evidence of precipitation. They considered only monodentate formation thus:

$$Fe^{3+} + Si(OH)_4 \rightarrow FeOSi(OH)_3^{2+} + H^+ \qquad 32$$

An equation was derived relating the ratio of solution absorption per mole of iron to the molar absorptivity coefficient for $FeOSi(OH)_3^{2+}$ and the inverse of the equilibrium constant for reaction. Furthermore, it was suggested that a plot of the data conforming to the derived equation would be linear only over the range for which the monodentate complex predominated.

Plots of data for 1. $[Fe_T] = 5.6 \times 10^{-5}$ M (3.136 mg Fe/L) and $[Si_T] = 5 \times 10^{-2}$ M (3000 mg SiO_2/L), and 2. $[Fe_T] = 4.2 \times 10^{-4}$ M (23.52 mg Fe/L) and $[Si_T] = 4.0 \times 10^{-2}$ M (2400 mg SiO_2/L) each at 280, 290 and 300 nm were presented. The plots were linear between pH 1.69 and pH 3.0, and nonlinear between pH 3.0 and 4.80. Nonlinearity was attributed to polymerization effects. Execution of the experiments at multiple temperatures allowed the measurement of several thermodynamic data for equation 32: ΔG° = + 0.80 kcal/mole, ΔH° = + 3.73 kcal/mole, S° = +

9.83 cal/mole-deg. The equilibrium constant for the equation was: K = 0.250 (25°C, μ = 0.1 ± 0.02). Alternative measurements based on polarographic data (half-wave potential) yielded K = 0.34.

Both of the values for K were similar to but less than the value (K = 0.57) obtained by Weber and Stumm (40). Spectral curves obtained agreed with patterns from the literature for Fe^{3+} and $FeOH^{2+}$ but not for $FeOH(H_2O)_5^{2+}$.

Although the experimental silica concentrations exceeded the solubility of amorphous silica, the authors thought that speed of execution eliminated preexperimental SiO_2 polymerization as a factor in the outcome of the experiments. Furthermore, the lack of precipitate formation after several days of equilibration, for the one system tested in this way, and the linearity of the relevant plots seemed to confirm that SiO_2 polymerization was not a factor between pH 1.5 and 3.0. Silicic acid polymerization rates are lowest at ~pH = 1 and increases with increasing pH (21). The use of Fe concentrations in excess of 2.8 mg/L, the lower limit for the formation of polynuclear Fe-OH complexes (40), did not seem to be a factor at pH < 3.0.

An additional role demonstrated by silicic acid is as a catalyst in the oxidation of ferrous iron by molecular oxygen (12). Schenk and Weber (12) observed that within the tested concentration range, 0.1 to 1m$\underline{M}$, silicic acid enhanced the oxidation of ferrous iron (< $5 \times 10^{-5}\underline{M}$). This augmented oxidation rate occurred in addition to the well-documented hydroxyl effect (7) and is presented in the following equation:

$$\frac{-d[Fe(II)]}{dt} = (KP_{O_2}[OH^-]^2 + K_{Si}[H_4SiO_4]^{0.5}[OH^-]^{0.5})[Fe^{2+}] \quad 4$$

where

$K = 2.1\ (\pm 0.5) \times 10^{13} L^2\ mole^{-2} atm^{-1} min^{-1}$,

and $K_{Si} = 1.8\ (\pm 0.3) \times 10^3\ L\ mol^{-1}$

It was suggested that the rate constant K_{Si} may have been a function of the P_{O_2} of the system.

Notably, these authors also observed that monomeric silica retarded the hydrolysis of ferric iron. Silica concentrations in the < 120 mg SiO_2/L and iron in the 0.56 to 56 mg Fe/L ranges were utilized. In a solution of 5.6 mg Fe/L, it was observed that after 100 minutes there was 7.5 and 3 times as much filterable (< 0.45 μm) iron in systems containing 60 and 6 mg SiO_2/L, respectively, as in the silica-free system. However, these experiments were conducted at pH 3.5, and it is unclear as to the extent to which these silica-derived differences can be extrapolated to higher more common natural pH levels.

Colloidal Interactions

This discussion deals with the interaction of silica in the dissolved and crystalloidal or colloidal forms with metal ions, primarily ferric, hydrolyzed and polymerized to varying extents. The primary interest in these types of investigations is an assessment of the role of silica species in the sequestration of iron, either directly from

experiments with ferric iron or, alternatively, by analogy from other metal ions.

Hazel (42) investigated the ability of sodium silicate solutions to convert the surfaces of iron oxide sols from positively to negatively charged, a process favoring dispersion of these colloids. Silicates employed ranged in SiO_2/Na_2O ratio from 1/1 to 4/1. Solutions of the silicates at 2000 mg/L SiO_2 were prepared fresh daily and diluted immediately to 200 mg/L with water or 0.02 N HCl, and appropriate volumes used in the tests. Iron oxide sols, aged for 1 week, were diluted to 200 mg iron oxide/L immediately before use. The concentration of iron oxide in actual test systems was 80 mg iron oxide/L.

It was observed that when the initial pH levels of the silicate solutions were unadjusted, the more alkaline silicates (lower SiO_2/Na_2O ratio) discharged the iron oxide surface at lower SiO_2 concentrations. In contrast, when varying initial silicate pH was eliminated by pre-adjusting the silicate pH to a given level, the reverse trend prevailed, i.e., the more silicious silicates (higher SiO_2/Na_2O ratios) discharged the surfaces at lower concentrations. In general, decreasing the initial silicate pH shifted the recharging concentrations to higher values and extended the observed coagulation over a wide range of silica concentrations. Also, for a decreasing initial pH, the more silicious, higher ratio silicates were more effective than the more alkaline silicates. Thus, it is apparent than the more polymeric

silicates are the more effective at changing the surface charge of ferric oxide sols from positive to negative, starting from a given pH.

Also, aging the silicates for 24 hours only affected the performance of the higher ratio silicates, reducing their effectiveness. This result is consistent with the aging of silica polymers at certain concentrations which produces a lesser charged material, and thus less effective counterions (21). One-to-one electrolytes such as NaCl had no effect on the mobility of the ferric oxide sols. In contrast, $CaCl_2$ at 66.6 mg/L Ca increased the silica concentration needed to produce negative mobility. This observation is readily explained by classical colloidal double layer theory invoking the Schultze-Hardy charge ratio rule (10), and by specific adsorption of Ca^{2+} by the ferric oxide surfaces (43). For each of the silicates, beyond the isoelectric point of ferric oxide sols, as additional silicate was added to ferric oxide surfaces became more negative and passed from a zone of coagulation to one of dispersion.

Relatedly, Cameron and Liss (44) conducted laboratory experiments to see what substances including metasilicates could hold iron at 1 mg Fe/L in dissolved form (< 0.45 μm) in oxygenated water at pH 6 to 7. Metasilicate stabilized iron (90% < 0.45 μm) at a silicate-to-iron ratio of 1000, i.e., 687 mg SiO_2/L, whereas at 77.4 and 7.8 mg SiO_2/L only 11% and 0%, respectively, of the iron was stabilized. It was acknowledged that iron-silicate complexes might have been playing a role, but it was also suggested, without actual testing, that the adsorption of excess negatively charged silicic acid sols on positive

colloidal iron oxide particles may have been important in producing the observed iron stabilization. Notably, among the metasilicate concentrations used, only 687 mg SiO_2/L was high enough to allow the existence of multimeric/ polymeric forms of silica.

Interactions of other metals with silicates can elucidate Fe-Si interactions by analogy. Hazel et al. (45) investigated the interaction between Zn^{2+} and various sodium silicates. A series of potentiometric titration curves (pH vs mls or meq of NaOH or Na silicate) showing an inflection point that varied with both the form of silicate and the anion of the zinc salt was presented. Orthosilicate (SiO_2/Na_2O ratio = 1/2), metasilicate (SiO_2/Na_2O = 1/1) and "E" brand silicate (SiO_2/Na_2O = 3.29/1) were used as silicate titrants. Titration of 0.4$\underline{N}$ $ZnSO_4$ with 0.1$\underline{N}$ titrant shifted the point of inflection from 75% equivalents with NaOH to 100.2, 104, and 109% of base as the silica content of the titrant increased. The results obtained with the NaOH were consistent with the previously observed formation of the basic salt, $3Zn(OH)_2 \cdot ZnSO_4$. Shifts in the inflection point beyond 100% equivalents of base were considered to be a measure of the amount of free base (silicate anion, hydroxyl ion) absorbed by the precipitate.

The titration of zinc sulfate with a combination of titrants, i.e., a predetermined volume of metasilicate followed by titration to completion with NaOH, moved the inflection point progressively from 75% equivalents to 104% equilivalents, as the proportion of sodium metasilicate was increased from 0 to 100%. In the titration of $ZnSO_4$ with the 3.29 ratio silicate the slow settling of precipitate was attributed to the

peptizing action of adsorbed colloidal silicic acid. The similarity between this observation and the dispersive action of high-ratio silicates on ferric oxide sols (42) is obvious. Further, in general, the amount of silica in precipitates was variable but increased with the silica content of the titrant.

Notably, under certain circumstances, silicates containing a high proportion of silica reacted with Zn^{2+} ions without the formation of a precipitate, although the usual precipitation plateau of $Zn(OH_2)$ was exhibited by the potentiometric curve. This phenomenon is attributable to a "silica"-associated inhibition of particle association and growth or possibly dispersion. In the titration of Zn with E brand silicate the reaction is the same with and without precipitation. Precipitation was a function of the zinc concentration, higher concentrations producing more precipitation, and of mixing rate during titration, higher rates leading to less precipitation. The ability of E brand silicate to delay the precipitation of Zn^{2+} is analogous to observations made with Fe^{3+} with similar silicate solutions by Dart and Foley (5, 6).

Falcone (30) also examined the role of silicate polymerization on the interaction of silicate with Ca^{2+}, Mg^{2+},Cu^{2+}. Silicates with SiO_2/Na_2O ratios of 0.5, 2.0 and 3.8, and NaOH were compared with their ability to lower the activity of Ca^{2+}, Mg^{2+}, Cu^{2+} in chloride or perchlorate solutions, as measured by ion selected electrodes. At a given pH, for both Ca^{2+} and Mg^{2+}, NaOH and orthosilicate (0.5 ratio) produced similar cation activity reductions. Progressively higher ratio silicates yielded correspondingly greater reductions in Ca^{2+}. For Mg^{2+}

little differences in performance was observed between the 2.0 and 3.8 ratio silicates although in both instances the cation activity reduction was greater than for NaOH or orthosilicate. Similar trends were observed for Cu^{2+} but, drift in the current data made the magnitude of differences in activity reduction among dilutions less clear. It should be noted that although the 3.8 ratio silicate tended to yield a greater activity reduction than the 2.0 ratio silicate at an equivalent pH, because of its lower base strength, the 3.8 ratio system contains more SiO_2 when the solution pH values are equivalent. Significantly, in the Ca^{2+} and Mg^{2+} studies, precipitates, when observed, appeared immediately. In contrast, for Cu^{2+}, which is chemically more similar to Fe^{3+} than to Ca^{2+} or Mg^{2+}, precipitation occurred only on aging. The presence in the higher ratio solutions of colloidal size silicate anions with more acidic surface silanol groups that readily adsorbed nucleating metal ion hydroxides was offered as an explanation for the silica-enhanced metal ion activity reduction.

Iron Treatment by Sodium Silicate and Chlorine

The primary alternative to conventional iron treatment by removal from water supplies has been the treatment with sodium silicate and chlorine. The latter treatment does not remove the iron from the water but seeks only maintain the iron in a form that produces neither a visible settleable precipitate nor a highly colored water. Earliest published record of this technique occurred in 1950 (46), but it was not well exploited until the late 1960's to early 1970's (5, 6).

Despite moderate to good success, this treatment process is not widely used, being limited largely to the relatively small municipal systems in Ontario, Canada.

In 1950 in Miami, Florida, concentrated sodium silicate was used by Henry to prevent the settlement of iron from chlorinated unsoftened water, as an interim measure until the completion of a conventional softening plant (46). Preliminary experiments were conducted with samples of unaerated groundwater taken carefully at the well head so as to exclude air (O_2) and then, with a few exceptions, dosed in the field at the time of collection and brought to the laboratory for analysis. The chemicals tested included polyphosphates, mono-, di- and trisodium phosphate, as well as concentrated sodium silicate (SiO_2 / Na_2O = 3.22) solution. Based on the results of these preliminary tests, the sodium silicate and polyphosphate were field-tested on a small well-built up subdivision on well water. Sodium silicate gave good treatment, in sharp contrast with polyphosphates which yielded poor treatment and/or objectionable turbidity. In the field treatment, the silicate was diluted 9-fold to provide a 3.2% SiO_2 feed solution and dosed continuously at 15 mg SiO_2/L. In the field, the iron was held in suspension for 3 days, only half as long as for comparable laboratory systems. Significantly, the observation of the Tyndall effect from clear successfully-treated waters, suggested that the iron was in fact present as small particles, perhaps colloidal, rather than in true solution.

Conflicting results were evidenced with regard to the ordering of chlorination and silicate applications. Henry (46) observed that

chlorine-before-silicate provided the best treatment. This is in contrast to the findings of F. E. Hale, cited by Henry (46) as a personal communication. Hale obtained best treatment of groundwater in Jamaica, New York by applying sodium silicate before chlorine. The treatment was not implemented in Jamaica, NY because there was an associated yellow color. It was also found in laboratory tests that with "activation" of the silicate by bubbling with CO_2 prior to dilution, the treatment was ~ 100% more effective (46). However, this modification was not field-tested.

Dart and Foley (5, 6) of the Ontario Ministry of Environment examined iron treatment problems in Ontario, Canada. It was noticed that groundwaters high in silica (30-40 mg SiO_2/L) were resistant to conventional iron treatment, but that in systems with 0.3-10 mg Fe/L and high silica, there were few "red water" complaints although the iron had not been removed satisfactorily. Based on this experience as well as Henry's (46) and Hazel's (42), it was decided to explore the silicate-chlorine treatment procedure as a means of bypassing the filtration needs for waters with low levels of iron (5, 6).

Initial laboratory evaluations of the chlorine/silicate treatment using 3.22 ratio sodium silicate yielded the following conclusions (5):

1. Higher pH favored silicate stabilization of iron, a pH of > 7.5 was best.

2. Silica-to-iron requirements were not linear. Higher iron concentrations required increasingly higher silica doses for stabilization.

3. Hardness increased silica requirements.

4. Fresh concentrated silicate was more effective than dilute or "activated" silicate at stabilizing iron.

5. Simultaneous addition of silicate and chlorine provided the best treatment.

6. Rapid mixing and cold water improved stabilization of iron.

Based on successful laboratory results the procedure was tested on four municipal water systems. The chemical composition of the raw waters along with critical treatment parameters for these four systems are presented in Table 1. These water systems were all low-iron systems three of them having $\leq$ 0.7 mg Fe/L and the other, Gravenhurst, 1.45 mg Fe/L. The pH levels were neutral or slightly above. Gravenhurst was a soft water system while the other three provided medium hardness waters. In all instances about 2/3 of the hardness was calcium hardness. Background silicate concentrations ranges from 15 to 20 mg SiO_2/L. Silicate feed was at or near full strength in the three instances (all except Gravenhurst) for which the requisite information was given. Satisfactory treatment was achieved with low in-stream silicate additions of 2.7 to 6 mg SiO_2/L. An important prerequisite for successful treatment was considered to be total and immediate oxidation of all iron at the point of silicate application.

Subsequently laboratory tests of the iron filterability in response to 3.22 ratio silicate treatments using a filter of asbestos fibers matted in a Gooch crucible, were performed. Results showed that for each of the three waters tested there was a plateau of low iron filterability followed by an abrupt and significant increase in filterability

Table 1. Chemical Composition and Critical Treatment Parameters for Successfully Field-Treated Water Systems (Dart and Foley (5)).

Characteristic[a]	Water System			
	Town of Markham	Markham Township	Borden[d]	Gravenhurst[e]
Iron, Fe	0.5	0.2-0.7	0.40	1.45
pH	7.6-8.0	7.7-7.8		7.1
Total Hardness, $CaCO_3$	150	300		96
Calcium Hardness, $CaCO_3$	98	220		55
Alkalinity, $CaCO_3$	200	c		56
Total Kjeldahl, N	1.4	0.54		c
Free Ammonium, N	0.99	0.02		c
Nitrate, N	b	0.02		0.014
Dissolved Solids	220	460		180
Sodium, Na	24	22		12
Chloride, Cl	15	55		c
Silica, SiO_2	19	20	15.0	19

Table 1. (continued)

Characteristic[a]	Water System			
	Town of Markham	Markham Township	Borden[d]	Gravenhurst[e]
Sulfate, SO_4	b	50		28
Phosphate, PO_4	b	0.12		c
Potassium, K	b	1.7		3.6
Manganese, Mn	b	0.0		c
Adequate Silica dose, SiO_2	2.7	4.6	5.4	6
Silica Feed Strength, % SiO_2	28.7	28.7	20	c
Chlorination; Dosing Point	just before silica addition	with silica addition or slightly after	several seconds before silica addition	with silica addition

a. Silica feed strength as % SiO_2 all other characteristics except pH reported as mg/L
b. Undetectable
c. Not listed
d. Identical to Markham Township except of those characteristics listed
e. Chlorination by hypochlorite

at a certain threshold silicate dose. For the one instance where a direct comparison could be made, i.e., for Markham (town) water, the threshold dose observed in the laboratory, ~7 mg SiO_2/L, was significantly lower than the dose needed to achieve satisfactory treatment in the field, 2.7 mg SiO_2/L. In other laboratory experiments it was also noted that the more alkaline oxidants had lower silicate requirements. Thus, hypochlorite chlorination required the least, hydrogen peroxide somewhat more, and gaseous chlorine chlorination of the greatest amount of silicate for iron stabilization (5).

The success of the silicate treatment in the stabilization of filterable iron was hypothesized by Dart and Foley to be due to the formation of the silicate iron (FeIII) complex, $FeSiO(OH)_3^{2+}$, which prevented or at least inhibited the polymerization of ferric iron into iron flocs. In support of that contention Dart and Foley (5) provided calculations to show that at pH 7.5, orthosilicate at ~12 mg SiO_2/L and iron at ~11 mg Fe/L, the iron would exist primarily almost exclusively in the complexed form. However, iron precipitates were not considered. Data provided by subsequent experimentation (6) suggested to Dart and Foley alternative explanations (to be discussed later) for the observed phenomena. Significantly, no exact dose formula based on standard water analyses has yet been provided.

In their later work Dart and Foley (6) extended the silicate-chlorine treatment to several other communities with the restriction that the iron content of the waters be $\leq$ 1.3 mg Fe/L. From all reports the treatments were successful with maximum in-stream dosage levels of 6.2

mg SiO_2/L. In the absence of a valid dosage formula on-site jar-tests were developed and standardized. One percent (1%) sodium hypochlorite and freshly prepared ~1% SiO_2 silicate solutions were used in these tests leading to the requisite dosage. It was observed, as before (5), that on exceeding a critical level of SiO_2 addition the amount of filter-retained iron dropped abruptly to much lower and usually insignificant levels (6).

Most importantly, characterization of the stabilized iron was attempted, using strong and weak base as well as strong and weak acid resins, as cited below:

1. Anion exchange resins
    a. Chloride form
        1. strong base (Nalcite SBR)
        2. weak base (NC-2077-1)
    b. Hydroxyl form
        1. strong base (Nalcite SBR)
        2. weak base (NC-2077-1)
2. Cation exchange resins
    a. Sodium form
        1. strong acid (Permutit Q)
    b. Hydrogen form
        1. strong acid (Permutit Q)
        2. weak acid (Nalcite CCR-2)

Quantitative removal of all of the stablized iron was obtained with each of the anionic exchange resins tested. In contrast, simultaneously quantitative silica removal was observed consistently on only the

strong base and the weak base resin in the hydroxyl form. Only one of the seven tests on chloride-form resins provided anything approaching quantitative (98%) silica removal. Iron removal on cation-exchange resins was inconsistent and, in general, poor. Silica removal by the same cation exchange resins was, with the exception of one water, nil. For the cationic Fe-Si complex proposed earlier by Dart and Foley (5), quantitative removal of Fe and of Si by a cation exchange resin would be expected.

However, these results suggest that the iron in the treated waters was consistently in the anionic form regardless of the contribution of the silicate to the complex. Furthermore, and perhaps significantly, silica removal on the OH-form resins for which the effluent pH was >11, was quantitative, whereas removal by the Cl-form with effluent pH 8.5-9.4 resin was poor. For the one water providing quantitative removal on the Cl^--form weak base resin the effluent pH was pH 9.8 All of this, together with the fact that the pKa of silic acid is 9.5-9.8 (depending on the source) (10), suggests that the silica may be retained by the resins in the silicate ion form, unassociated with iron. However, all previous evidence indicates that it is the combination of silicate in some form and the iron together that produces the stabilized form of iron. Thus, it would appear that the resin experiments (6) produced questionable results, and perhaps there is a reaction occurring at the surface of the resin that splits the stabilizing complex into its Fe and Si components.

In this regard, Dart and Foley (6) also observed, in filtration experiments, that when silicate-stabilized iron contacted precipitated iron (hydrous ferric oxide) retained by the filter the stabilized iron was removed from solution, i.e., negating the effect of the silicate. Conceivably, a similar mechanism may have been responsible for the conflicting ion exchange results presented above.

Nevertheless, Dart and Foley (6) offered a mechanism for the role of the silicate on the stabilization of iron. They invoked the intervention of monovalent orthosilicate anion in the normal iron polymerization by suppression of positive catalysts, such as dihydroxyl ferric ion. Their suggested sequence of reactions in the absence of silicate was as follows:

$$Fe(OH)_2 \cdot 4H_2O^+ + Fe(OH)_4 \cdot 2H_2O^- \rightarrow (OH)_2Fe\text{-}O\text{-}Fe(OH)_2 \cdot 6H_2O + H_2O \qquad 34$$

$$(HO)_2Fe\text{-}O\text{-}Fe(OH)_2 \cdot 6H_2O + H^+ \rightarrow (OH)_2Fe\text{-}O\text{-}Fe(OH) \cdot 7H_2O^+ \qquad 35$$

$$(HO)_2Fe\text{-}O\text{-}Fe(OH) \cdot 7H_2O^+ + Fe(OH)_4 \cdot 2H_2O^- \rightarrow (OH)_2Fe\text{-}O\text{-}Fe(OH)\text{-}O\text{-}Fe(OH)_2 \cdot 9H_2O + H_2O \qquad 36$$

However in the presence of orthosilicate anion the resultant reaction was hypothesized to be:

$$Fe(OH)_2 \cdot 4H_2O^+ + H_3SiO_4 \cdot 2H_2O^- + OH^- \rightarrow Fe(OH)_3OSi(OH)_3 \cdot 5H_2O + H_2O \quad 37$$

They also recognized the silicate-iron complex as a metastable state.

Detracting from the theory of Dart and Foley (6) is the fact that at pH 7 and 8, the pH of most of treated waters, orthosilicate anion provides a very small fraction of the added silicate (pK_a H_4SiO_4 = 9.5-9.8). Also, several critical questions regarding their results remain unaddressed, such as:

1. Why were freshly prepared 3.22 silicate dilutions more effective at iron-stabilization than the silicate, presumably orthosilicate, negative to the untreated waters?
2. Why were freshly prepared silicate dilutions more effective than aged ones?
3. Why were undiluted or only moderate (e.g., 1/50) dilution of 3.22 silicate concentrate more effective in treatment than more dilute silicate "solutions"?
4. Why does the Ca^{2+} ion increase the SiO_2 dose required for iron stabilization although it forms neither strong complexes nor insoluble precipitates with silicate?

These and other questions will be addressed in the experimental research to be reported in this investigation.

In their earlier work Dart and Foley (5) found that hardness increased the silicate dose required for iron stabilization. More recently, Dart (47), went further to state that because silicate is inactivated by calcium and magnesium ions, hard water cannot be dosed with silicate prior to oxidation of the iron unless the total silica in the treated water exceeds the total hardness equivalents

available. This would leave some silicate free for combination with the iron. Dart (47) provided a dosage formula:

$$\text{mg } SiO_2/L \text{ addition} = [(\text{total } CaCO_3 \text{hardness}) * 0.6 + 1.07 * (\text{mg/L Fe+ Mn})] - [(\text{mg/L } SiO_2 \text{ of raw } H_2O)] \quad 38$$

This formula was recommended for waters of hardness < 30-40 mg/1 $CaCO_3$ and iron < 10 mg/L Fe. Holden (48) examined the effect of calcium ions on iron treatment with 3.22 ratio sodium silicate and could find no simple stochiometric rule for determining the necessary silica dosage in the presence of calcium. Furthermore, the literature provides no evidence of a strong calcium-silicate interaction. Spectulation suggests perhaps a double-layer counterion effect due t the calcium ions. However, the need for further experimentation to clarify the role of calcium (and magnesium) in the silicate treatment of iron is obvious. Other results of Holden (48), indicated that in contrast with calcium which increased the necessary sodium silicate dosage for iron stabilization, sodium, chloride, sulfate, and bicarbonate had much smaller effects and did not increase silicate dosage significantly.

III. METHODS AND MATERIALS

Kinetic Characterization of Silicate Solutions

Silicate solutions to be used in the treatment of iron systems were characterized in terms of their distribution of nomeric and polymeric silica species. This characterization was effected indirectly by quantifying the rates of reaction with molybdic acid of monomeric silica whether present in the original solution or resulting from the subsequent depolymerization of more complex forms of silica. The procedure was carried out according to the method of O'Connor (31). The molybdic acid reagent as described by Alexander (35) was prepared by combining 40 ml of ammonium molybdate solution (10 g/100 ml) with 100 ml of 1N H_2SO_4 and making the combined solution up to 1 liter. This molybdic acid reacted with monomeric silica to produce β-silicomolybdate initially (49). An aliquant of appropriately aged silicate solution, 10 µl to 5 ml, was added to a dry 400 ml glass beaker, 200 ml of molybdic acid added rapidly to the beaker and the mixture well-agitated by a magnetic stirrer. After two minutes of mixing, a portion was transferred to a 1 cm quartz cell and the rate of color development at 400 nm measured on a Perkin-Elmer Hitachi 200 double-beam spectrophotometer for a period sufficient to allow full color development. Experiments were conducted at 21 and 25°C. Duplicate samples of the β-silicomolybdate formed in each experiment were heated in capped linear polyethylene (LPE) bottles at $\geq$ 90°C for $\geq$ 3 hr, sufficient for complete conversion to α-silicomolybdate. Because β-silicomolybdate converts spontaneously to α-silicomolybdate, this latter measurement with extended heating is

necessary, along with the ratio of extinction coefficients for the two species, to calculate the optical density of β-silicomolybdate corresponding to the total amount of SiO_2 present. The ratio of extinction coefficients for β- as compared with α-silicomolybdate is 1.77 at 400 nm (31).

Mathematical analysis of the pattern of color development allowed derivation of coefficients indicative of the degree of silica polymerization as well as of the proportion silica in the polymerized form. A measure of the color development is given by:

$$\% \text{ color developed} = \left[\frac{0.435K_1}{K_o - K_1} - 0.565\right] P_o e^{-K_1 t} + 0.435 \left[100 - P_o \left(1 + \frac{K_1}{K_o - K_1}\right)\right] e^{-K_o t} + 56.5 \qquad 27$$

where

K_1 = the rate constant for the formation of β-silicomolybdate complex from depolymerization of polysilicate,

P_o = the initial level of polysilicate,

K_o = the rate constant for the spontaneous conversion of β-silicomolybdate to the less color absorbent α-silicomolybdate complex

An index of the % SiO_2 remaining uncomplexed by molybdic acid is given by (31):

$$100(OD_T - OD_t)/OD_T = 100 - \% \text{ color developed} \qquad 39$$

where

OD_t = the optical density of the solution at time t, and OD_T is the total optical density of the β-silicomolybdate complex corresponding to the total amount of SiO_2 present.

Analysis of experimental data for the % SiO_2 remaining uncomplexed by molybdic acid, by means of NLIN a nonlinear regression program (50) using fixed values for K_o, allowed estimation of values for K_1 and P_o.

Silicate Dilutions

Four different commercial silicate solutions produced by the Philadelphia Quartz Corporation, i.e., S35, N, Star, and Starso, with molar SiO_2/Na_2O ratios of 3.75, 3.22, 2.50, and 1.80, respectively, were used in this investigation. The properties of these silicates are presented in Table 2. In addition to the undiluted silicate solutions themselves, four dilutions of each -- 1/10, 1/50, 1/100, and 1/500, were tested routinely. One dilution of 1/25 of the N silicate was used for one experiment. Dilutions were prepared by dispensing 1.0 or 2.0 mL of the undiluted solution by means of a gas-tight syringe (Hamilton Gastight #1005) into an appropriately-sized volumetric flask and made up to volume, with mixing, with freshly deaerated, deionized distilled water. A positive displacement syringe, as opposed to the more commonly used gravity-drained volumetric pipettes, was needed for the accurate dispensation of the undiluted silicate solutions which were viscous and dried rapidly upon exposure to the atmosphere. The dilutions were aged for 10 min or 24 hr as appropriate for the designated experiments regarding rate of reaction and/or iron filterability.

Table 2. Properties of Liquid Silicates Used in Investigations (26)

Product Name	Weight Ratio SiO_2/Na_2O	SiO_2 Content %	Density[a] g/cm^3	pH
S35	3.75	25.3	1.31	11.1
N	3.22	28.7	1.38	11.3
Star	2.50	26.5	1.40	11.9
Starso	1.80	24.1	1.43	12.9

a. at 20 °C

Iron Filterability (<0.1 μm)

In each of these experiments a standard model groundwater was prepared having a pH of 7.0, dissolved oxygen (DO) ~ 0 mg/L, iron as Fe^{2+} at ~ 2 mg/L, and an alkalinity of 150 mg/L as $CaCO_3$ added as $NaHCO_3$. Experimental variables included forms and amounts of silicate added, pH control/no control, mixing regimes at silicate dosing, and the lag between silicate and hypochlorite additions. Silicate doses ranged from 8 to 14 mg SiO_2/L. Experiments were conducted in a constant temperature room at 20-21°C.

Preparation and treatment of the standard model groundwater was as follows: 1. 22 liter of deionized distilled water (turbidity $\leq$ 0.08 NTU, specific conductance $\leq$ 1 μS) were collected in an acid-washed Nalgene carboy modified to have a spigot at the base; 2. this water was chilled to 20-21°C in the constant temperature room for 18-24 hr; 3. the water was sparged with filtered (< 0.45 μm), prepurified nitrogen (99.999% N_2) gas at ~ 3 L/min to reduce the DO to < 0.1 mg/l; 4. dry sodium bicarbonate, dissolved rapidly in a small volume of deaerated water was added to the bulk of the water to provide an alkalinity of 150 mg/L as $CaCO_3$; 5. the pH of the water (8.6-8.7) was then adjusted to pH 7.0 by adding CO_2 to the N_2 continuously sparging the model groundwater; 6. dry ferrous chloride, $FeCl_2 \cdot xH_2O$, was dissolved rapidly in about 100 mL of deaerated water taken from the carboy and then added to the remainder of the model groundwater; 7. the solution was allowed to equilibrate for 15 min while mixing was provided by the vigorous

sparging of the N_2-CO_2 gas mixture with the DO and pH being monitored continously; 8. Samples for the measurement of turbidity were taken; 9. model groundwater was dispensed via the spigot at the base of the elevated reservoir (carboy) into a 2 liter LPE bottle under the same anaerobic N_2-CO_2 atmosphere used for sparging. All sampling and dosing for the 2 liter bottles were conducted under an N_2-CO_2 atmosphere except when there was no pH control; 10. a 10 mL sample was taken from the 2 liter bottle for Fe^{2+} analysis; 11. the solution in the 2 L bottle was dosed with silicate and sodium hypochlorite as follows: a) silicate was added rapidly to quiescent model groundwater; (b) at time, t = 0, i.e., when all of the silicate was added, the solution was mixed vigorously for 15 seconds with the stirrer set at maximum (velocity gradient, $G = 5900\ sec^{-1}$); c) at t = 15 sec, 15 seconds of no active mixing was initiated; d) at t = 30 sec 7 ml of 0.1% sodium hypochlorite solution were added: 3) at t = 40 sec, 45 seconds of vigorous mixing at maximum stirring rate were initiated; 12. post-dosage samples were then drawn for turbidity, total iron and filterable iron analyses. The withdrawal of each sample for iron analysis was preceded by 15 seconds of mixing at maximum stirrer rate; for filterable iron the filtrate from passing sample through a 0.1 μm cellulose Micro Filtration Systems (MFS) membrane was used; 13. pH and DO were then measured on the dosed system and samples taken for the measurement of free chlorine (100 mL) and alkalinity (100 mL); 14. the head space of the dosed bottle was then filled with N_2-CO_2 mixture, the bottle capped and put in the shaker; 15. steps 8 through 14 were repeated for each treatment.

On days 1, 3, 5, 7, and 10, samples were taken routinely for the measurement of turbidity, total iron, and filterable iron. The pH was measured directly on the solution/suspension before and after the mixing associated with the sampling which was as follows: 1. 30 seconds at the maximum mixing setting; 2. 10 seconds at a setting of 4; 3. withdrawal of sample for turbidity analysis; 4. 10 seconds of mixing at a setting of 10; 5. withdrawal of sample for filterable iron; 6. 10 seconds of mixing at 10; 7. withdrawal of sample for total iron analysis; 8. if appropriate, fill bottle headspace with N_2-CO_2 mixture and return bottle to shaker for continued shaking at 1 rpm. Where pH control was maintained, it was effected by performing all mixing and sampling under an N_2-CO_2 mixture appropriate for a pH of 7.0 in the solution/suspension and then filling the headspace with the same N_2-CO_2 mixture for the intervening periods.

Iron Filterability (Ultrafiltration)

Samples for ultrafiltration were prefiltered through a 0.1 μm MFS cellulose nitrate membrane filter to reduce potential clogging problems with the ultrafiltration membranes. The resultant filtrate was then passed through either a 1000 molecular weight (MW) cut off or a 200,000 MW cutoff MFS ultrafiltration membrane. The 1000 MW cut off membrane system was run under a pressure of 55 psig, whereas for the 200,000 MW cut off system a pressure only slightly greater than atmospheric was sufficient to provide adequate filtrate flow. Immediately before ultrafiltration the prefiltered solution to be processed was made 0.1M

in NaCl with dry salt, to reduce polarization effects. The volume of solution for processing was initially ~ 60 mL for each unit; ~ 5 mL were used to rinse the insides of the ultrafiltration unit, the first 5 mL of ultrafiltrate were discarded, the next 25 mL saved for analysis and the remaining retentate discarded. Ultrafiltration membranes were soaked for at least 25 hr in ~ 0.01N H_2SO_4, then for 10-15 min in deionized distilled water and then finally, flushed with deionized distilled water (~10 mL and ~ 90 mL for the 1000 MW cut off and the 2000,000 MW cut off membrances, respectively) prior to sample processing.

Transmission Electron Microscopy

A transmission electron miscroscopy (TEM) investigation of formvar (polyvinylformate)-coated copper grids plated with particulates produced by the silicate-hypochlorite treatment was conducted. The particulates were examined at 100 KV in bright field (BF) and by selected area electron diffraction (SAD) using a Philips Model No. EM300. The camera constant for selected area diffraction pattern (SAD) analysis was calibrated using an aluminum diffraction standard. Identification of crystalline particles was effected using a PDP-11/34 computer (RSX-11M operating system), equipped with software for analyses of particles/phases having known d-spacings. The program DSPACE was employed and required initial inputs including the d-spacing for the sample, the maximum acceptable error in the diffracted (transmitted) radiation angle, minimum intensity of lines, and the data base to be searched for

comparisons. Supplementary inputs included the elements that were required to be in the sample (Fe, O_2, H_2) and optional elements (Si, Na). The output from DSPACE was processed through another program, CARD, which printed out the names and d-spacing of the matched compounds determined by DSPACE.

The deposition of particulates on the forvmar-coated grids was accomplished as follows. The grid was placed in a circular recessed area machined into the transverse face of cylindrical carbon stub (1 x X 0.25 in) retained in place by a thin steel wire wrapped vertically around the stub in a single strand. The stub, with the grid gacing upward, was then placed in a glass centrifuge tube which was then filled with the test fluid (suspension). The tube (along with others similarly prepared) was then centrifuged at 2700 rpm and for 30 min. The grid was then elutriated gently in situ three times with freshly deionized distilled water and then dried at room temperature.

Routine Chemical Analyses

Solution/suspension pH values were measured after equilibration for $\geq$ 1 min, with a combination glass electrode using an Orion Model 407-A Ionanalizer. Turbidities were measured on a Hach 2100A turbidimeter after ~ 1 min equilibration. Total iron was determined on acidified filtered or unfiltered samples by atomic absroption spectrometry at 248.3 nm primarily on a Perkin-Elmer Model 403 and in the final stages of the investigation on an Analytical Laboratories Video 12 spectrophotometer. Ferrous iron was determined by the method of Stumm and

Lee (7) using bathophenonthroline which forms a highly-colored complex with ferrous (Fe^{2+}) but not with ferric (Fe^{3+}) iron. This complex was extracted from the aqueous system into hexanol and the absorption measured at 533 nm. Reactive silica and total silica were determined by the formation of silicomolybdate complex followed by the measurement of absorption at 410 nm (51). For the total silica analysis the color reaction phase was preceded by digestion at ~100°C in the presence of excess bicarbonate. Total silica was also measured using the Video 12 absorption spectrophotometer at 251.6 nm. Alkalinities were determined by potentiometric titration (51). Free chlorine was measured by the N, N - diethyl-p-phenylenediamine (DPD) method (51) as modified by Hach (52) for rapid field determinations. Dissolved oxygen (DO) concentrations were monitored with a Yellow Springs Instrument Company Model 54 meter using a submersible polarographic probe. Samples for iron analysis by atomic absorption spectrophotometry were acidified routinely to < pH 2 with ultrapure concentrated nitric acid as recommended by the USEPA (53).

Statistical Analysis

The experimental iron filterability data were transformed and grouped in accordance with data availability and desired goals, and then examined by multiple linear regression analysis by the Statistical Analysis systems (SAS) (50) general linear models (GLM) package. In the first data grouping which included only those filterability experiments involving dilution of 3.22 ratio silicate, the dependent variable was t_{50}, the time taken for the filterability to decrease to 50%, and

the independent variables were silica dose, and the silicate reactivity coefficients K_1 and P_0. For both of the other two data groupings, the dependent variable was % iron filterability and the independent variables time, silica dose, K_1 and P_0. However, while one grouping included only undiluted silicate treatments for all of the four silicate types used, the other grouping was restricted to data from experiments with the various dilutions of the 3.22 ratio silicate.

The objective of the statistical analysis was to develop, in each instance, an equation (model) that would be a good predictor of the dependent variable. Interpretation of the statistical significance of the various independent variables in such equations was then used to generate a mechanism for treatment effectiveness.

IV. RESULTS AND DISCUSSION

The broad objective of this investigation was to establish the factors controlling the ability of various types of sodium silicates at different dilution levels to sequester aqueous ferric iron, generated in situ. Treatment effectiveness was judged primarily by the resultant iron filterability through a 0.1 μm membrane filter although turbidity and total iron were also instructive. In addition, for a few selected instances the iron filterability was evaluated further by means of ultrafiltration. Furthermore, to assist in understanding the mechanisms controlling their performance, the various silicate solutions were also characterized in terms of their reactivity coefficients with molybdic acid.

In the discussion to follow, the silicate characterization data are presented first. These are followed by the analysis of data for the iron filterability and associated parameters. This format facilitated the logical incorporation of silicate characteristics into the discussion of associated iron filterability patterns.

Silicate Characterization

Four types of commercial sodium silicate solutions were examined. These silicates were identifiable by their individual SiO_2/Na_2O ratios, i.e., 3.75, 3.22, 2.50, and 1.80. The corresponding product names and other relevant properties are presented in Table 2. Clearly, these dense, viscous, concentrated, alkaline "solutions" would require special care in handling if used in the undiluted form. Of special importance

was the fact that higher SiO_2/Na_2O ratio silicates show higher levels of silica polymerization (21). Earlier evidence suggested that silicate dilution (6, 48) and silicate SiO_2/Na_2O ratios (42) likely played a significant role in the effectiveness of silicates in maintaining iron filterability (6, 48) or dispersing iron oxide sols (42). As a result, at the outset of this investigation, the level of silica polymerization in the feed silicate solutions was hypothesized as the key element in treatment success. The level of silica polymerization was varied by two methods: (1) by using different types of sodium silicates to provide a range of SiO_2/Na_2O ratios as given in Table 2, and (2) by varying the silicate concentration of the feed stock (or dilution of the original concentrate) used for dosing, viz., undiluted concentrate, and 1/10, 1/50, 1/100, and 1/500 dilutions of the concentrate. If the chemical nature of the silica in these different silicate solutions could be readily determined, then the mechanism by which they effect iron sequestration could be ascertained with more certainty.

Characterization of the silicate solutions was based on the analysis of the rate of color development (absorbance) at 400 nm produced by the reaction of the silicate solution with molybdic acid (31), in accordance with equation 27 discussed earlier. Typical absorbance data necessary for the mathematical analysis are provided in Figure 3 and Tables A1 - A4, for undiluted silicates with SiO_2/Na_2O ratios, hereinafter also referred to as m-ratios, of 3.75, 3.22, 2.50, and 1.80, respectively. It was clear from the figure that these silicates, although dosed at similar final in-beaker concentrations of 17 to 20 mg

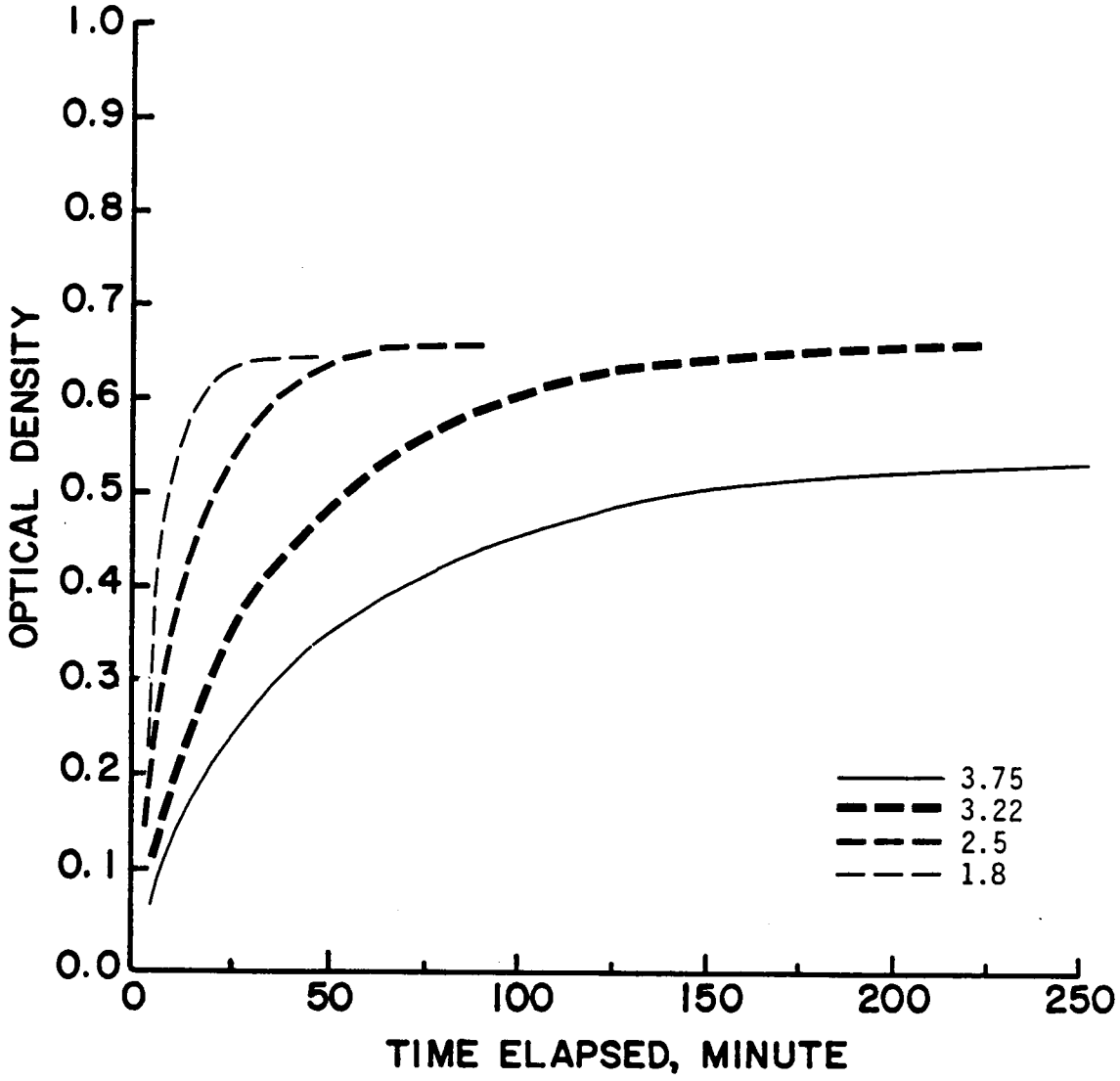


Figure 3. Optical Density vs. Time for the Reaction of Molybdic Acid with Undiluted 1.8, 2.5, 3.22, and 3.75 Ratio Sodium Silicates at 25-26°C.

SiO_2/L, each exhibited its own distinct pattern of color development with time. The rate of approach to maximum optical density decreased with increasing m-ratios. Because molybdic acid reacts only with the monomeric silica, this pattern was indicative of the increasing silica polymerization with increasing m-ratios (31). Higher polymers depolymerize more slowly than the lower ones.

Transformation of the raw optical density data to give the pattern of change of percent unreacted silica with time was done by use of the formula (31):

$$\% \text{ unreacted } SiO_2 = 100\ (OD_T - OD_t)/OD_T \qquad 40$$

where

OD_t = optical density at time t

OD_T = maximum optical density for total silicate as β-silicomolybdate.

These data for the undiluted silicates with m-ratios of 3.75, 3.22, 2.50 and 1.80 are included in Tables A1 - A4, respectively, and plotted in Figure 4. Predictably, the rate of decrease of the percentage of unreacted silica was most rapid and slowest for the silicates with m-ratios 1.80 and 3.75, respectively. The development of characteristic coefficients from the data in Figure 4 was done in accordance with the equation (31):

$$\% \text{ color developed} = \left[\frac{0.435K_1}{K_0 - K_1} - 0.565\right] P_0 e^{-K_1 t} + 0.435 \left[100 - P_0 \left(1 + \frac{K_1}{K_0 - K_1}\right)\right] e^{-K_0 t} + 56.5 \qquad 27$$

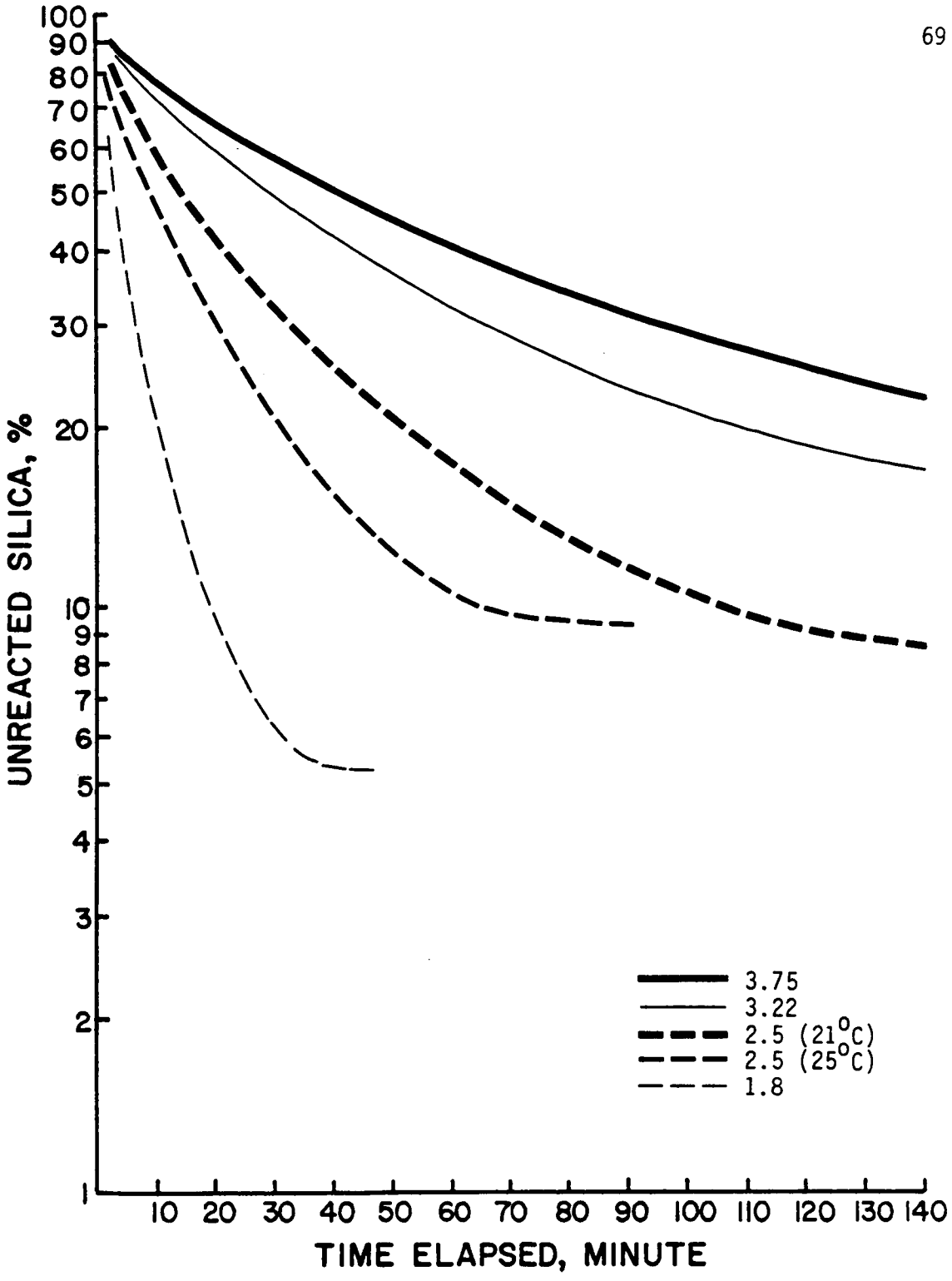


Figure 4. Percent Unreacted Silica vs. Time for the Reaction of Molybdic Acid with Undiluted 1.8, 2.5, 3.22, and 3.75 Ratio Sodium Silicates at 25-26°C and 2.5 Ratio at 21°C.

where

K_1 = the rate constant for the formation of β-silicomolybdate complex from depolymerization of polysilicate,

P_0 = the initial level of polysilicate,

K_0 = the rate constant for the spontaneous conversion of β-silicomolybdate to the less color absorbent α-silicomolybdate complex.

The percentage of unreacted silica is given by:

$$\% \text{ unreacted silica} = 100 - \% \text{ color developed} \qquad 41$$

Equations 40 and 41 only approximate the amount of silica remaining unreacted or uncomplexed because of the continuous conversion of β- to α-silicomolybdate complex, which has a lower extinction coefficient, as discussed earlier (31). Nonetheless, valid vaues for K_1 and P_0 were derived from the system of analysis used, because of the inclusion of K_0 in equation 27 to correct for the conversion of β- to α-silicomolybdate. The derived reaction coefficients are presented in Table 3 for the reaction of the undiluted silicates with molybdic acid at 25-26°C. By the technique used, K_1 was indicative of the complexity of the major silica fraction present and P_0 indicative of the fraction of the total silica represented by this polymer.

For the silicates tested the magnitude of K_1 increased as the m-ratio decreased. Thus, K_1 increased progressively from 0.012 to 0.133 min^{-1} as the corresponding m-ratios decreased from 3.75 to 1.80 (Table 3). These results were consistent with earlier findings of Iler

Table 3. Reaction Coefficients Derived from the Reaction of Undiluted Sodium Silicates with Molybdic Acid with Time at 400 nm and 25-26°C[a]

SiO_2/Na_2O ratio	K_1 min^{-1}	P_0 %
3.75	0.012	87.0
3.22	0.016	85.7
2.50	0.045	81.1
1.80	0.133	81.2

a. $K_0 = 0.00117\ min^{-1}$ for 25°C (31)

(21). It was reasoned that the rate-limiting step in the color development for the reaction of complex silicates with molybdic acid was the depolymerization of the complex silicates to monosilicic acid (31). Furthermore, the more complex silicates with more multiple bonding would depolymerize more slowly than the simpler silicates (31). The data also showed a positive correlation between the P_0 and m-ratio values, although the values for the 2.50 and 1.80 ratios silicates were effectively identical. Also included in Figure 4 is a plot for undiluted silicate with m-ratio = 2.50 at 21°C. The corresponding optical density data are given in Table A5. As might be expected a comparison of the traces for the 2.5 ratio silicate at the two temperatures, i.e., 21 and 25°C, showed a faster reaction, i.e., a more rapid decrease, at the higher temperature. Because the filterability experiments were conducted at 20-21°C, it was decided to collect most of the silicate-molybdic acid reactivity data at 21°C. Silicate reactivity data collected at both temperatures would be useable with validity, provided the data from each temperature group are applied separately.

Reactivity data were also obtained for the silicate with m-ratio = 3.22 in greater detail. This silicate, also called N silicate (Table 2) is the most commonly used commercial liquid silicate. Moreover, it is the only silicate, so far, that has been reported as being applied to the sequestration of iron in water treatment (5, 6, 26). Thus, N silicate was tested in undiluted form, and as 1/10, 1/50, 1/100 and 1/500 dilutions as well.

For any given dilution of concentrated silicate, determinants of the distribution of silicate moieties include the manner of dilution and the age of the resultant system. The greater the time of aging the more likely that the distribution of silicate species will be in accordance with an equilibrium system as represented by Figure 2. After some preliminary testing with solutions aged for 10 minutes and for 24 hours, it was decided to utilize solutions aged for 24 hours, primarily because it was considered to be in better agreement with the likely field application conditions. The silicate dilutions were prepared by diluting the appropriate aliquot of undiluted silicate to the appropriate volume with mixing, within a few minutes.

Raw and transformed optical density data for the reaction of undiluted and four dilutions of 3.22 m-ratio silicates with molybdic acid, at 21°C are presented in Tables A6 to A10. The corresponding semilog plots of percent unreacted silica vs. time, and the derived reactivity coefficents are presented in Figure 5 and Table 4, respectively. The patterns for the various dilutions were readily distinguishable from each other. A qualitative assessment of these patterns, shown in Figure 5, suggested that as the feed solutions became more diluted the initial decrease in percent unreacted silica was more rapid, as was the transition to a flatter plateau. The plot for the undiluted silicate is truncated at 140 minutes for the convenience of uniform presentation in the figure; it actually continues decreasing until 340 minutes have elapsed, down to about 9% (Table A6). In the examination of Figure 5, the reader is reminded that the Y-axis is on a logarithmic

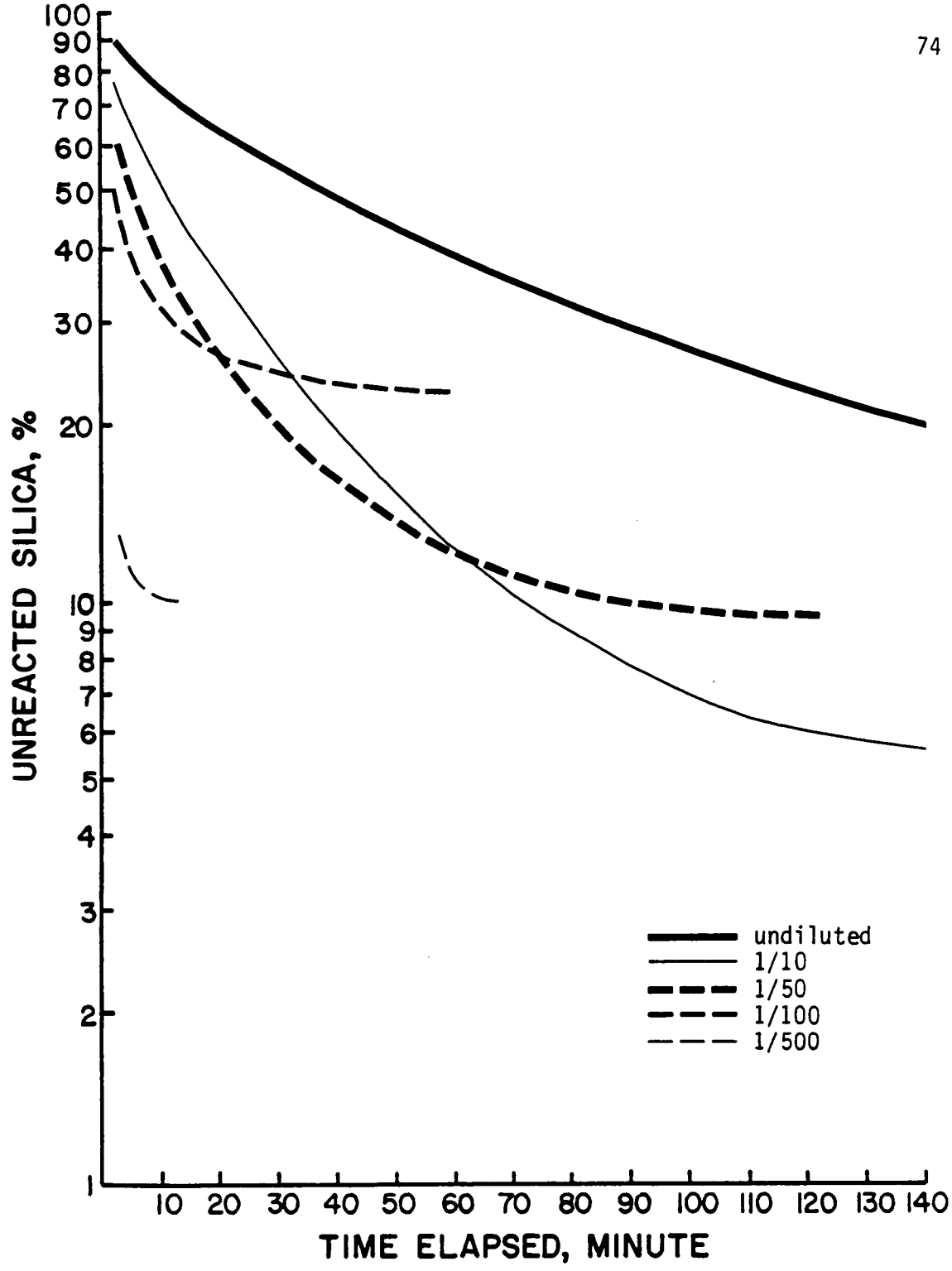


Figure 5. Percent Unreacted Silica vs. Time for the Reaction of Molybdic Acid with Undiluted, and 1/10, 1/50, 1/100, and 1/500 Dilutions of 3.22 Ratio Sodium Silicate at 20-21°C.

Table 4. Reaction Coefficients for Dilutions of 3.22 Ratio Sodium Silicate at ~21°C, and ~14 mg SiO_2/L

Dilution	SiO_2 %	K_0 used $min^{-1}x10^4$	K_1 $min^{-1}x10^2$	P_0 %
undiluted	28.7	2.77	1.19 (±3.4%)[a]	86.5 (±1.2%)
		3.02	1.19 (±3.3%)	86.6 (±1.2%)
1/10	2.87	2.77	3.78 (±3.3%)	80.4 (±1.5%)
		3.02	3.79 (±3.2%)	80.4 (±1.5%)
1/50	.574	2.77	3.63 (±6.4%)	59.6 (±2.9%)
		3.02	3.64 (±6.3%)	59.6 (±2.9%)
1/100	.287	2.77	1.20 (±12.7%)	39.5 (±3.05%)
		3.02	1.20 (±12.7%)	39.5 (±3.06%)
1/500	.0574	2.77	2.58 (±17.2%)	13.6 (±3.8%)
		3.02	2.59 (±17.2%)	13.6 (±3.8%)

a. Number in parentheses is standard deviation as a % of the estimate

scale and as such, except for the 1/100 dilution, the silica concentrations at which the individual traces plateau are not markedly different from each other. The anomalous behavior of the 1/100 dilutions is unexplained at this time. A quantitative assessment of these curves is represented by the values presented in Table 4. The trends in these values are better illustrated in Figure 6. The P_0 values showed a significant positive correlation with the concentration of silicate in the feed solution. This pattern was very similar to that obtained by O'Connor (31). Notably, the undiluted, and 1/10, 1/50, 1/100 and 1/500 dilutions of the 3.22 ratio silicate provided % SiO_2 concentrations of 28.7, 2.87, 0.574, 0.287, and 0.0574, respectively, and corresponding P_0 values of 86.6, 80.4, 59.6, 39.5, and 13.6%, respectively. O'Connor used 3.3 ratio silicate and obtained P_0 values of 65 to 90% for solutions with silica concentrations of 2 to 30%, respectively. These results all suggested that as the solutions were made more dilute there was an associated decrease in the proportion of silica in a polymeric form (as indicated by P_0 values).

In contrast, the relationship between derived K_1 values and the SiO_2 concentration was not nearly as clear. Figure 6 showed a distinctly parabolic relationship between K_1 and log %SiO_2 values with a maximum occurring at about 1.8% SiO_2. This concentration corresponded to about a 60/100 dilution of the 3.22 ratio silicate. O'Connor observed a monotonic increase in K_1 values as the 3.3 ratio silicate was diluted from 30 to 2% SiO_2. This pattern corresponded well with the results presented here for 3.22 ratio silicate for similar silica

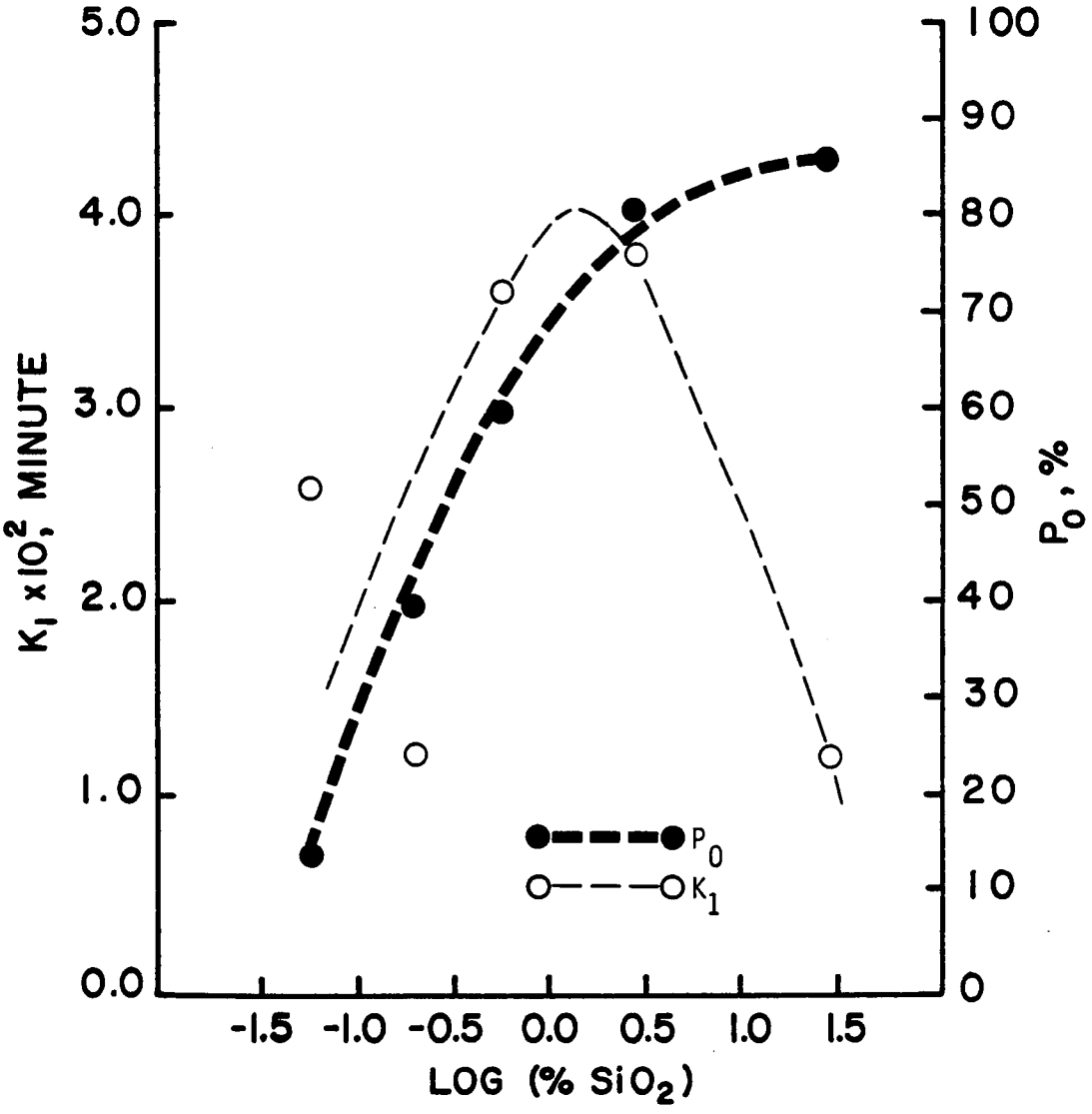


Figure 6. Silicate Reactivity Coefficients Derived from the Reaction of Molybdic Acid with Dilutions of 3.22 Ratio Sodium Silicate at 21°C.

concentrations. However, for the current investigation three of the test concentrations (corresponding to 1/50, 1/100, and 1/500 dilutions), occurred significantly below the lowest concentration tested by O'Connor (31).

Currently, it is unclear as to the extent to which the decrease in K_1 at greater dilutions (lower concentrations) is real or due to artifacts attributable to our method of curve analysis. It was observed that as the traces (Figure 5) showed increasing curvature with increasing dilution, the NLIN curve-fitting program (50) experienced greater difficulty in regenerating (predicting) the early limb of the individual curves. This inadequacy produced increasing errors in the derived parameter values (Table 4), and probably also greater inaccuracies in K_1 as well. Nonetheless, these values for K_1 and P_0 will be used in the interpretation of the iron filterability data, with due allowance for error. Although the other silicates with m-ratios 3.75, 2.5, and 1.8, were not examined in as great detail, it is logical to expect that similar patterns of P_0 and perhaps K_1 would prevail for the same combination of dilutions.

Thus, on the basis of the silicate-molybdic acid reactivity analyses, the following conclusions will be carried forward to the next section on iron filterability: (1) higher ratio silicates exhibit a higher level of silica polymerization as reflected in K_1 and P_0 values; (2) for a given ratio silicate, greater dilutions produce lower levels of silica polymerization in the resultant "solutions". These ideas will be examined quantitatively for the various silicate systems, in accordance with the data at hand.

Iron Filterability

The primary objective of this investigation was to examine the fundamentals of the treatment process with a focus on the role of silica polymerization in selected stock silicate "solutions" in effecting the stabilization of aqueous iron. In the standardized test system, ferrous iron at 2 mg/L, present in a water with alkalinity at 150 mg/L as $CaCO_3$ added as $NaHCO_3$, was treated by sodium hypochlorite and sodium silicate to sequester the iron. Because at pH levels near or above neutrality hypochlorite oxidizes ferrous iron almost instantaneously (54), it was assumed that upon addition of excess hypochlorite, under the prevailing experimental conditions here, the iron present initially as ferrous was converted rapidly and completely to ferric iron.

Testing the various hypotheses for this investigation required that, initially, essentially all of the iron present be in the ferrous form. For example, to determine the importance of the sequencing of oxidation of the ferrous iron and the introduction of the sodium silicate, all of the iron needed to be in the ferrous form initially. Furthermore, if it were found (as was in fact the case) that the silicate needed to be added before iron oxidation, then it would always be necessary that the iron be completely in the ferrous form, for good treatment effectiveness by the silicate application technique.

Accordingly, testing for ferrous iron at the time of treatment was a critical part of this investigation. The results of ferrous iron testing are presented in Table 5. These values represented averages for samples taken either (1) before and after all treatments as a

Table 5. Fraction of Total Iron Present as Ferrous Iron at the Start of Individual Treatments within Various Experiments

Experiment No.	Description	Fraction of total iron present as ferrous: Average %	Coefficient of Variation %
II	Lag-time	96[a]	1.2
III	No pH control testing	99	1.6
V	pH control/no control testing	95	0.85
VI	Silica dose optimization	96	1.5
X	Dilution effects 3.22 and 3.75 silicates	94	2.0
XI	Dilution effects 3.75 and 2.5 silicates	94	1.6
XII	Dilution effects 2.5 and 1.5 silicates	96	2.0
XIII	Ultrafiltration	99	0.76

a. For this experiment three samples were taken before the application of the first treatment and three more at the application of the last treatment.

group, as was the case for the lag-time experiments or (2) immediately after the transfer of water for each bottle (treatment), as for the remainder of the experiments. Thus, one way or the other, there was at least one ferrous iron value for each test treatment (2 liter bottle). The average fractions of the total iron as ferrous iron ranged from 94 to 99%, and the coefficient of variation, a measure of the variability among individual values, ranged from 0.76 to 2.0% (Table 5). These results verify that, for all of the experiments in this investigation, the iron was present substantially in the ferrous form for the initiation of each of the applied treatments.

For the development of a standardized testing system that would best reveal differences in the effectiveness of the primary target comparisons, some preliminary testing was done. Accordingly, early testing examined of the effect of (1) experimental mixing/dosing conditions, and (2) control of the pre-and post-treatment pH levels.

In general, for this investigation the primary indicator of treatment success was the level of iron filterability (<0.1 μm) achieved, higher filterabilities being preferable. Measurements of the other routinely measured parameters--turbidity, pH, and total iron, provided corroborative evidence/explanations or the controls necessary for the interpretation of the observed iron filterability patterns with time.

In the presentation of the data for each of the iron filterability experiments, the full details are provided in tabular form. This is in contrast with the corresponding figures in which only selected representative data are plotted where the inclusion of all of the data would produce a crowded confusing picture.

Lag-Time Effects

The effects of the lag-time, i.e., the time elapsed between the sodium silicate and sodium hypochlorite additions, were investigated by varying this experimental condition all the way from adding the hypochlorite two minutes ahead of the silicate, to adding the hypochlorite 2½ minutes after the silicate addition. The results are presented for iron filterability, turbidity, pH, and total iron in Figures 7,8,9, and 10, respectively, and also in Table 6. In each instance the silicate was added in undiluted form and the pH was uncontrolled.

Figure 7 showed that the optimal treatment sequence was--addition of silicate ahead of hypochlorite with a lag-time of 15 to 150 seconds--,as evidenced by the associated iron filterabilities of 95 to 100%. In sharp contrast, where the hypochlorite was added before the silicate, the iron filterability was essentially zero from the time of initial combination of reactants. Adding the silicate and hypochlorite simultaneously was less than optimal, and that occurrence was readily explained by an examination of the prevailing mixing conditions. The volume of undiluted viscous sodium silicate needed to provide the desired dosage was a very small, ~0.05 mL, as contrasted with the ~7 mL of 0.1% sodium hypochlorite solution, and both were combined into a treatment volume of 2L. Consequently, for the simultaneous addition of hypochlorite and silicate, the hypochlorite, i.e., the oxidant, was effectively mixed in before the silicate. The resultant reduced iron filterability was consistent with the finding for the other instance where hypochlorite was added before the silicate.

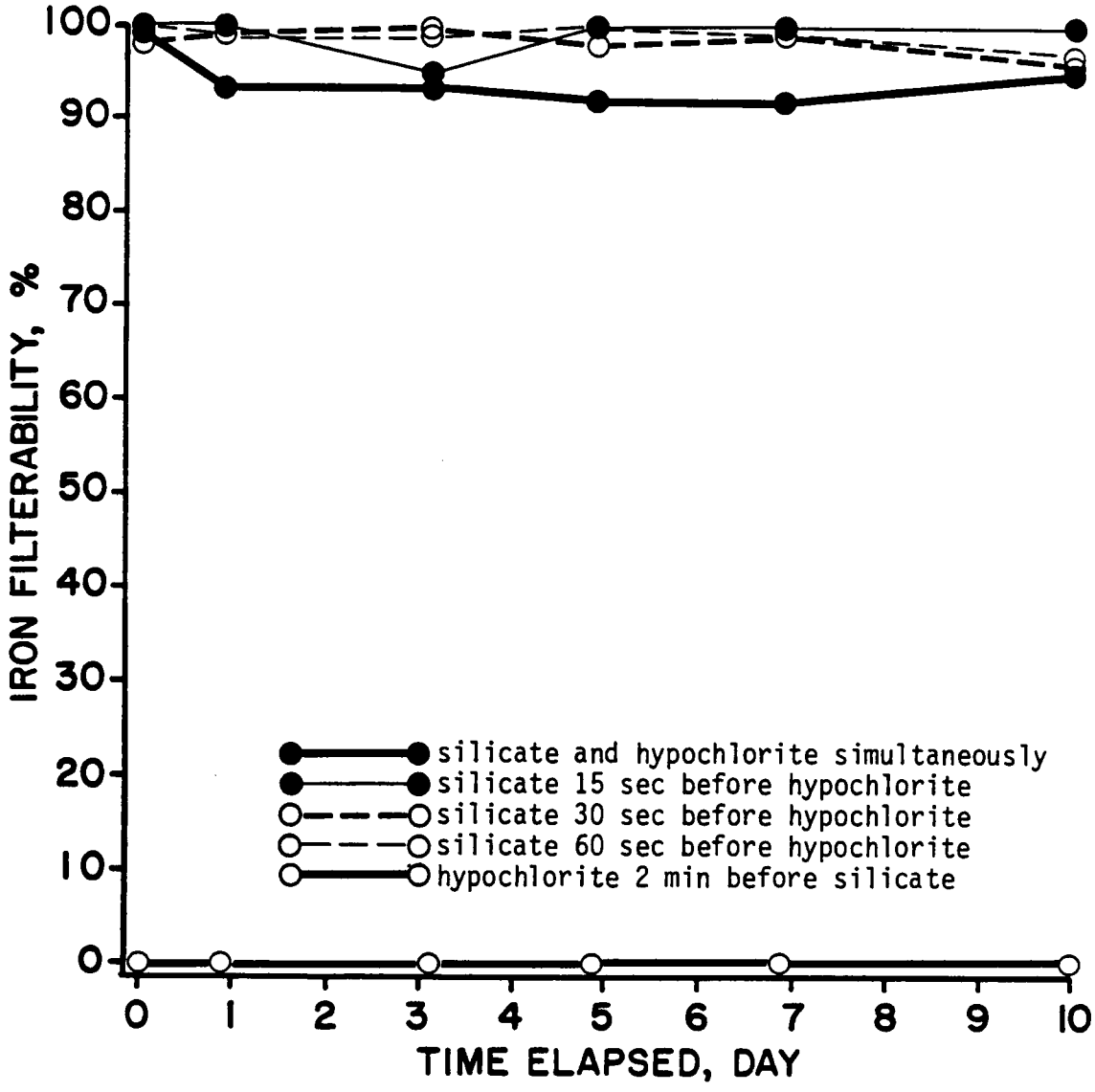


Figure 7. Lag-Time Effects for Undiluted 3.22 Ratio Sodium Silicate: Iron Filterability.

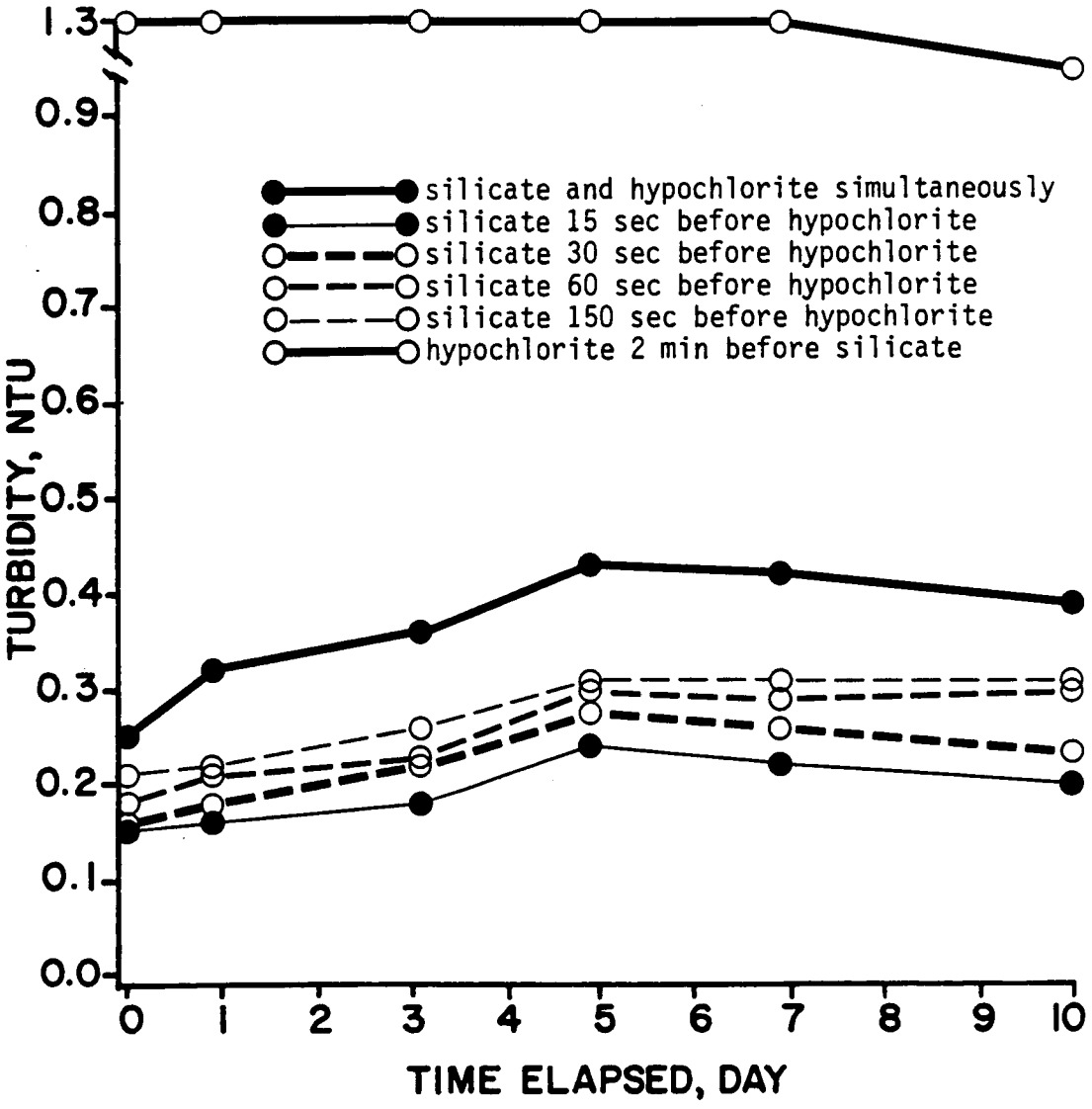


Figure 8. Lag-Time Effects for Undiluted 3.22 Ratio Sodium Silicate: Turbidity.

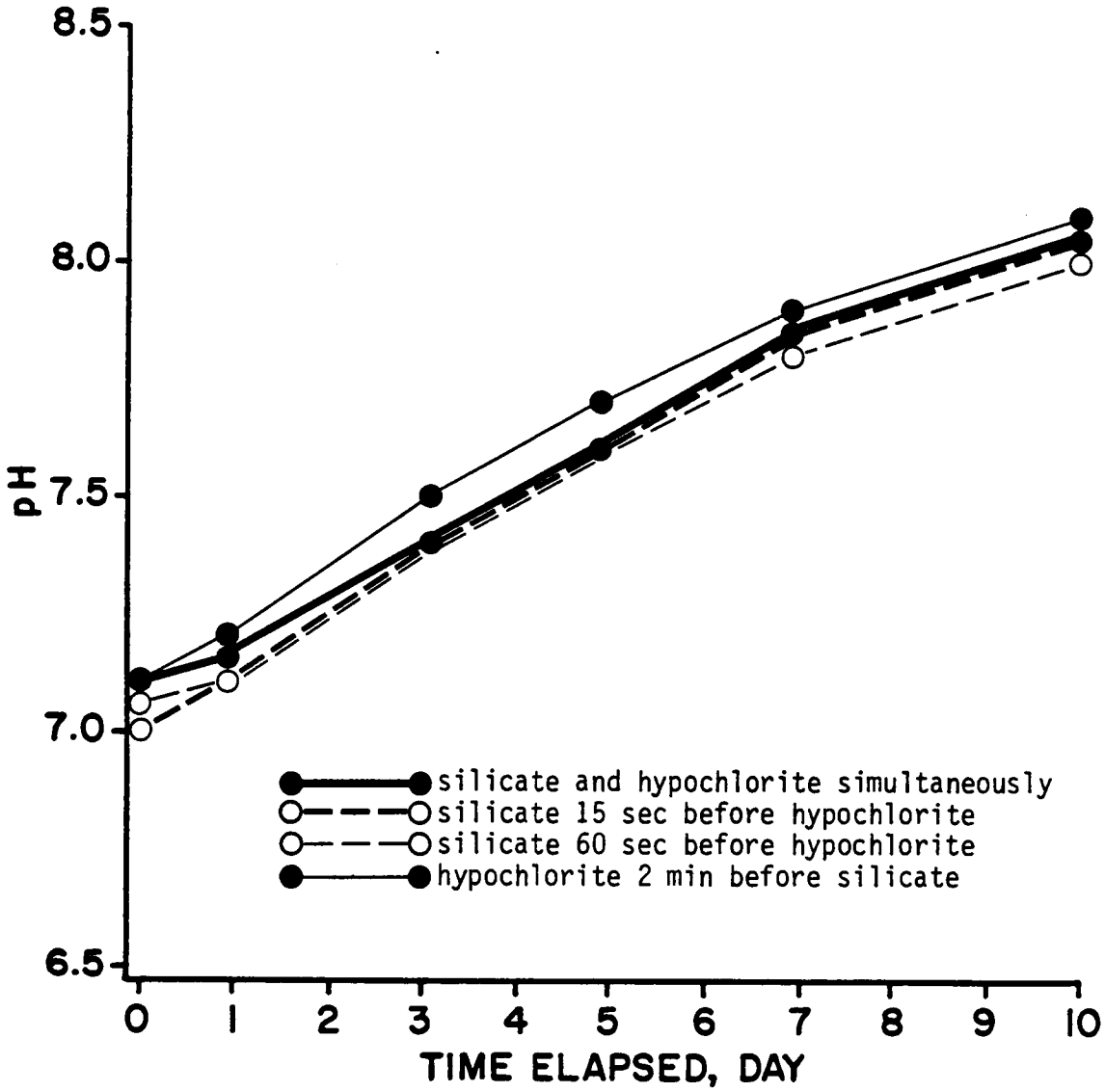


Figure 9. Lag-Time Effects for Undiluted 3.22 Ratio Sodium Silicate: pH.

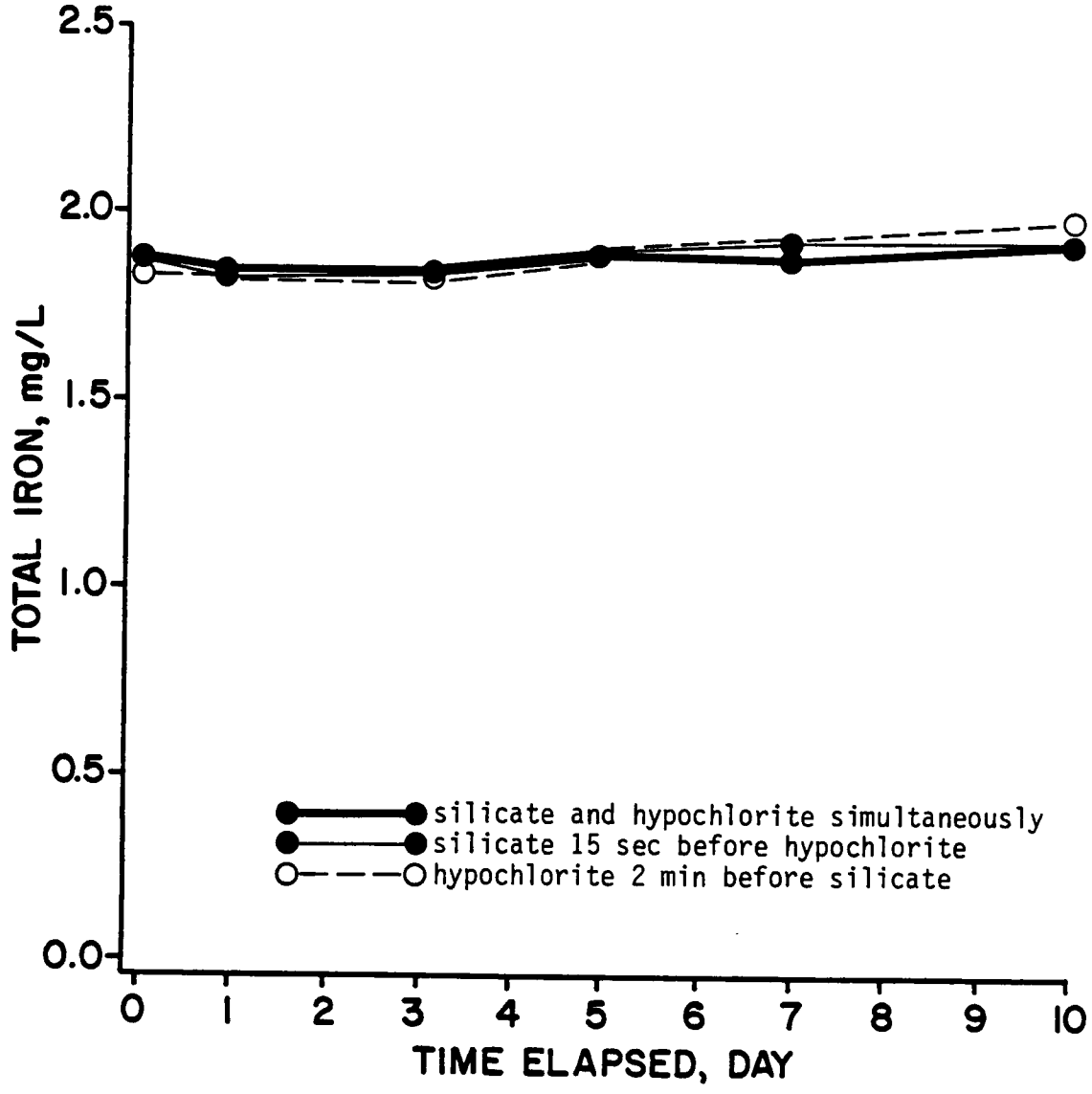


Figure 10. Lag-Time Effects for Undiluted 3.22 Ratio Sodium Silicate: Total Iron.

Table 6. Data on Lag-Time Effects for 3.22 Ratio Sodium Silicate at 9-10 SiO_2/L with No pH Control

	Silicate			Day																							
				0				0.9				3.1				4.9				6.9				10.0			
Jar No.	SiO_2/Na_2O Ratio[2]	Dose[a]	Dilution	Turb[b]	Tot Fe[c]	Filt[d]	pH	Turb	Tot Fe	Filt	pH	Turb	Tot Fe	Filt	pH	Turb	Tot Fe	Filt	pH	Turb	Tot Fe	Filt	pH	Turb	Tot Fe	Filt	pH
1[e]	3.22	9.8	Undil.	0.25	1.88	99	7.1	0.32	1.86	93	7.15	0.36	1.86	93	7.4	0.43	1.90	92	7.6	0.42	1.89	92	7.85	0.39	1.94	95	8.05
3	3.22	9.4	Undil.	0.15	1.88	100	7.0	0.16	1.84	100	7.1	0.18	1.86	95	7.4	0.24	1.90	100	7.6	0.22	1.94	100	7.85	0.20	1.94	100	8.05+
5	3.22	10.0	Undil.	0.16	1.88	98	7.05	0.18	1.86	99	7.1	0.22	1.84	100	7.4	0.275	1.90	88	7.6	0.26	1.92	99	7.8	0.235	1.97	96	8.0
6	3.22	8.9	Undil.	0.18	1.88	100	7.05	0.21	1.88	99	7.1	0.23	1.80	98	7.4	0.30	1.90	100	7.6	0.29	1.94	99	7.8	0.30+	1.94	97	8.0
7	3.22	10.0	Undil.	0.21	1.88	98	7.05	0.22	1.86	99	7.1+	0.26	1.84	97	7.45	0.31	1.93	96	7.7	0.31	1.94	100	7.9	0.31-	1.92	98	8.1
8	3.22	10.0	Undil.	0.28	1.86	92	7.1	0.26	1.86	95	7.1+	0.41	1.89	91	7.4	0.46	1.90	92	7.6	0.46	1.94	92	7.8	0.485	1.99	93	8.0
9[f]	3.22	10.3	Undil.	1.3	1.84	0	7.1	1.3	1.84	0	7.2	1.3	1.84	0	7.5	1.3	1.90	0	7.7	1.3	1.94	0	7.9	1.25	2.00	0	8.1

a. Reported as mg SiO_2/L

b. Turbidity, NTU

c. Total iron, mg Fe/L

d. Iron filterability, %

e. 1, 3, 5, 6, 7, 8 corresponds to lag-times of silicate 0, 15, 30, 60, 150, and 0 seconds, respectively, ahead of hypochlorite

f. Hypochlorite added 120 seconds as ahead of silicate

The implications of the results from the iron filterability tests were corroborated by the result for the turbidity studies (Figure 8, Table 6). For consistent experimental conditions, higher turbidities were associated, broadly, with lower filterabilities. Accordingly, based on turbidities, the optimal treatment sequence was----addition of silicate ahead of hypochlorite with a lag of 15 of 150 seconds. The higher turbidities for the simultaneous silicate and hypochlorite addition (>0.30 NTU) and for the addition of hypochlorite ahead of the silicate (1.3 NTU) were consistent with the lower iron filterabilities.

Figure 9 showed that over the duration of the experiment there was a progressive increase in pH from ~7.0 to ~8.0, and also that there were no significant differences in pH among the various treatments. The increase in pH with time was attributable to the gradual equilibration of the treatment systems, for which the alkalinity is due in major part to "carbonate", with atmospheric carbon dioxide (CO_2). The biggest difference in hydrogen ion concentration amoung the treatments occurred initially, where the pH values ranged from 7.0 to 7.1. The similarities in pH values and in trends among the treatments indicated that the observed differences in iron filterabilities were not pH effects. Similarly, the constancy of total iron values among treatments and over the duration of the experiment (Figure 10, Table 6), eliminated variability of total iron concentrations as a determinant of the observed variability in iron filterability values among treatments.

These results from the lag-time experiment demonstrated the inability or at least the reduced ability of silicate to intervene in the growth of ferric hydrolysis product particles unless the silicate was

already present when the ferric iron was formed. These conclusions agree in large part with the findings of Dart and Foley (5). For successful iron sequestration, they found that the optimal application of silicate always proved to be near-simultaneous with chlorination (oxidation), and that lower efficiencies commenced at plus or minus 15 seconds from the time of iron oxidation. However, these results were in sharp contrast with those of Henry (46) who obtained best iron stabilization when chlorination was applied before the sodium silicate treatment. Henry (46) also found that polyphosphate needed to be applied ahead of chlorination for satisfactory iron stabilization. There was no obvious explanation for these differences. However, it may have been due to (1) the presence of extraneous constituents in the natural waters tested, or to (2) peculiarities of his test system which used sedimentation out of the top two inches of water, rather than filtration, to examine for iron sequestration.

pH Control/No Control Effects with Silicate Dilutions

The pH of the system has been found to play a significant role in the success of the treatment. Thus, reduced silica dosages for satisfactory treatment have been observed at higher pH levels (>7.5) (5). Also, pH controls the speciation of treatment chemicals as well as being a critical design parameter for many chemical treatment systems. For these reasons, pH was selected as a test variable in this investigation. Furthermore, to broaden the applicability of the pH testing, silicate dosage, and dilution in the stock feed solution were also included as associated experimental variables.

Attempts to establish useful experimental conditions led initially to the examination of several variables including pH, dilution of silicate in stock feed solutions and mixing conditions. For both the controlled and uncontrolled pH systems, the initial pH was 7.0. However, for the uncontrolled system with the equilibration of with atmospheric CO_2, as favored by the periodic mechanical mixing at sampling, the pH gradually drifted upwards. In contrast, for the controlled pH system the pH was returned to 7.0 at each sampling, as described in the Methods and Materials section. Figures 11,12,13, and 14, and Table 7, show the effect of stock feed solution dilution on iron filterability, total iron, turbidity and pH, in the absence of pH control. Iron filterability was essentially 100% for the undiluted silicate and the low dilution (1/10 and 1/50) stock feed solutions. The 1/500 dilution system was unfilterable from the earliest measurements at time zero. The 1/100 dilution system was initially filterable (80%) but this value decreased within the first day to zero. However, the 1/100 dilution was applied at a dosage of ~4.9 mg SiO_2/L, while the remaining dilutions were applied each at about 10 mg SiO_2/L. The pH results (Figure 12) showed a general upward trend with time, attributable, as before, to a gradual equilibration with atmospheric CO_2. The values were bracketed by the "plots" for the 1/10 and 1/50 dilution systems on the low side and by the undiluted system on the high side. The 1/100 and 1/500 dilution systems exhibited intermediate pH values that were quite similar to those of the undiluted silicate system. Differences in system pH values among treatments did not explain (contribute significantly to) the observed differences in filterability. Higher pH levels favored

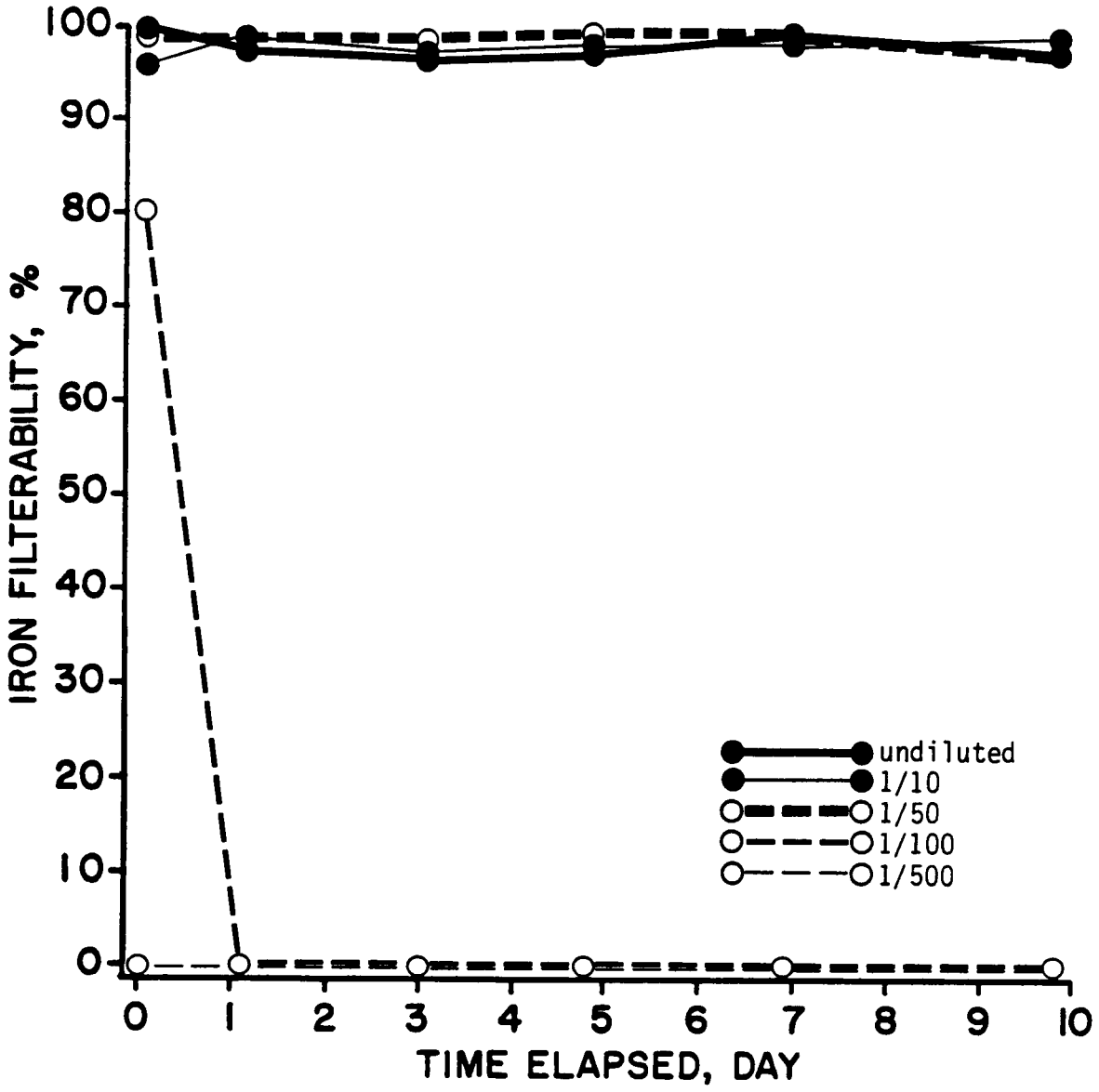


Figure 11. Dilution Effects for 3.22 Ratio Sodium Silicate at ~10.5 mg SiO_2/L--No pH Control: Iron Filterability.

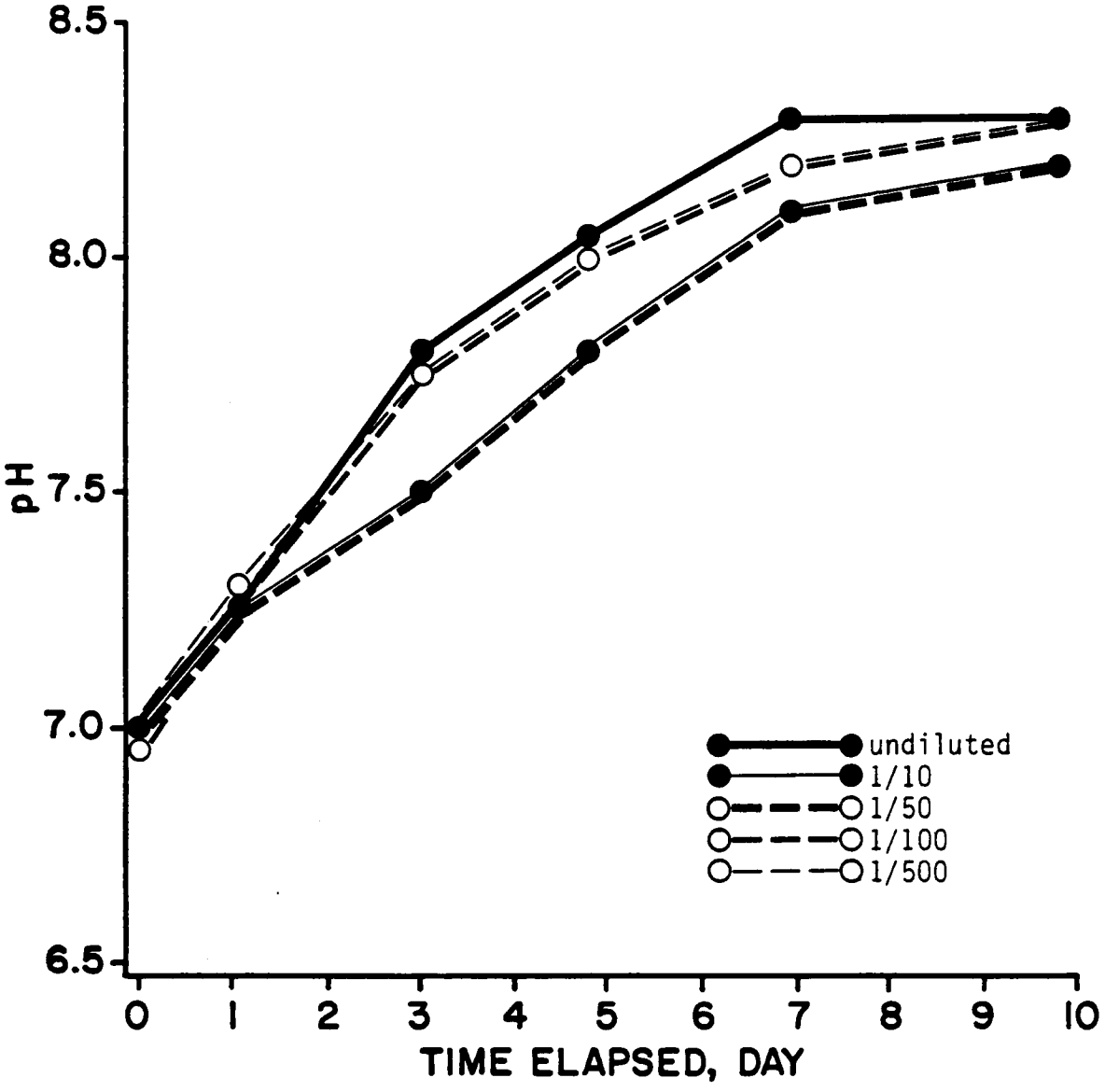


Figure 12. Dilution Effects for 3.22 Ratio Sodium Silicate at ~10.5 mg SiO_2/L--No pH Control: pH.

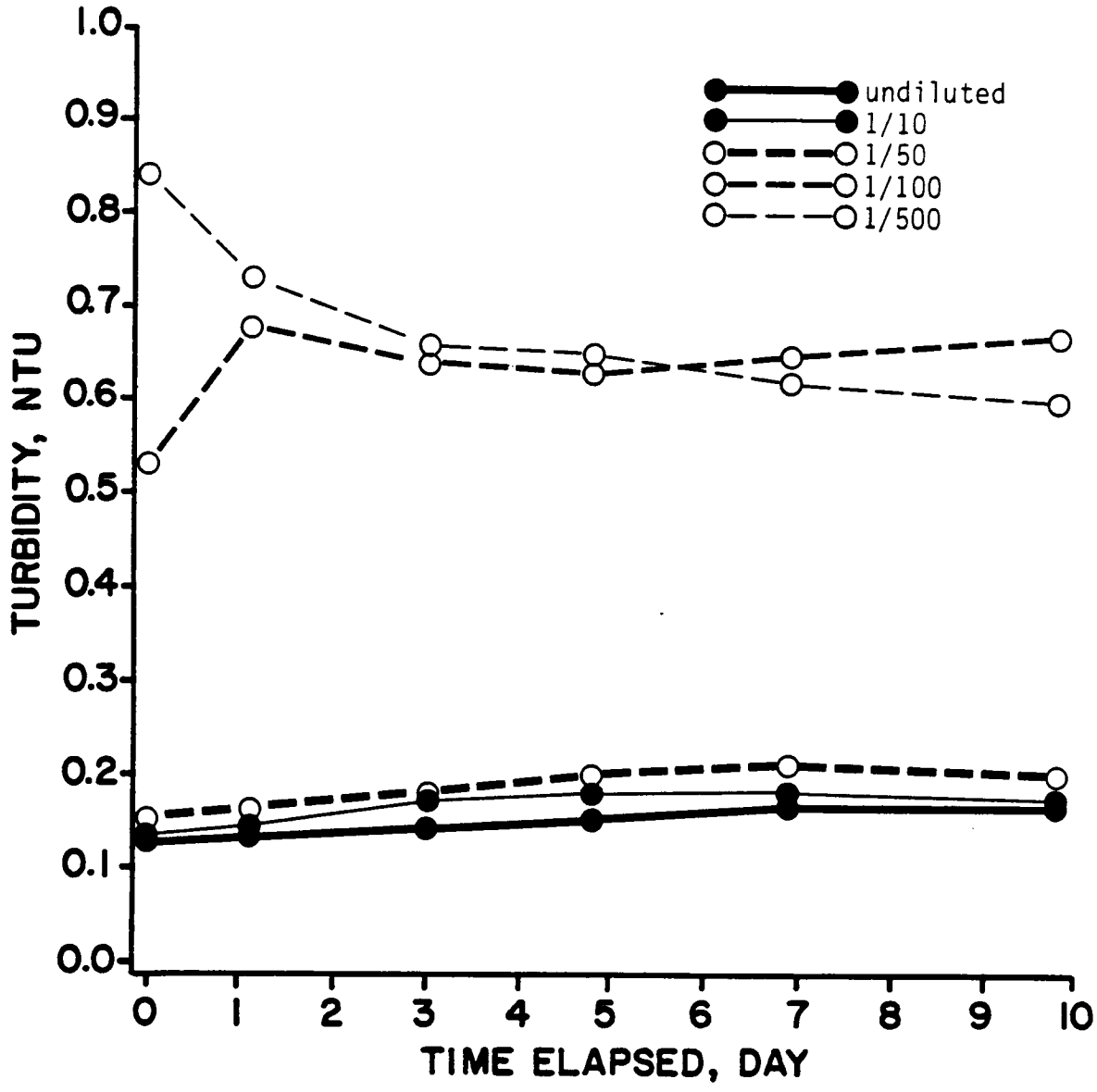


Figure 13. Dilution Effects for 3.22 Ratio Sodium Silicate at ~10.5 mg SiO_2/L--No pH Control: Turbidity.

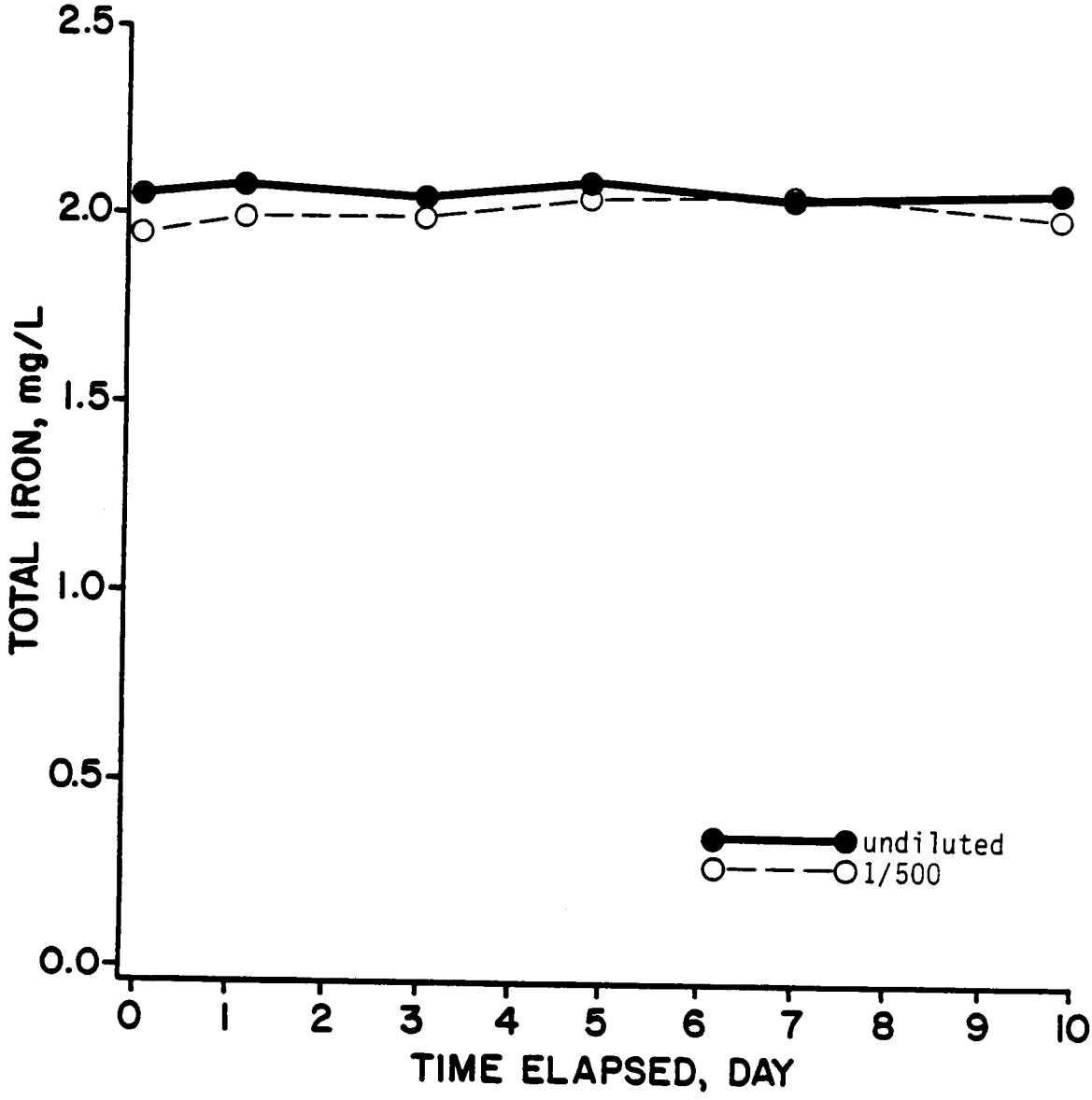


Figure 14. Dilution Effects for 3.22 Ratio Sodium Silicate at ~10.5 mg SiO_2/L--No pH Control: Total Iron.

Table 7. Data on Dilution Effects for 3.22 Ratio Sodium Silicate at ~ 10.5 mg SiO_2/L with No pH Control

	Silicate			Day																			
				0				1.1				3.0				4.8				6.9				9.8			
Jar No.	SiO_2/Na_2O Ratio	Dose[a]	Dilution	Turb[b]	Tot Fe[c]	Filt[d]	pH	Turb	Tot Fe	Filt	pH	Turb	Tot Fe	Filt	pH	Turb	Tot Fe	Filt	pH	Turb	Tot Fe	Filt	pH	Turb	Tot Fe	Filt	pH
1[e]	3.22	10.5	Undil.	0.125	2.04	100	7.0	0.13	2.08	98	7.25	0.14	2.05	97	7.8	0.15	2.09	98	8.05	0.16	2.05	100	8.3	0.16	2.08	98	8.3
3[e]	3.22	10.7	1/10	0.13	2.01	96	7.0	0.145	2.06	99	7.25	0.165	2.05	98	7.5	0.175	2.10	99	7.8	0.18	2.08	99	8.1	0.17	2.05	100	8.2
8	3.22	10.7	1/10	0.18	0.95	100	7.0	0.22	2.02	100	7.3	0.22	2.04	99	7.8	0.225	2.08	100	8.05	0.23	2.08	98	8.2	0.225	2.04	100	8.2
5[e]	3.22	10.5	1/50	0.15	1.97	99	7.0	0.16	2.05	99	7.25	0.18	2.04	99	7.5	0.20	2.02	100	7.8	0.21	2.04	100	8.1	0.20	2.05	98	8.2
6[e]	3.22	4.9	1/100	0.53	1.95	80	6.95	0.68	2.01	0	7.25	0.64	1.96	0	7.75	0.63	1.96	0	8.0	0.65	1.90	0	8.2	0.67	1.86	0	8.3
7[e]	3.22	10.4	1/500	0.84	1.94	0	7.0	0.73	1.99	0	7.3	0.66	1.98	0	7.75	0.65	2.06	0	8.0	0.62	2.06	0	8.2	0.60	2.01	0	8.3

a. Reported as mg SiO_2/L

b. Turbidity, NTU

c. Total iron, mg Fe/L

d. Iron filterability, %

e. Plotted in Figure 11

increased iron filterability according to Dart and Foley (5) and yet the 1/500 dilution system, despite its higher pH levels, showed significantly lower Fe filterabilities than the 1/10 and 1/50 dilution systems which showed higher pH values.

The turbidity patterns (Figure 13) corroborated the iron filterability results, higher turbidities being associated, grossly, with lower filterability. Accordingly, the turbidities for the undiluted, 1/10 and 1/50 systems were similar and low (0.11 to 0.23 NTU) whereas for the 1/100 and 1/500 dilution systems the turbidities were substantially higher (0.53 to 0.84 NTU). Constancy in the total iron patterns eliminated this parameter as a factor causing the observed differences among treatments (Figure 14).

Overall, these results showed that, under uncontrolled pH conditions the higher dilution (more dilute) stock silicate solutions were less effective than the lower ones (more concentrated) at maintaining significant iron filterability. It is likely that for some dosage lower than 10 mg SiO_2/L, a difference in iron filterability would be observed among the undiluted, 1/10 and 1/50 dilution systems, under conditions otherwise similar to those prevailing for Figures 11, 12, 13,and 14.

The next experiment provided a comparison of varying silicate dilution systems, under controlled and uncontrolled pH conditions. The data for iron filterability, total iron, turbidity, and pH are given in Table 8 and Figures 15 to 19. Figure 15 showed that for the dosage of ~9 mg SiO_2/L, under controlled pH conditions, all except the 1/500 dilution systems exhibited almost maximal iron filterability through

Table 8. Data on Dilution Effects for 3.22 Ratio Sodium Silicate at ~ 9 mg SiO_2/L, pH Controlled and Uncontrolled

Jar No.	Silicate SiO_2/Na_2O Ratio	Dose[a]	Dilution	Day 0 Turb[b]	0 Tot Fe[c]	0 Filt[d]	0 pH	1.0 Turb	1.0 Tot Fe	1.0 Filt	1.0 pH	3.0 Turb	3.0 Tot Fe	3.0 Filt	3.0 pH	5.0 Turb	5.0 Tot Fe	5.0 Filt	5.0 pH	6.7 Turb	6.7 Tot Fe	6.7 Filt	6.7 pH	9.8 Turb	9.8 Tot Fe	9.8 Filt	9.8 pH	161 Turb[b]	161 Tot Fe[c]	161 Filt[d]	161 pH	164 Turb	164 Tot Fe	164 Filt	164 pH
1[e,g]	3.22	7.5	Undil.	0.15	2.03	98	7.1	0.13	2.06	97	7.25	0.415	2.04	5	7.25	-	-	0	-	-	-	-	-	-	-	-	-								
2[e,g]	3.22	9.2	1/10	0.14	2.00	100	7.1	0.165	2.00	99	7.25	0.43	2.04	6	7.25	-	-	0	-	-	-	-	-	-	-	-	-								
3[e,g]	3.22	9.1	1/50	0.17	2.04	98	7.1	0.17	2.05	100	7.25	0.47	2.09	0	7.25	-	-	0	-	-	-	-	-	-	-	-	-								
5[e,h]	3.22	8.9	1/50	0.18	2.00	100	7.1	0.18	2.06	97.5	7.2	0.49	2.00	3	7.25	-	-	0	-	-	-	-	-	-	-	-	-								
6[f,h]	3.22	8.9	1/50	0.18	2.2	100	7.05	0.20	2.02	100	7.2	0.26	2.03	100	7.55	0.26	2.04	94	7.85	0.27	2.04	92	8.2	0.28	2.04	93	8.3	0.31	1.94	95	8.5	0.36	1.94	95	8.1[i]
6[i]	3.22	8.9	1/50																									-	-	-	7.0	0.54	1.91	0.5	7.1
8[e,g]	3.22	9.0	1/100	0.23	2.00	100	7.1	0.30	2.02	97.5	7.25	0.55	2.06	3	7.25	-	-	0	-	-	-	-	-	-	-	-	-								
9[e,g]	3.22	9.5	1/500	0.53	2.02	58	7.1	0.69	1.99	0	7.25	0.62	2.02	0	7.2	-	-	0	-	-	-	-	-	-	-	-	-								

a. Reported as mg SiO_2/L

b. Turbidity, NTU

c. Total iron, mg Fe/L

d. Iron filterability, %

e. Measurement made before any readjustment of pH

f. pH uncontrolled

g. Plotted in Figure 15

h. Plotted in Figures 15 and 16

i. Readjustment of pH of uncontrolled pH system in Jar No. 6

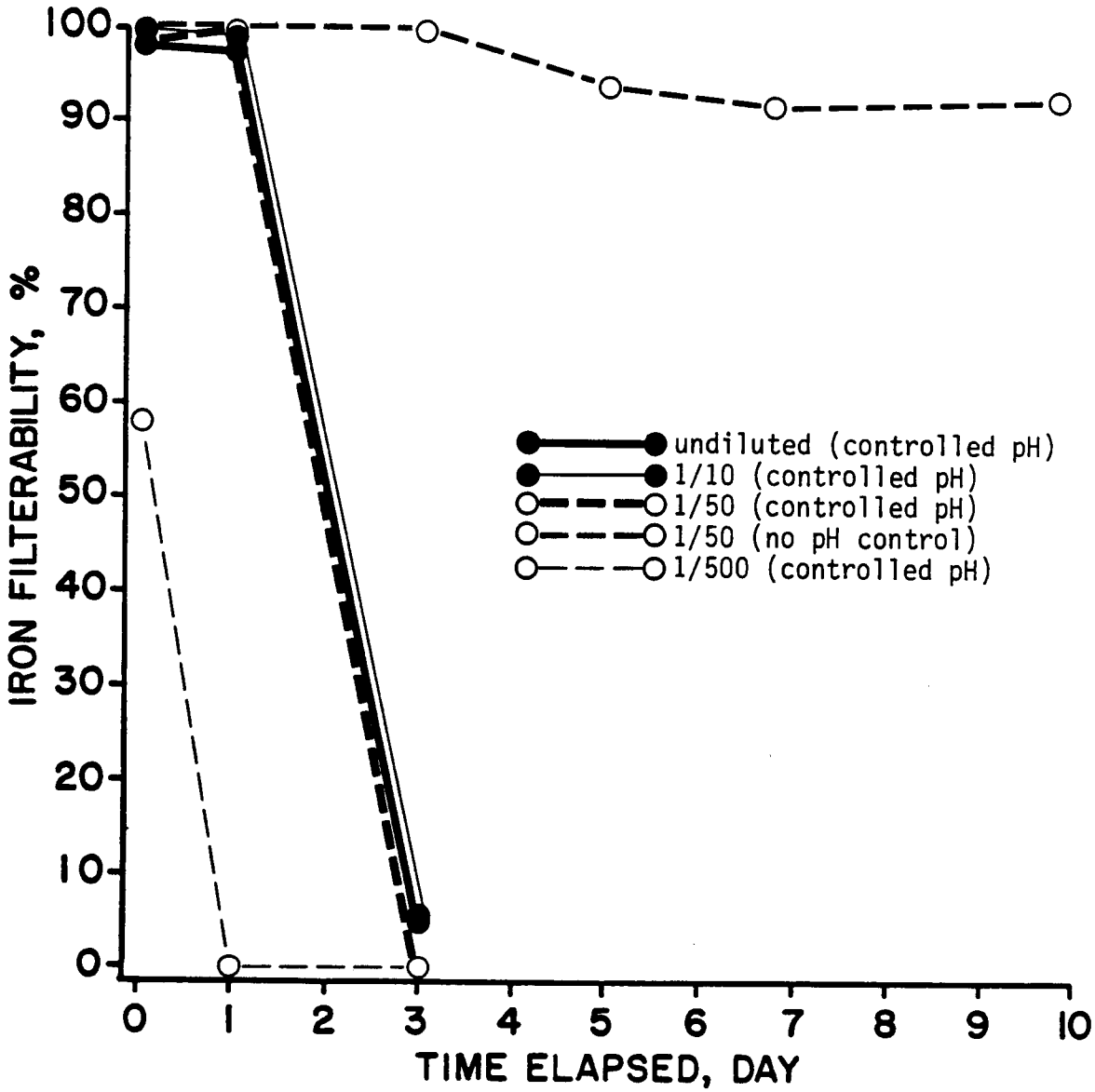


Figure 15. Dilution Effects for 3.22 Ratio Sodium Silicate at ~9 mg SiO_2/L--pH Controlled vs. Uncontrolled: Iron Filterability, 0 to 10 days.

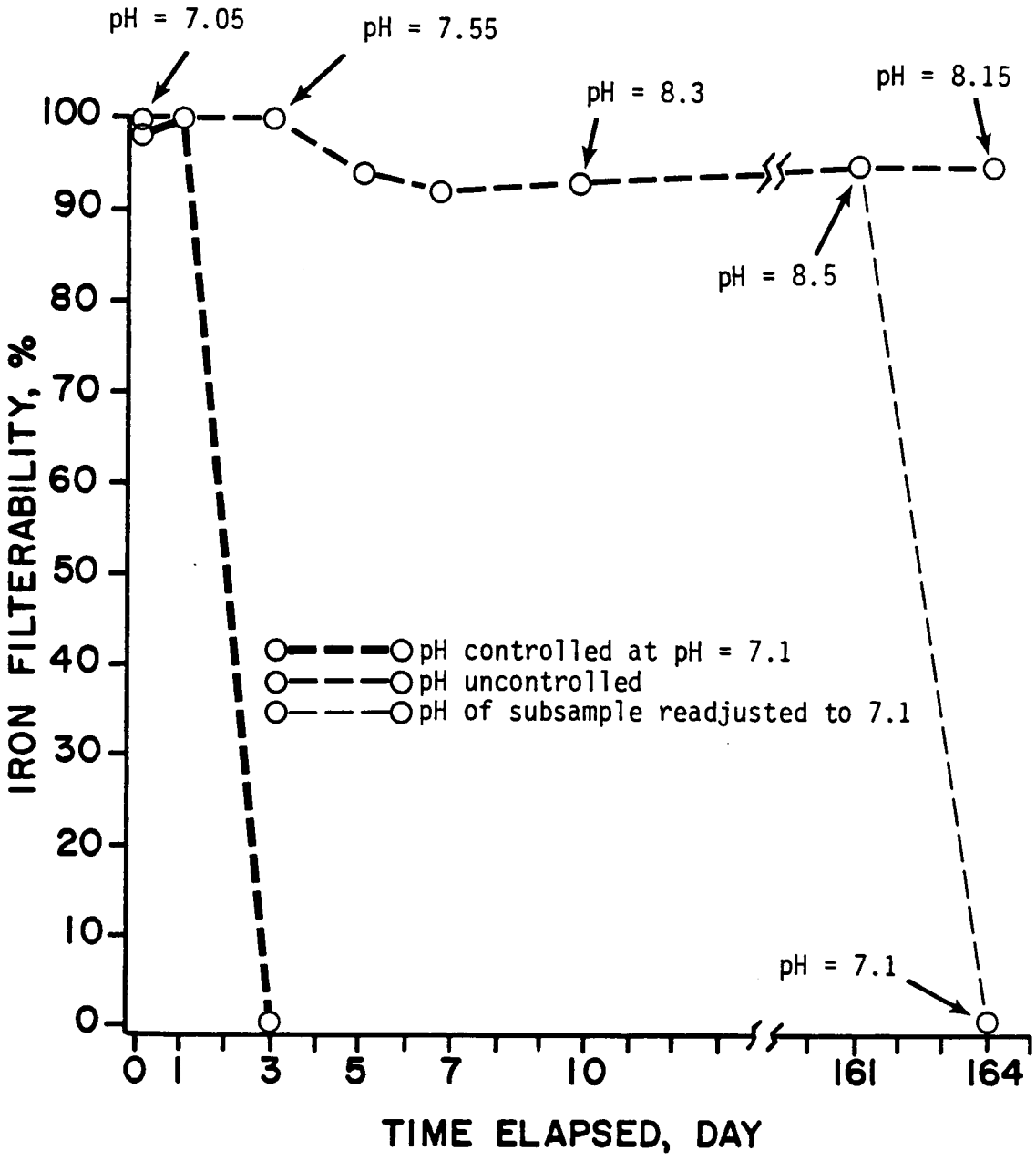


Figure 16. Dilution Effects for 3.22 Ratio Sodium Silicate at ~9 mg SiO_2/L--pH Controlled vs. Uncontrolled: Iron Filterability, 0 to 164 days.

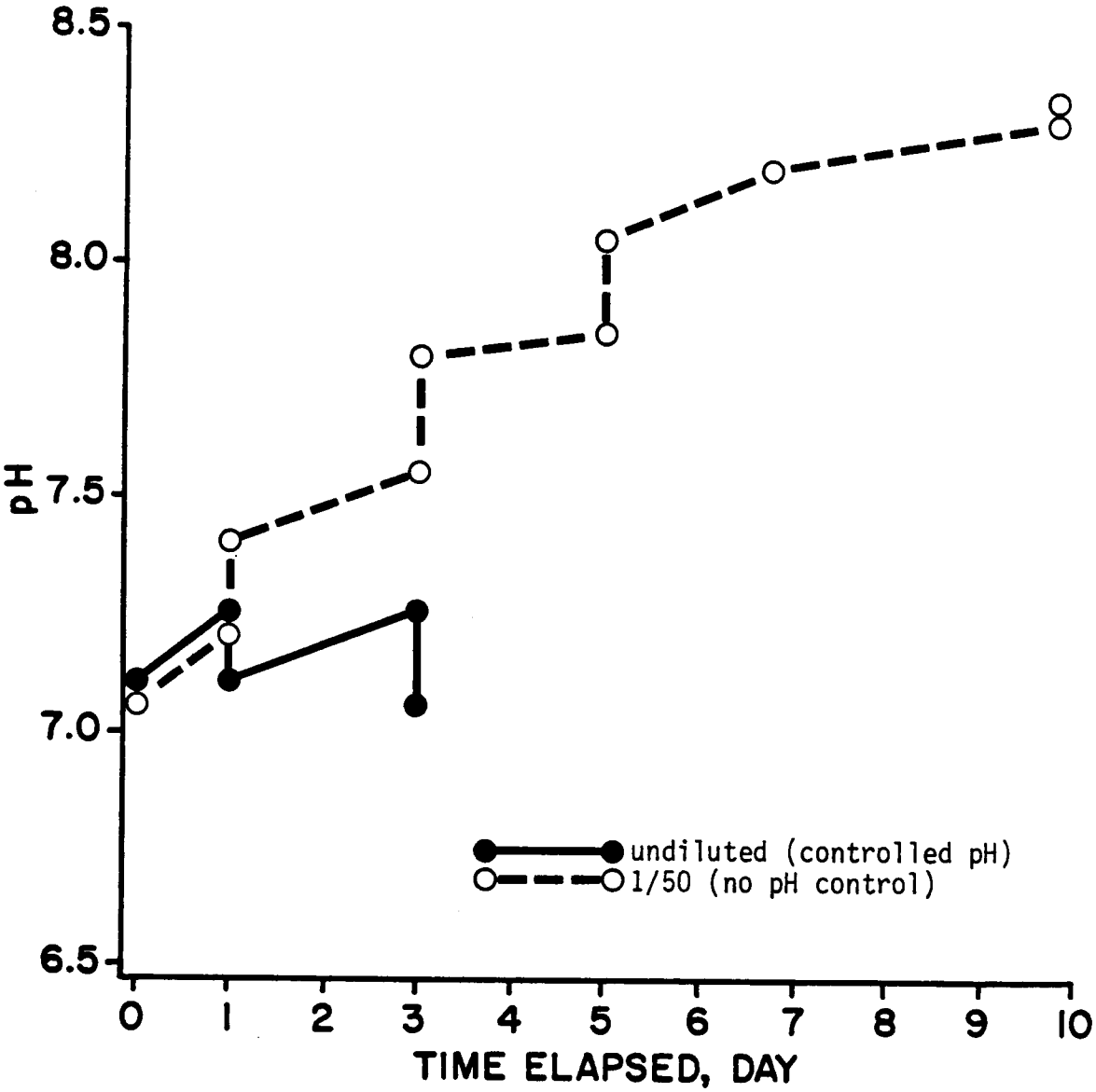


Figure 17. Dilution Effects for 3.22 Ratio Sodium Silicate at ~9 mg SiO_2/L--pH Controlled vs. Uncontrolled: pH.

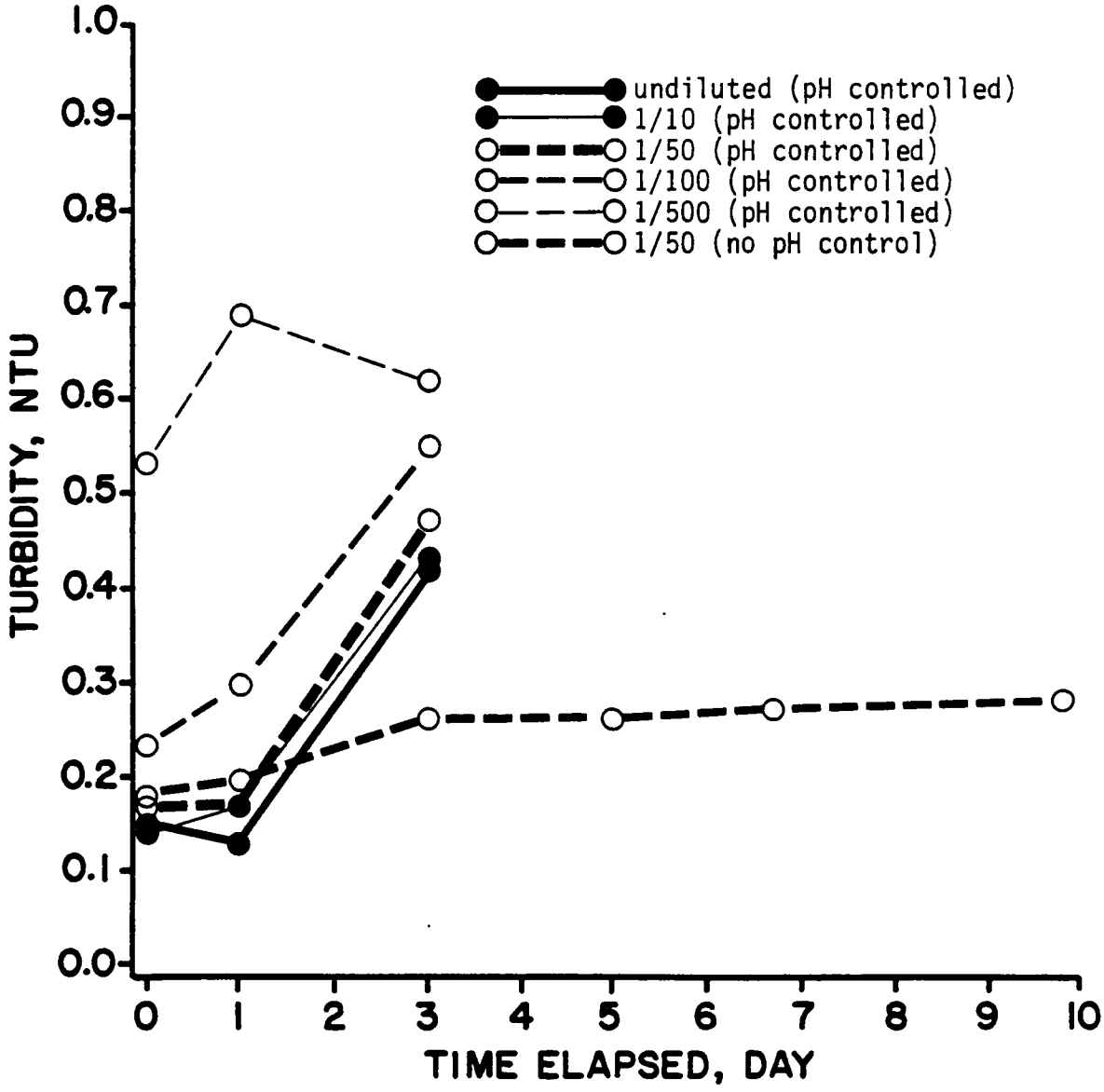


Figure 18. Dilution Effects for 3.22 Ratio Sodium Silicate at ~9 mg SiO_2/L--pH Controlled vs. Uncontrolled: Turbidity.

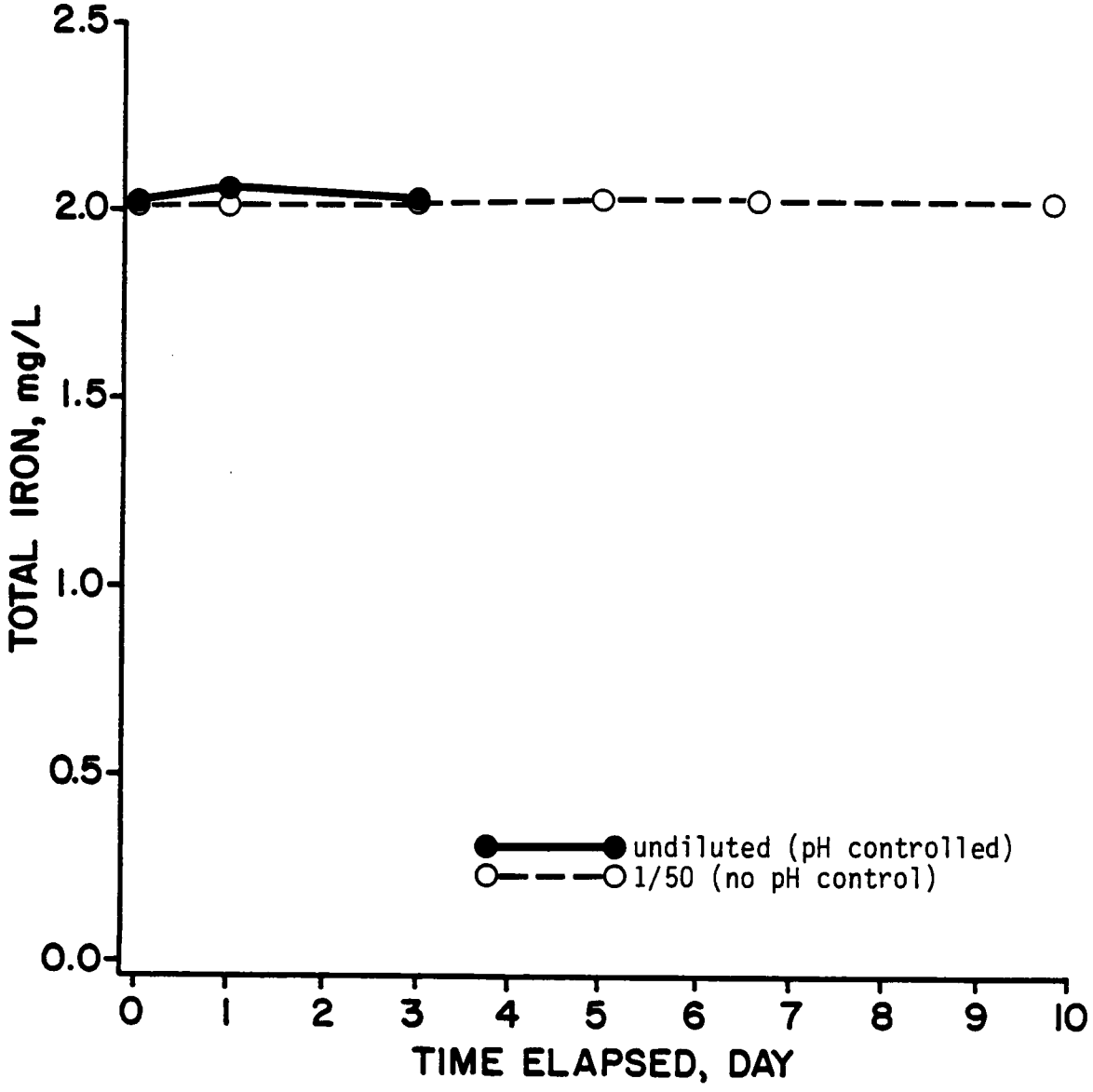


Figure 19. Dilution Effects for 3.22 Ratio Sodium Silicate at ~9 mg SiO_2/L--pH Controlled vs. Uncontrolled: Total Iron.

day 1, which then in every instance decreased to almost zero by day 3. For the 1/500 dilution system, the initial iron filterability was only 58% and decreased to zero by day 1. As for the previous test systems (Figures 11 to 14), here the conditions of dosage and pH did not allow differentiation in performance among most of the dilutions. For the systems with the pH controlled at ~7.0, higher doses of silica would be required to provide distinctions in performance among the various dilution systems.

In sharp contrast with controlled-pH systems, for the one treatment without pH control, i.e., the 1/50 dilution at a dose of ~9 mg SiO_2/L, the iron filterability remained at > 90% for up to 164 days. Moreover, the role of pH was demonstrated well by the fact that upon the adjustment to pH 7.0 of a subsample from the uncontrolled-pH system (day 161), the iron filterability fell to approximately zero within three days after the change (Figure 16).

Figure 17 showed the pH to be between 7.05 and 7.25 for the controlled pH systems, whereas for the uncontrolled pH system the pH rose to as high as 8.35 on day 10 and 8.5 on day 161 (not shown in Figure 17). The pH adjustment of the subsample of the uncontrolled pH system was also verified (Figure 16).

The turbidities (Figure 18) repeated previously observed patterns, i.e., low turbidities (0.14 to 0.30 NTU) were associated with high iron filterability, and high turbidities (0.41 to 0.69 NTU) with minimal iron filterability. Total iron concentrations remained between 1.91 and 2.09 mg Fe/L and indicated little or no abnormalities (Figure 19).

Because of the results of the pH control/no control experiments, it was felt that the controlled pH (at 7.0) would be a more stringent test of the iron treatment technique, would minimize pH variability with time as a factor, and would thus allow a clearer distinction among the performances of various silicate treatments. As a result the remaining iron filterability experiments were conducted under conditions that controlled the pH at ~7.0.

Silica Dose Optimization

The next experiment was conducted to demonstrate the effect of a range of silica doses on iron filterability. This represented an attempt to establish a dose of undiluted silicate that would produce maximal iron filterability for the entire 10 day experimental duration, and yet allow a distinction in performance among the corresponding test dilutions. The resultant data for iron filterability, total iron, turbidity, and pH are presented in Figures 20 and 21,22,23, and 24, respectively, and Table 9. These results showed that increased silica doses produced increased iron filterability, i.e., high filterability was maintained for a longer period, whether the feed silicate was an undiluted or a 1/100 dilution system. The undiluted silicate was more effective than the 1/100 dilution feed solution at maintaining high iron filterability, for any given dose. Thus, a dose of 11.2 mg SiO_2/L of undiluted silicate (Figure 20), maintained a 95% iron filterability until almost day 5, while 11.4 mg SiO_2/L of 1/100 dilution produced a $\geq$ 95% filterability until only 2½ days had elapsed. However, higher doses of the 1/100 dilution solution can be used to compensate for the superior effectiveness of undiluted

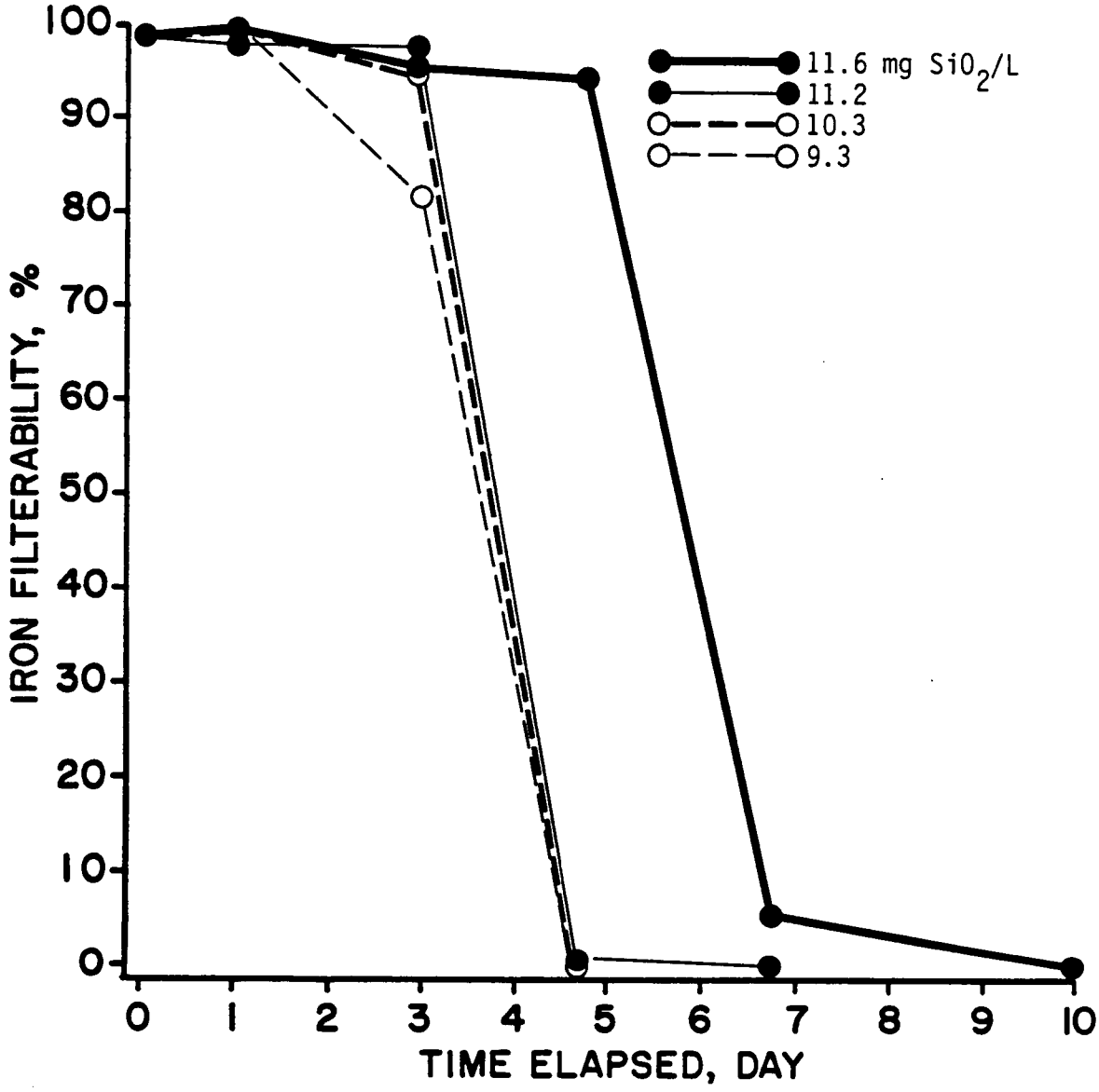


Figure 20. Silica Dose Effects for Undiluted 3.22 Ratio Sodium Silicate--pH Controlled: Iron Filterability.

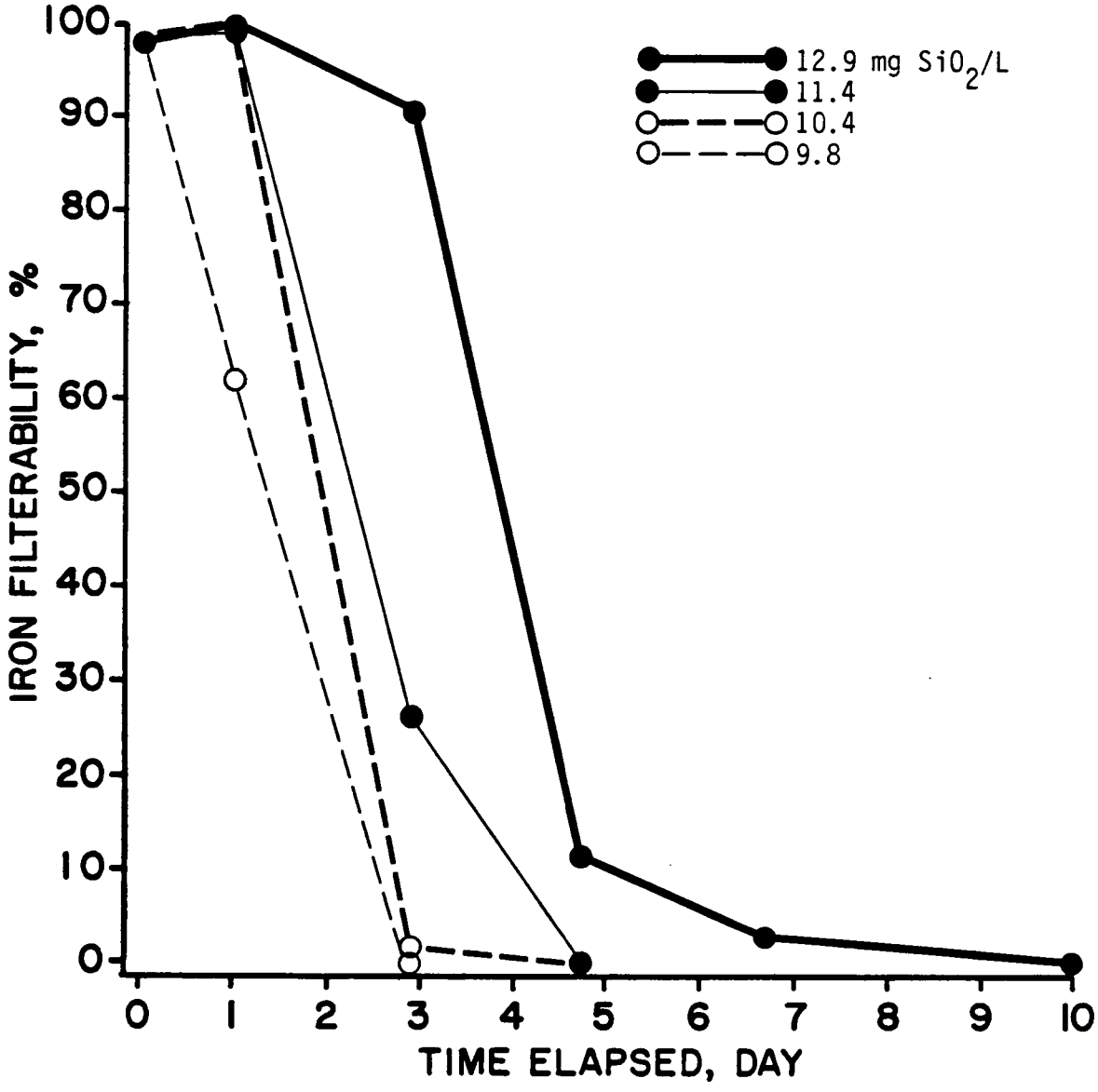


Figure 21. Silica Dose Effects for 1/100 Dilutions of 3.22 Ratio Sodium Silicate--pH Controlled: Iron Filterability.

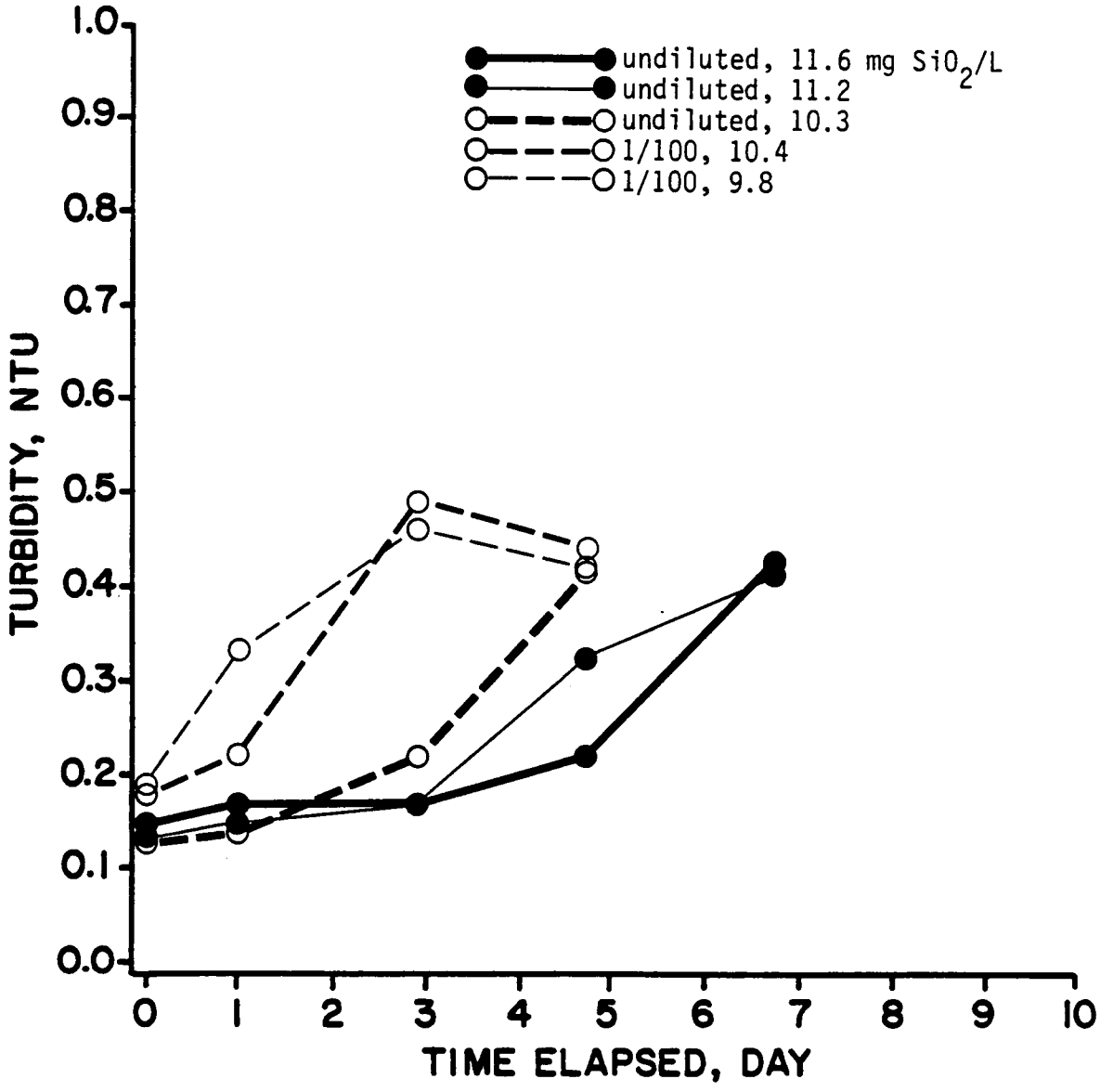


Figure 22. Silica Dose Effects for Undiluted and 1/100 Dilutions of 3.22 Ratio Sodium Silicate--pH Controlled: Turbidity.

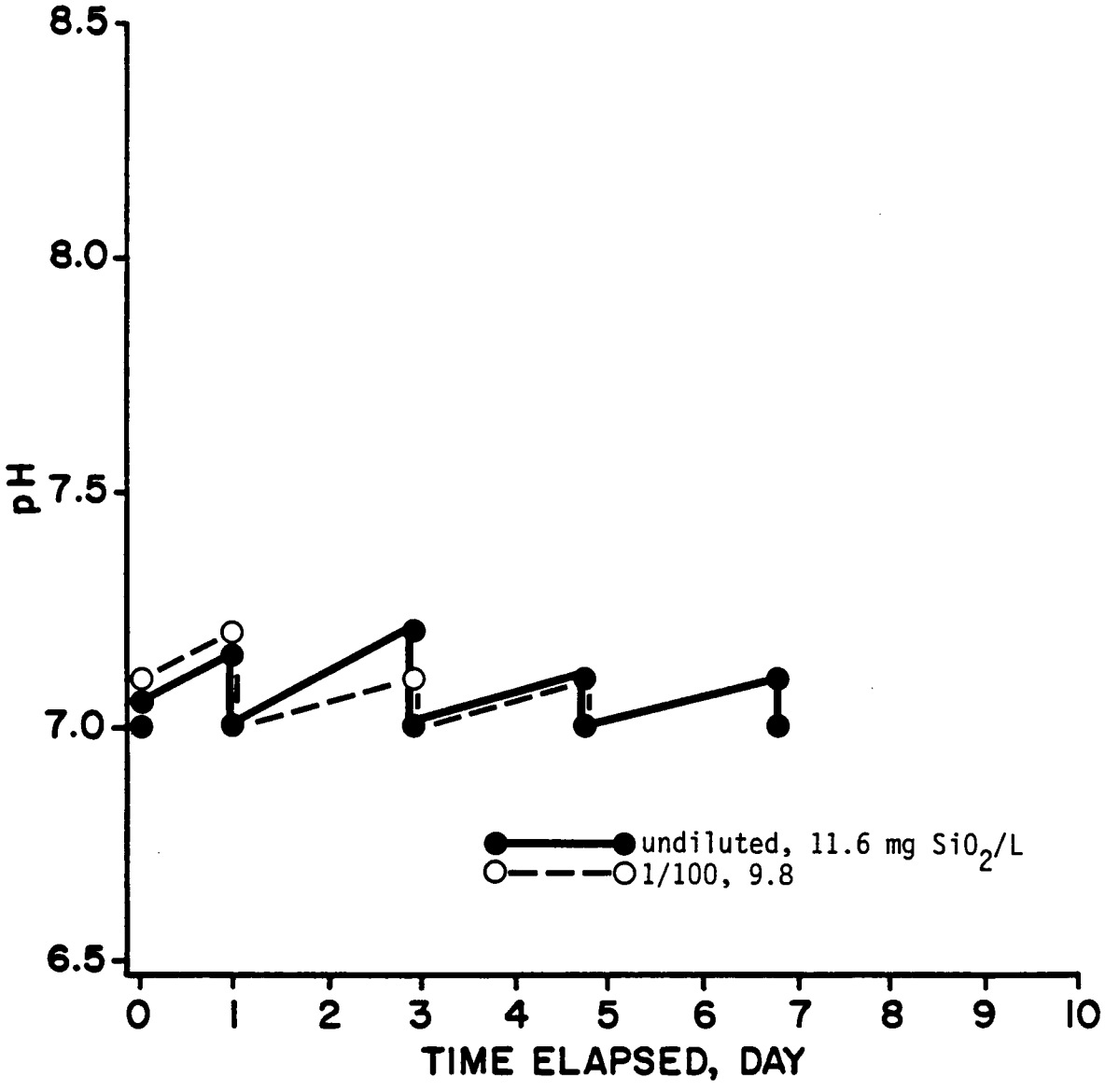


Figure 23. Silica Dose Effects for Undiluted and 1/100 Dilutions of 3.22 Ratio Sodium Silicate--pH Controlled: pH.

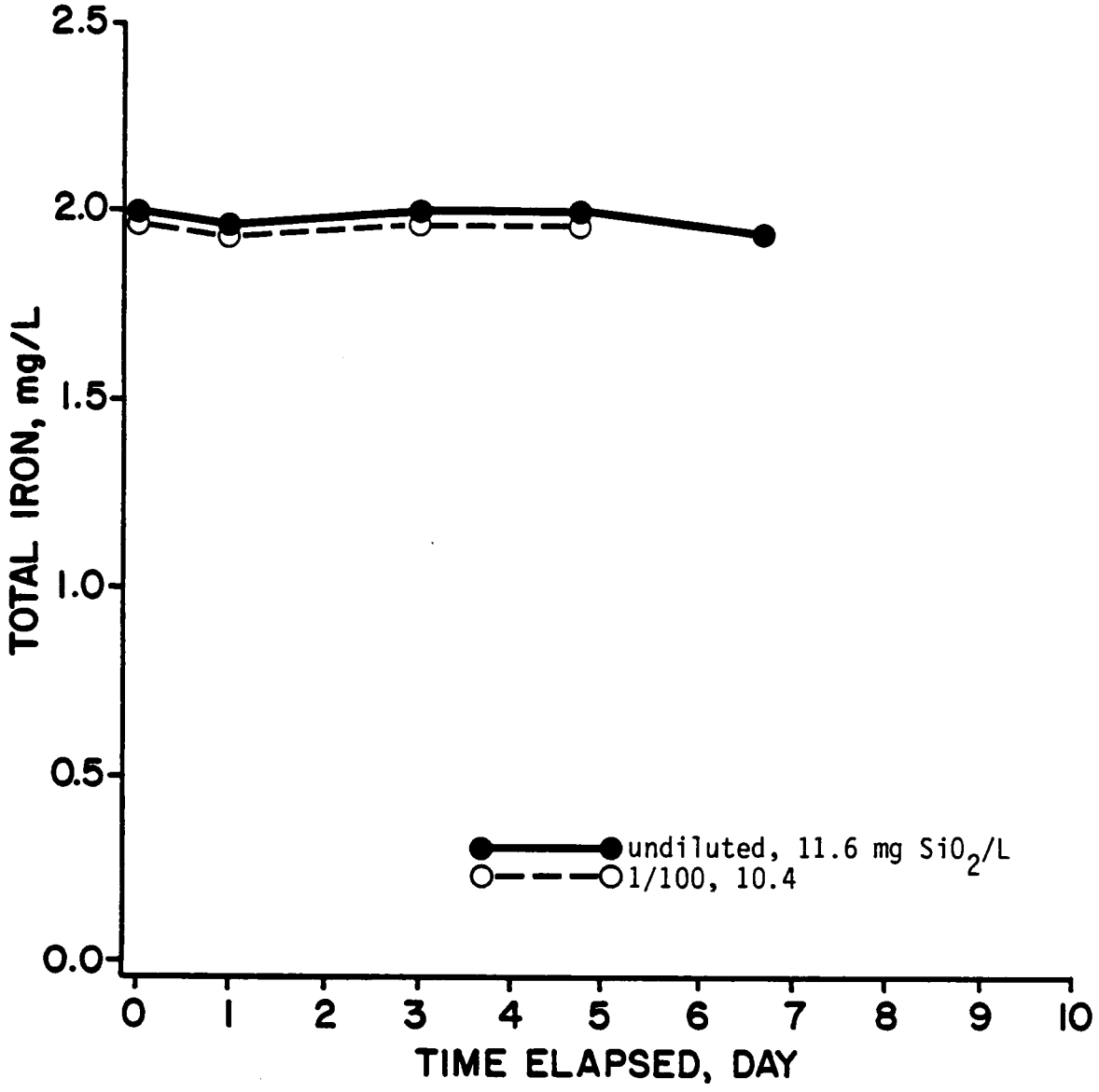


Figure 24. Silica Dose Effects for Undiluted and 1/100 Dilutions of 3.22 Ratio Sodium Silicate--pH Controlled: Total Iron.

Table 9. Data on Silica Dose Effects for Undiluted and 1/100 Dilution of 3.22 Ratio Sodium Silicate with pH Controlled

Jar No.	Silicate SiO_2/Na_2O Ratio	Dose[a]	Dilution	Day 0 Turb[b]	0 Tot Fe[c]	0 Filt[d]	0 pH	1.0 Turb	1.0 Tot Fe	1.0 Filt	1.0 pH	2.9 Turb	2.9 Tot Fe	2.9 Filt	2.9 pH	4.75 Turb	4.75 Tot Fe	4.75 Filt	4.75 pH	6.75 Turb	6.75 Tot Fe	6.75 Filt	6.75 pH	10 Turb	10 Tot Fe	10 Filt	10 pH
1[f]	3.22	9.3	Undil.	0.12	1.99	99.5	7.05	0.14	1.99	99.5	7.15	0.25	1.97	82	7.1	0.39	1.99	0	7.1	-	-	-	-	-	-	-	-
2[g]	3.22	9.8	1/100	0.19	1.97	98.5	7.1	0.35	1.98	62	7.2	0.46	1.96	0	7.1	0.42	1.97	0	7.1	-	-	-	-	-	-	-	-
3[f]	3.22	10.3	Undil.	0.13	1.99	98.5	7.05	0.14	1.95	99.5	7.2	0.22	1.99	95	7.1	0.415	1.99	0	7.1	-	-	-	-	-	-	-	-
5[g]	3.22	10.4	1/100	0.18	1.96	98.5	7.05	0.22	1.93	99.5	7.2	0.49	1.96	2	7.1	0.44	1.96	0	7.05	-	-	-	-	-	-	-	-
7[f]	3.22	11.2	Undil.	0.135	1.97	99.5	7.05	0.15	1.98	98	7.2	0.17	1.96	98	7.15	0.32	2.00	1	7.1	0.41	1.96	0	7.1	-	-	-	-
8[g]	3.22	11.4	1/100	0.18	1.96	98.5	7.05	0.22	1.95	99	7.1	0.415	1.94	26	7.1	0.47	1.96	0	7.1	-	-	-	-	-	-	-	-
9[f]	3.22	11.6	Undil.	0.15	1.99	99.0	7.05	0.17	1.96	100	7.15	0.17	2.00	96	7.2	0.22	2.00	95	7.1	0.425	1.94	5	7.1	-	-	0	-
17[g]	3.22	12.9	1/100	0.18	1.97	98.0	7.05	0.20	1.97	100	7.15	0.28	1.97	91	7.1	0.44	1.98	11	7.05	0.51	1.99	4	7.1	-	-	0	-

a. Reported as mg SiO_2/L

b. Turbidity, NTU

c. Total iron, mg Fe/L

d. Iron filterability, %

e. Measurement made before any readjustment to pH 7

f. Plotted in Figure 20

g. Plotted in Figure 21

silicate. For example, 11.4 mg SiO_2/L of 1/100 dilution solution maintained high iron filterability more effectively than 9.3 mg SiO_2/L of the undiluted silicate.

Turbidities (Figure 22) showed the characteristic pattern of low turbidity in association with high iron filterability and vice versa. The pH patterns (Figure 23) verified pH control to be at around 7.1, and the total iron data (Figure 24), showed that the total iron values were in fact around 2 mg Fe/L.

Effect of Silicate Dilution on Treatment Performance

A more detailed investigation of the role of feed stock solution dilutions dosed at ~13 mg SiO_2/L was presented for N silicate. These results are shown in Figures 25,26,27, and 28, and Table 10. A clear association between feed stock dilution and treatment effectiveness was demonstrated. Thus, for a given silica dose, increasingly dilute stock solutions produced progressively less effective maintenance of high iron filterability. In Figure 25, the effectiveness of the undiluted and the 1/10 dilution treatments were quite similar, with the latter being slightly better on day 7. The distinctions among the other dilutions were clearer. Thus, a level of 50% iron filterability was observed on days 1, 4.2, and 6.4, for the 1/500, 1/100, and 1/50 dilutions respectively. For a consistent trend, given that the undiluted and 1/10 dilution systems were dosed at the same level, 12.9 mg SiO_2/L, the former solution should have been more effective than the latter. The apparent reversal in effectiveness was attributed to errors in the filterability measurements; these are magnified on the sloping limbs of

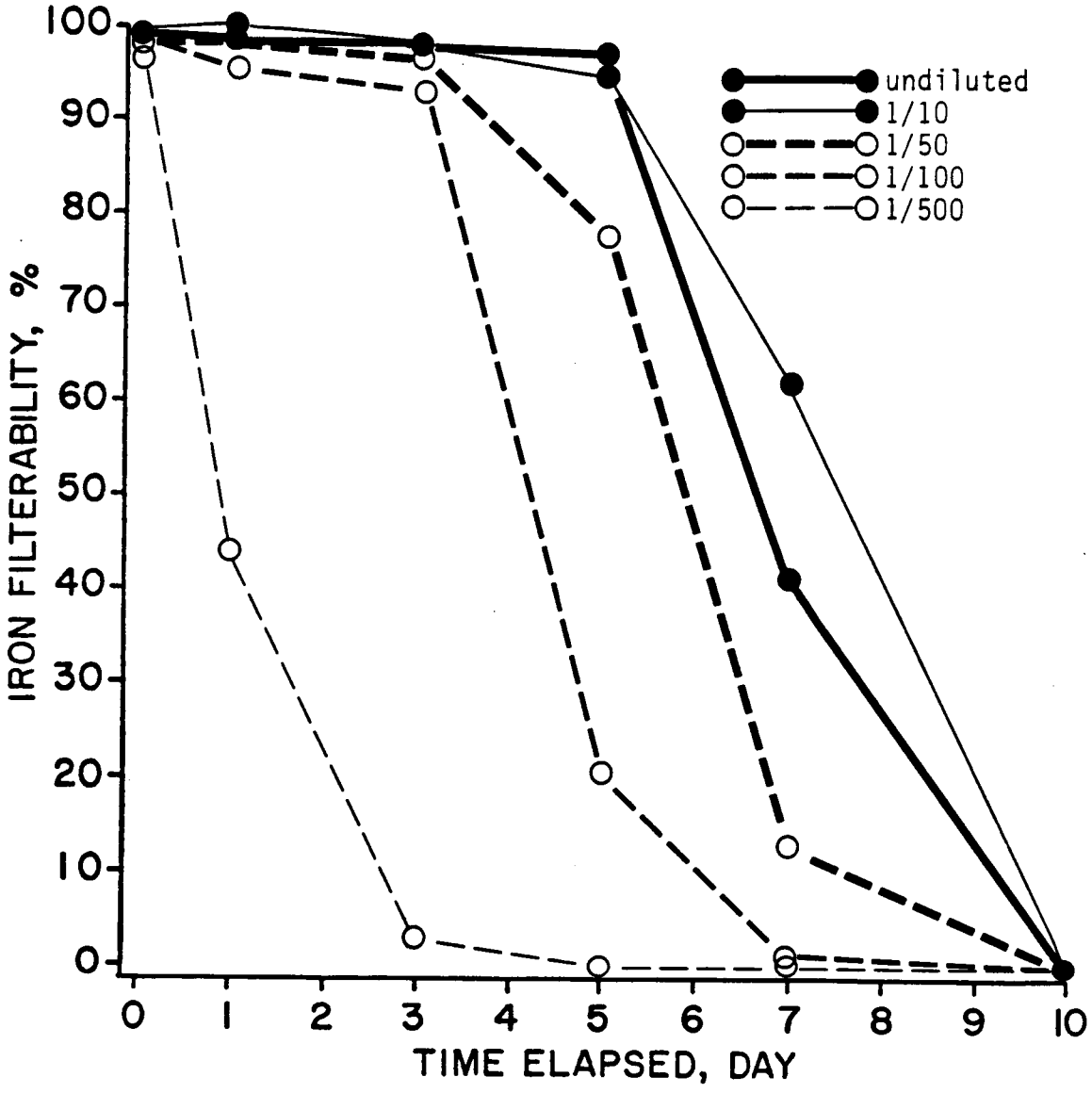


Figure 25. Dilution Effects for 3.22 Ratio Sodium Silicate at ~13 mg SiO_2/L--pH Controlled: Iron Filterability.

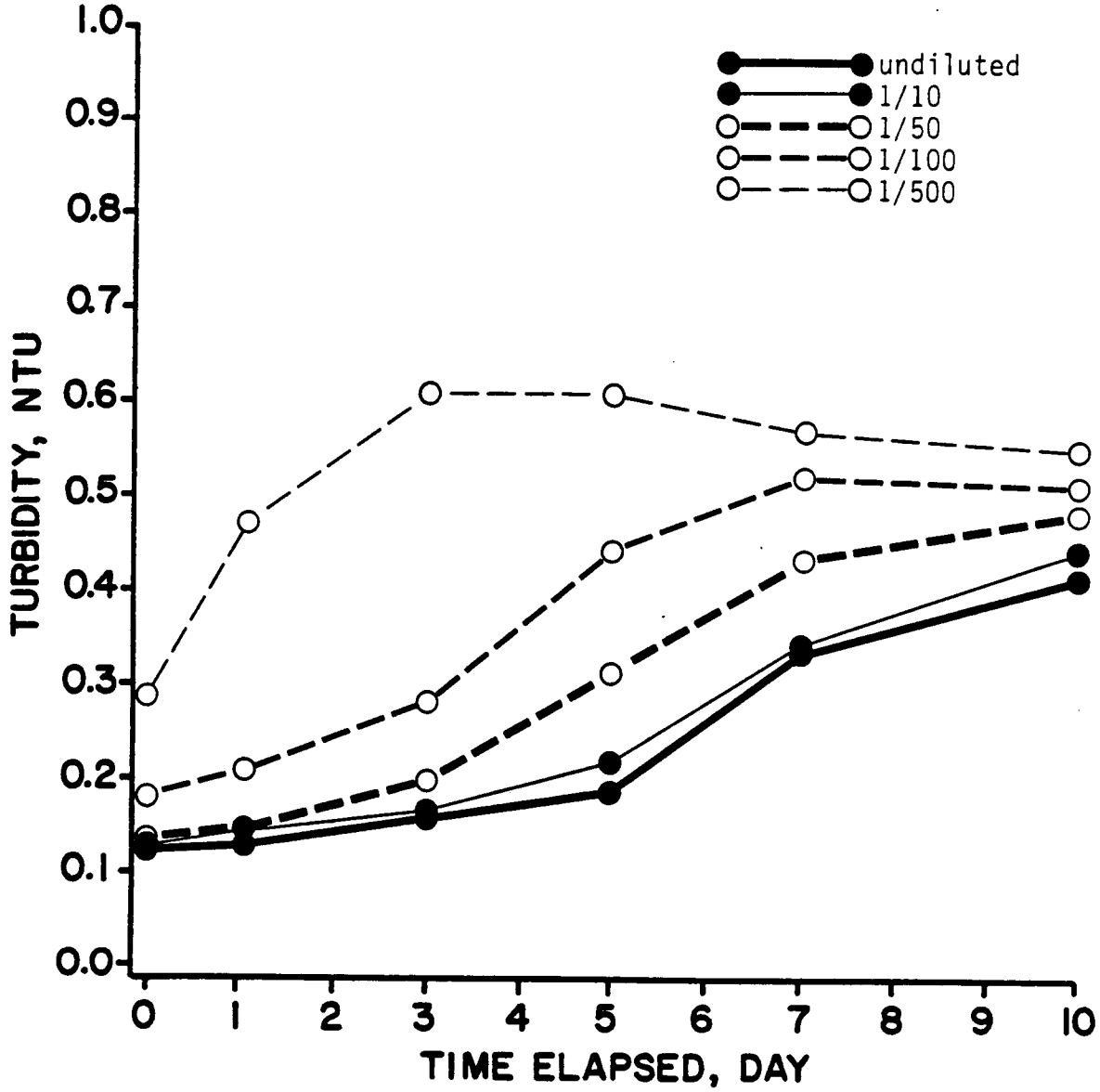


Figure 26. Dilution Effects for 3.22 Ratio Sodium Silicate at ~13 mg SiO_2/L--pH Controlled: Turbidity.

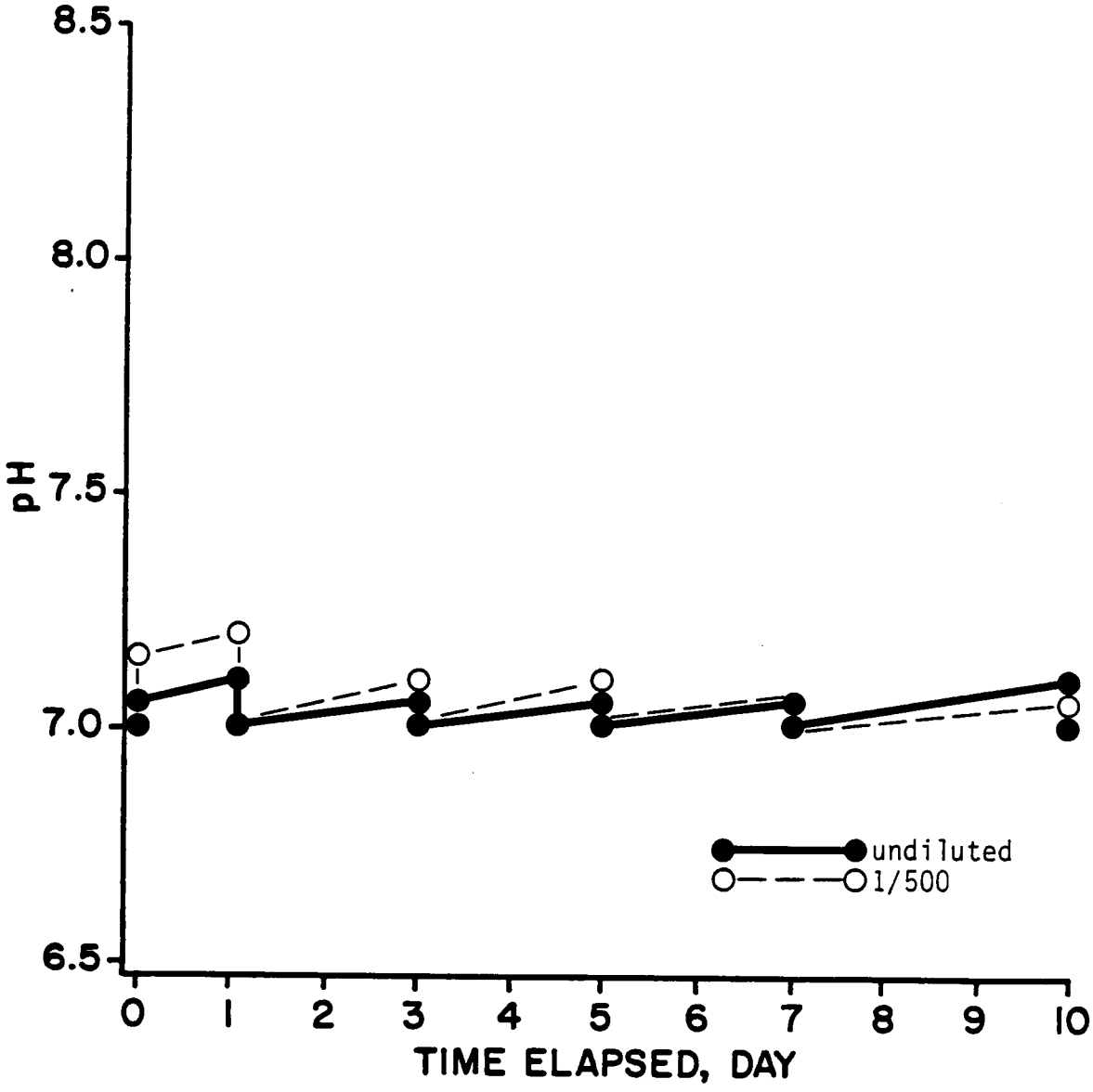


Figure 27. Dilution Effects for 3.22 Ratio Sodium Silicate at ~13 mg SiO_2/L--pH Controlled: pH.

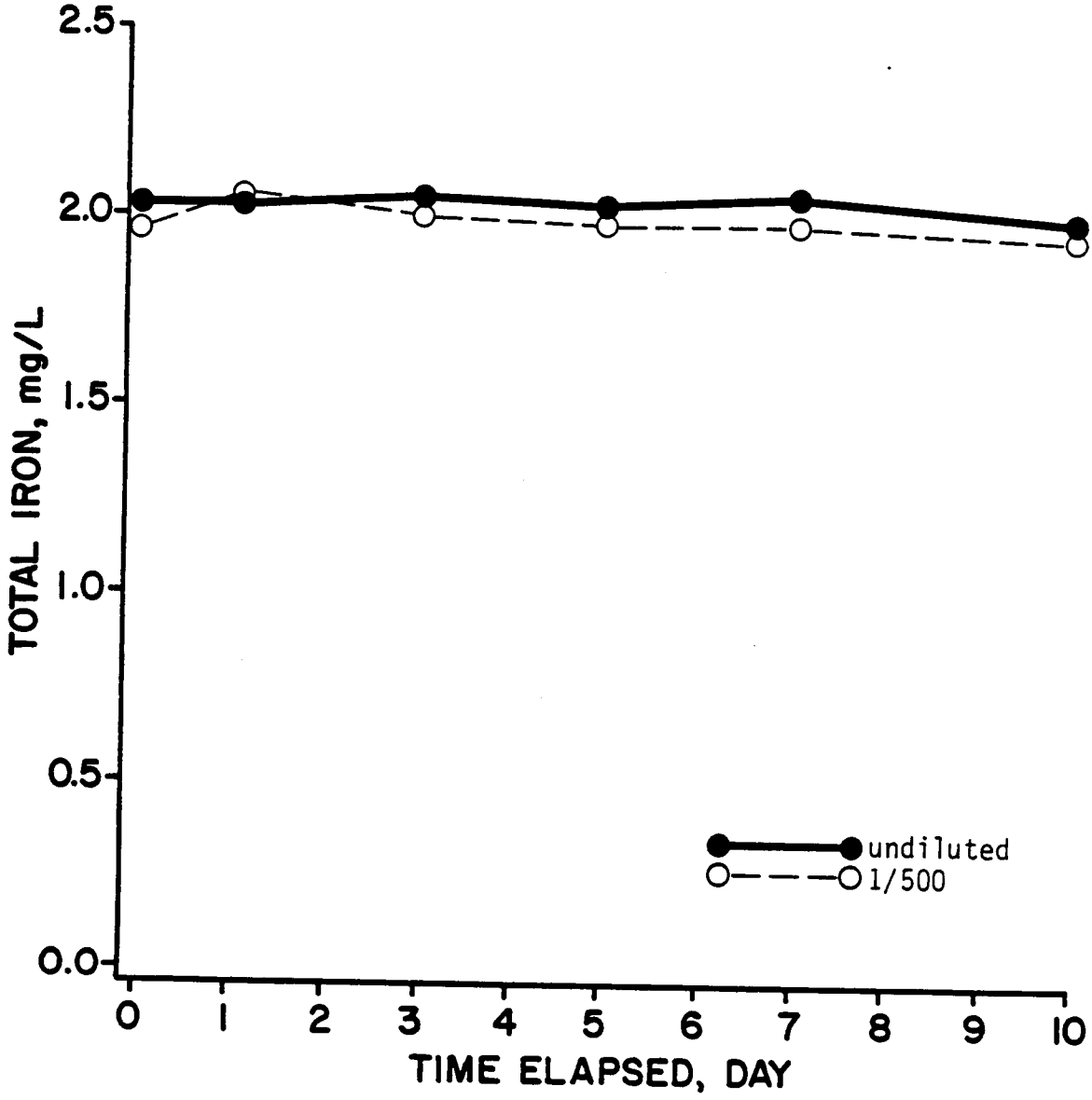


Figure 28. Dilution Effects for 3.22 Ratio Sodium Silicate at ~13 mg SiO_2/L--pH Controlled: Total Iron.

Table 10. Data on Dilution Effects for 3.22 and 3.75 Ratio Sodium Silicates at ~ 13 mg SiO_2/L with pH Controlled

Jar No.	Silicate SiO_2/Na_2O Ratio	Dose[a]	Dilution	Day 0 Turb[b]	0 Tot Fe[c]	0 Filt[d]	0 pH	1.0 Turb	1.0 Tot Fe	1.0 Filt	1.0 pH	3.1 Turb	3.1 Tot Fe	3.1 Filt	3.1 pH	5.0 Turb	5.0 Tot Fe	5.0 Filt	5.0 pH	7.0 Turb	7.0 Tot Fe	7.0 Filt	7.0 pH	10.0 Turb	10.0 Tot Fe	10.0 Filt	10.0 pH
6[f]	3.22	12.9	Undil.	0.125	2.04	99.5	7.05	0.13	2.04	98.5	7.1	0.16	2.06	98	7.05+	0.19	2.03	97	7.05	0.33	2.06	41	7.05	0.41	2.00	0	7.1
10[f]	3.22	12.9	1/10	0.13	2.04	99	7.05	0.15	2.01	100	7.1+	0.17	2.05	98	7.05	0.22	2.05	95	7.1	0.34	2.07	62	7.05	0.44	2.05	0	7.1
11[f]	3.22	13.0	1/50	0.14	2.05	98	7.05	0.15	2.06	98	7.1	0.20	2.05	96	7.05	0.31	2.01	78	7.05	0.43	2.02	13	7.05+	0.48	2.02	0	7.1
13[f]	3.22	13.3	1/100	0.175	2.01	98.5	7.05	0.21	2.06	95	7.1	0.28	2.01	93	7.05	0.44	1.97	20	7.1	0.52	2.03	1	7.0+	0.51	1.97	0	7.15
14[f]	3.22	13.6	1/500	0.29	1.97	96	7.15	0.47	2.06	44	7.2	0.61	2.96	44	7.2	0.61	2.01	3	7.1	0.61	1.98	0	7.05	0.55	1.96	0	7.05
15[g]	3.75	12.8	Undil.	0.18	2.01	99	7.05	0.23	2.07	97	7.15	0.23	2.00	99.5	7.05	0.25	1.99	98.5	7.1	0.31	1.99	98.5	7.05	0.46	2.04	46	7.1
16[g]	3.75	12.9	1/50	0.22	2.03	97.5	7.05	0.27	2.05	98	7.1	0.27	2.03	98	7.05	0.35	1.99	93	7.1	0.49	2.05	21.5	7.05	0.58	2.01	1	7.1
17[g]	3.75	13.6	1/100	0.25	2.00	98.5	7.05	0.30	2.06	98	7.1	0.32	2.02	95.5	7.05+	0.45	2.01	64	7.1	0.61	2.03	3	7.05+	0.58	2.00	0	7.1

a. Reported as mg SiO_2/L

b. Turbidity, NTU

c. Total iron, mg Fe/L

d. Iron filterability, %

e. Measurement made before any readjustment to pH 7

f. Plotted in Figure 25

g. Plotted in Figure 29

curves. Variability in silica concentration measurement probably also contributed to the apparent effect. Thus, while the average value for the silicate dose was 12.9 mg SiO_2/L for both dilutions, the coefficients of variability for undiluted and 1/10 dilution systems were 0.85% and 0.35%, respectively. The turbidity values presented in Figure 26 showed similar trends to the iron filterabilites patterns shown in Figure 22. As filterabilities went down the corresponding turbidities went up. Thus, the turbidities for the undiluted and 1/10 silicate solutions showed similar values and progressively higher turbidities were shown for the 1/50, 1/100, and 1/500 dilutions. Figures 27 and 28 showed the pH and total Fe values over time, and indicated that the desired control of these two parameters was achieved and that they did not contribute to the observed differences among treatments. In the examination of these data it should be noted that there are slight but real differences in the silica doses which help to determine the comparative effectiveness of various treatments.

Data for the comparison of the treatment effectiveness of various dilutions of 3.75 ratio silicate dosed at 13 to 13.6 mg SiO_2/L are presented in Figures 29 to 32 and in Tables 10 and 11. Figure 29 showed a clear progressive decrease in effectiveness at maintaining continued high iron filterability in going from the undiluted to higher dilutions of silicate solution. This finding agreed with the results obtained for the 3.22 ratio silicate, and was consistent with the notion that higher levels of polymerization in the feed silicate solution are more effective at the stabilization of aqueous ferric iron. The turbidity data (Figure 30) corroborated the findings for iron

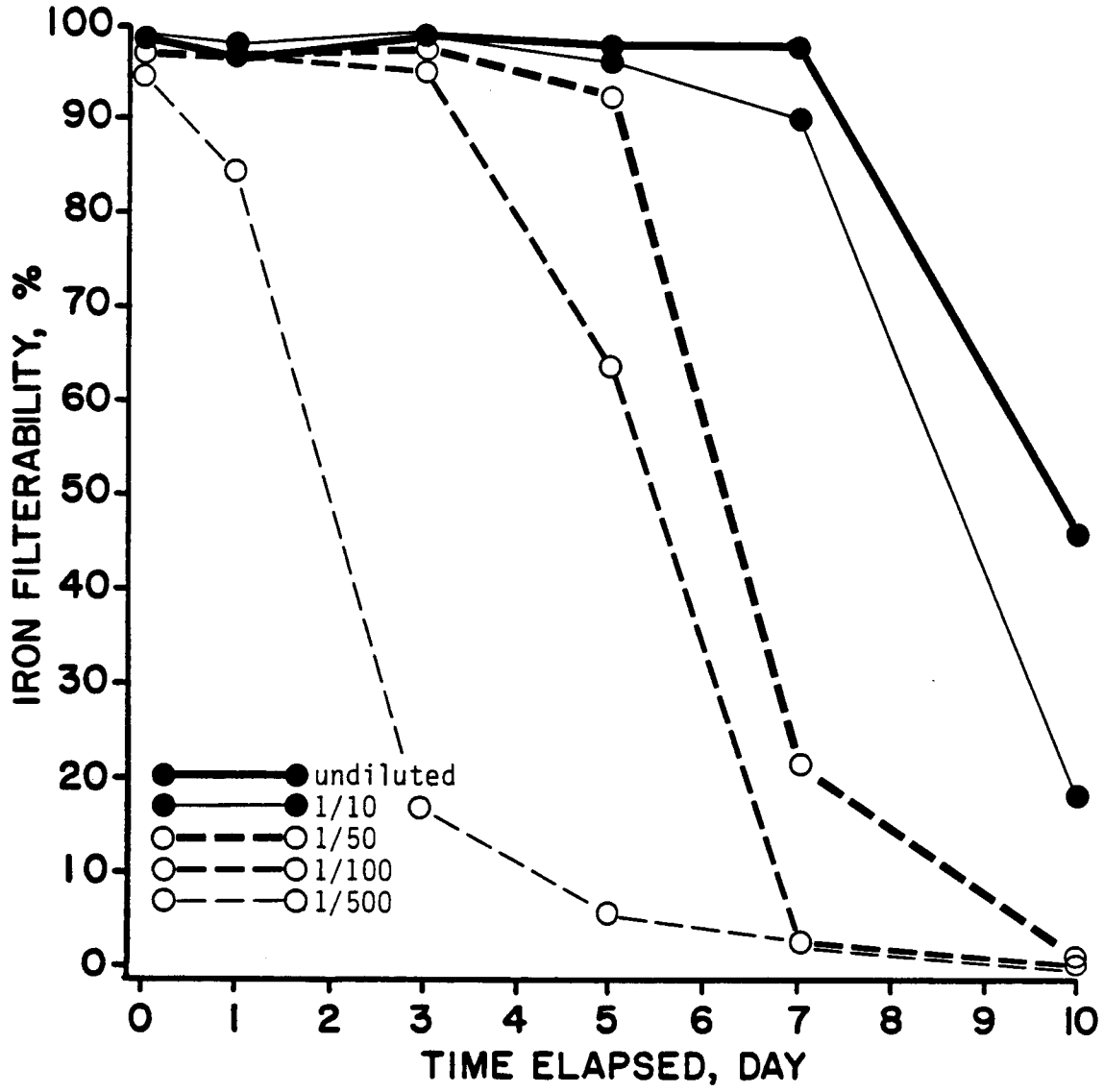


Figure 29. Dilution Effects for 3.75 Ratio Sodium Silicate at ~13 mg SiO_2/L--pH Controlled: Iron Filterability.

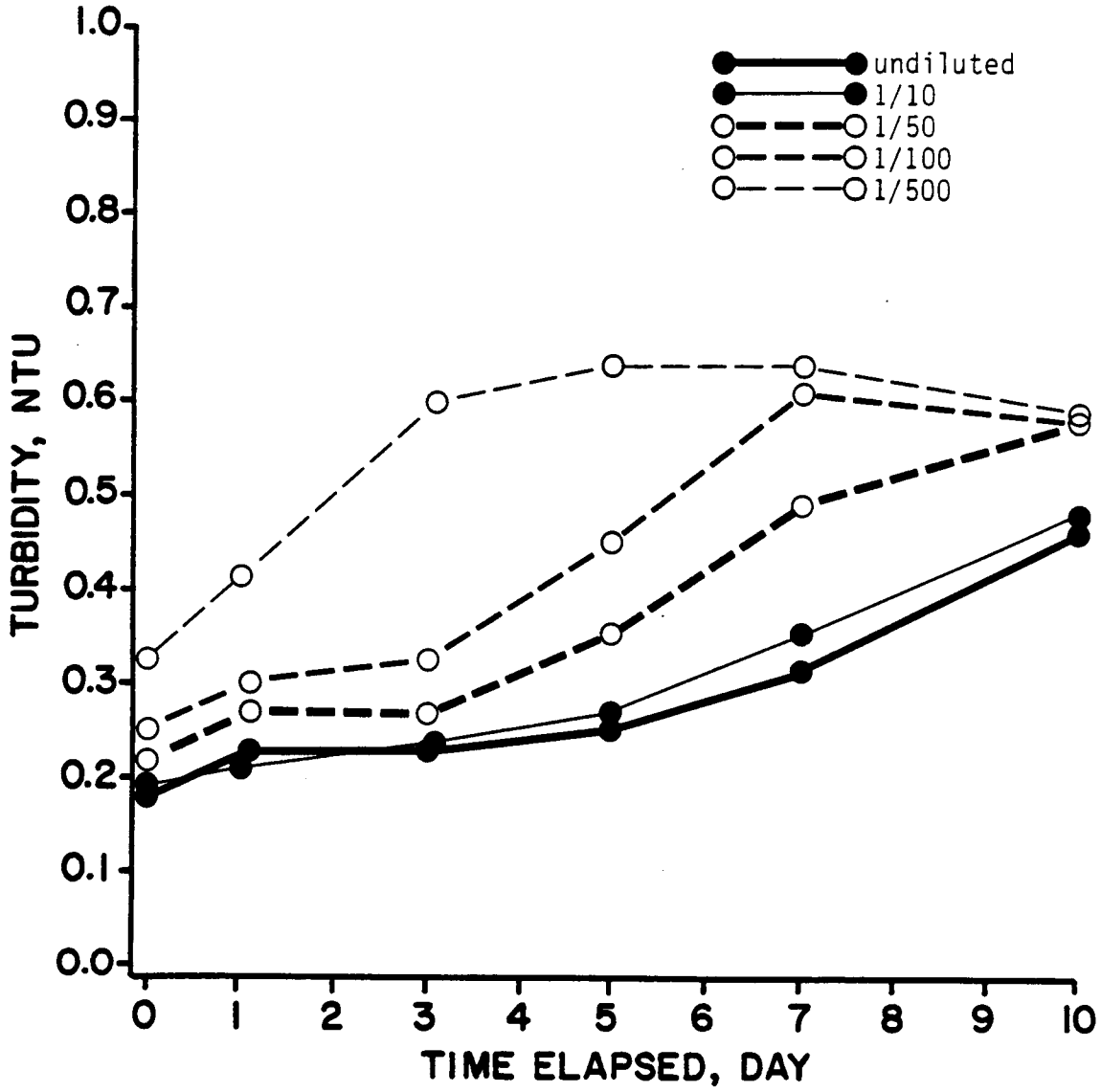


Figure 30. Dilution Effects for 3.75 Ratio Sodium Silicate at ~13 mg SiO_2/L--pH Controlled: Turbidity.

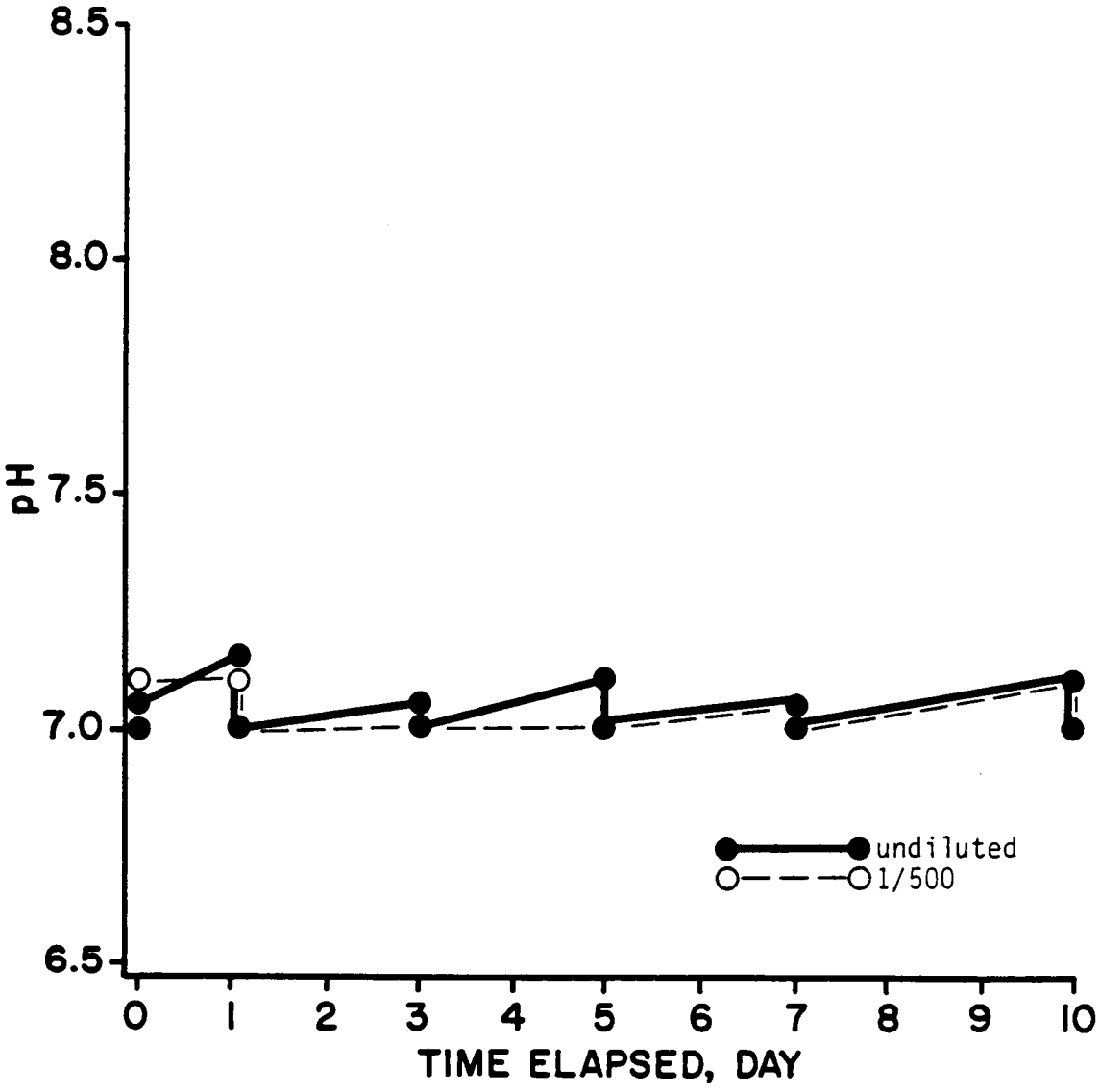


Figure 31. Dilution Effects for 3.75 Ratio Sodium Silicate at ~13 mg SiO_2/L--pH Controlled: pH.

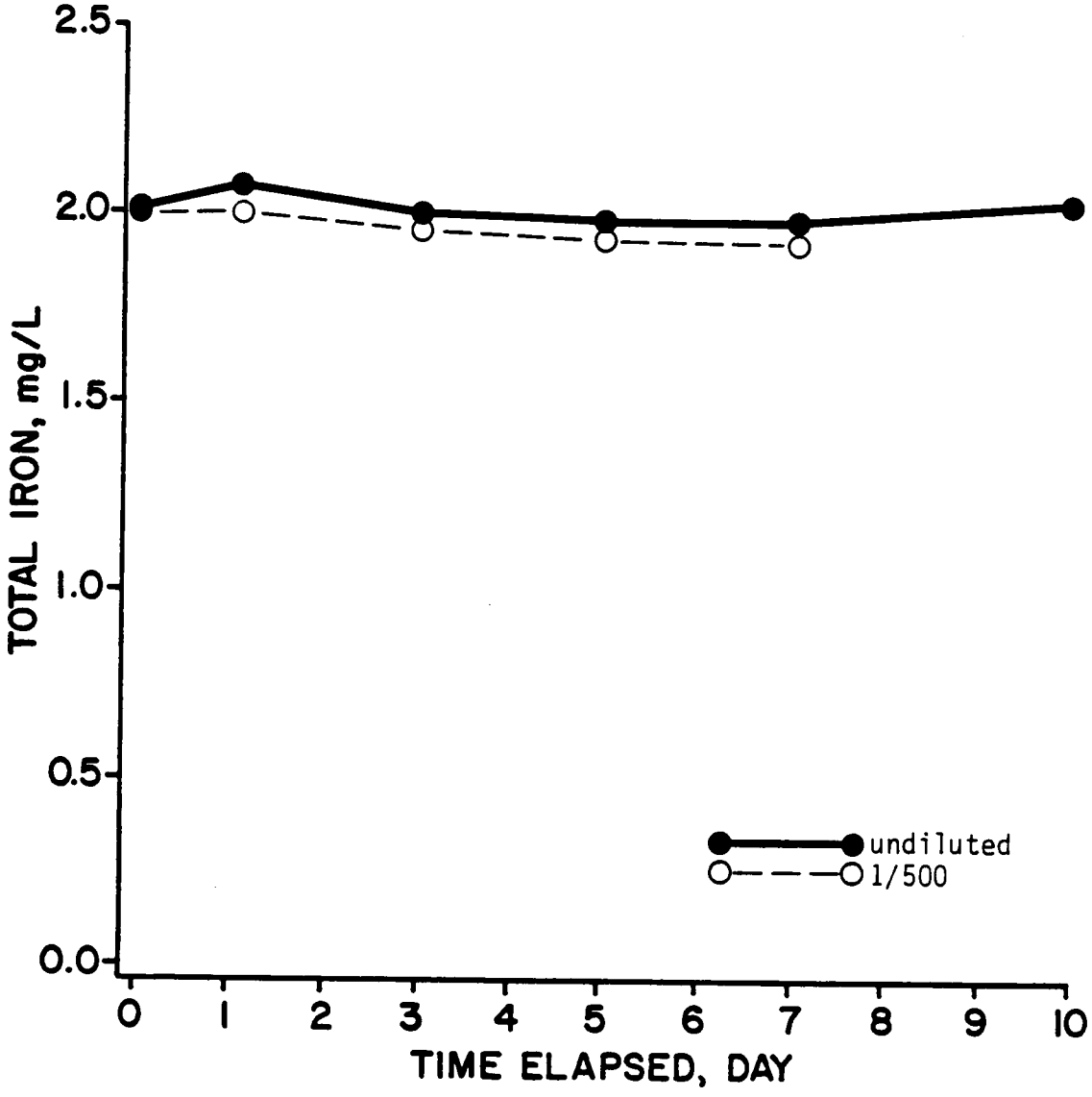


Figure 32. Dilution Effects for 3.75 Ratio Sodium Silicate at ~13 mg SiO_2/L--pH Controlled: Total Iron.

Table 11. Data on Dilution Effects for 2.5 and 3.75 Ratio Sodium Silicates at 13-14 mg SiO_2/L with pH Controlled

Jar No.	Silicate SiO_2/Na_2O Ratio	Dose[a]	Dilution	Day 0 Turb[b]	0 Tot Fe[c]	0 Filt[d]	0 pH	1.0 Turb	1.0 Tot Fe	1.0 Filt	1.0 pH	3.1 Turb	3.1 Tot Fe	3.1 Filt	3.1 pH	5.0 Turb	5.0 Tot Fe	5.0 Filt	5.0 pH	7.0 Turb	7.0 Tot Fe	7.0 Filt	7.0 pH	10.0 Turb	10.0 Tot Fe	10.0 Filt	10.0 pH
1[f]	2.5	13.3	Undil.	0.13	2.03	99	7.1	0.135	2.05	97	7.1	0.17	2.02	98	7.1-	0.27	2.04	84	7.1	0.43	2.03	6	7.1	0.465	2.03	2	7.1
2[f]	2.5	13.9	1/10	0.15	2.03	99.5	7.1	0.15	2.02	99	7.1+	0.26	2.00	95	7.1	0.48	2.01	3	7.0	0.48	1.98	1	7.1	0.45	-	0	7.0
3[f]	2.5	13.8	1/50	0.16	2.03	97	7.1	0.195	2.03	98.5	7.1+	0.31	2.00	90.5	7.1	0.55	2.04	3	7.05+	0.54	2.02	2	7.1	0.52	-	0	7.1
5[f]	2.5	13.5	1/100	0.18	2.01	99	7.1	0.19	2.00	100	7.1	0.35	1.99	81	7.1	0.52	2.01	2	7.0	0.52	1.99	1	7.5	0.48	-	0	7.1
7[f]	2.5	13.2	1/500	0.26	2.06	96	7.1	0.49	2.04	51.5	7.15	0.59	1.96	2	7.1	0.57	1.96	0	7.05+	0.58	1.92	0	7.1	0.56	-	0	7.1
8	3.75	14.5	Undil.	0.18	2.02	100	7.1	0.205	2.04	96	7.1	0.23	2.00	97.5	7.05	0.25	2.01	96	7.0+	0.29	2.00	95.5	7.1	0.44	2.02	28	7.1
9[g]	3.75	13.3	1/10	0.195	2.03	99.5	7.1	0.21	2.01	98.5	7.15	0.24	2.00	99	7.05-	0.27	2.02	96.5	7.05	0.35	2.02	90	7.05	0.48	2.02	18	7.1
17[g]	3.75	13.3	1/500	0.32	2.00	95	7.1	0.41	2.00	84	7.1	0.60	1.96	16	7.0	0.64	1.94	6	7.0+	0.64	1.93	3	7.05	0.59	-	0	7.1

a. Reported as mg SiO_2/L

b. Turbidity, NTU

c. Total iron, mg Fe/L

d. Iron filterability, %

e. Measurement made before any readjustment to pH 7

f. Plotted in Figure 33

g. Plotted in Figure 29

filterability in accordance with the previously demonstrated inverse relationship between those two parameters. The pH and total iron data (Figure 31,32, respectively) indicated good system control with no background anomalies.

Data for the comparison of the treatment effectiveness of various dilutions of 2.5 ratio silicate dosed at 13.2 to 13.9 mg SiO_2/L are presented in Figures 33 to 36 and in Table 11. Figure 33 showed a progressive decrease in effectiveness at maintaining extended high iron filterabilities in going from the undiluted to the higher dilution silicate solutions. The filterability patterns for the 1/10, 1/50, and 1/100 dilutions between days 3 and 5 were almost identical. This may well be, in part, a function the inadequate resolution resulting from too large a sampling interval. In other words, with a smaller sampling interval between days 3 and 5, the data would probably have shown steeper decreases for the higher dilutions resulting in a greater separation among these treatment filterabilities. Nonetheless, the overall trend fits the pattern of the previously discussed silicates--3.75 and 3.22 ratios. The turbidity data (Figure 34) supported the filterability patterns (Figure 33), as before. The pH and total iron data (Figure 35, and 36, respectively) again indicated good system control with no background anomalies.

Data for the comparison of the treatment effectiveness of various dilutions of 1.8 ratio silicate dosed at 13.2 to 14.6 mg SiO_2/L are presented in Figures 37 to 40 and in Table 12. Figure 37 showed only a small difference in performance among the undiluted and the three lowest dilutions (1/10, 1/50, 1/100) of this silicate. This was

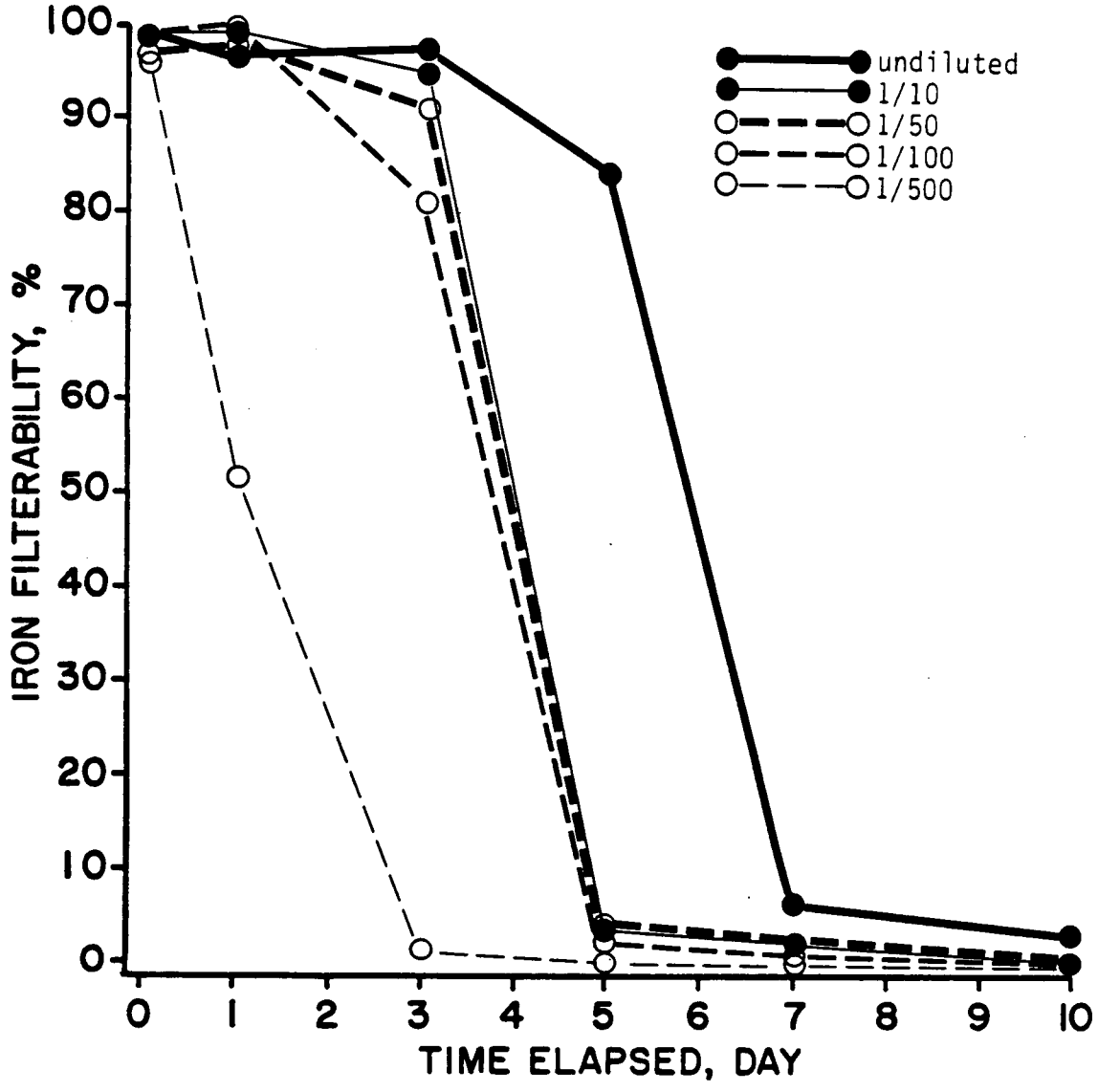


Figure 33. Dilution Effects for 2.5 Ratio Sodium Silicate at 13-14 mg SiO_2/L--pH Controlled: Iron Filterability.

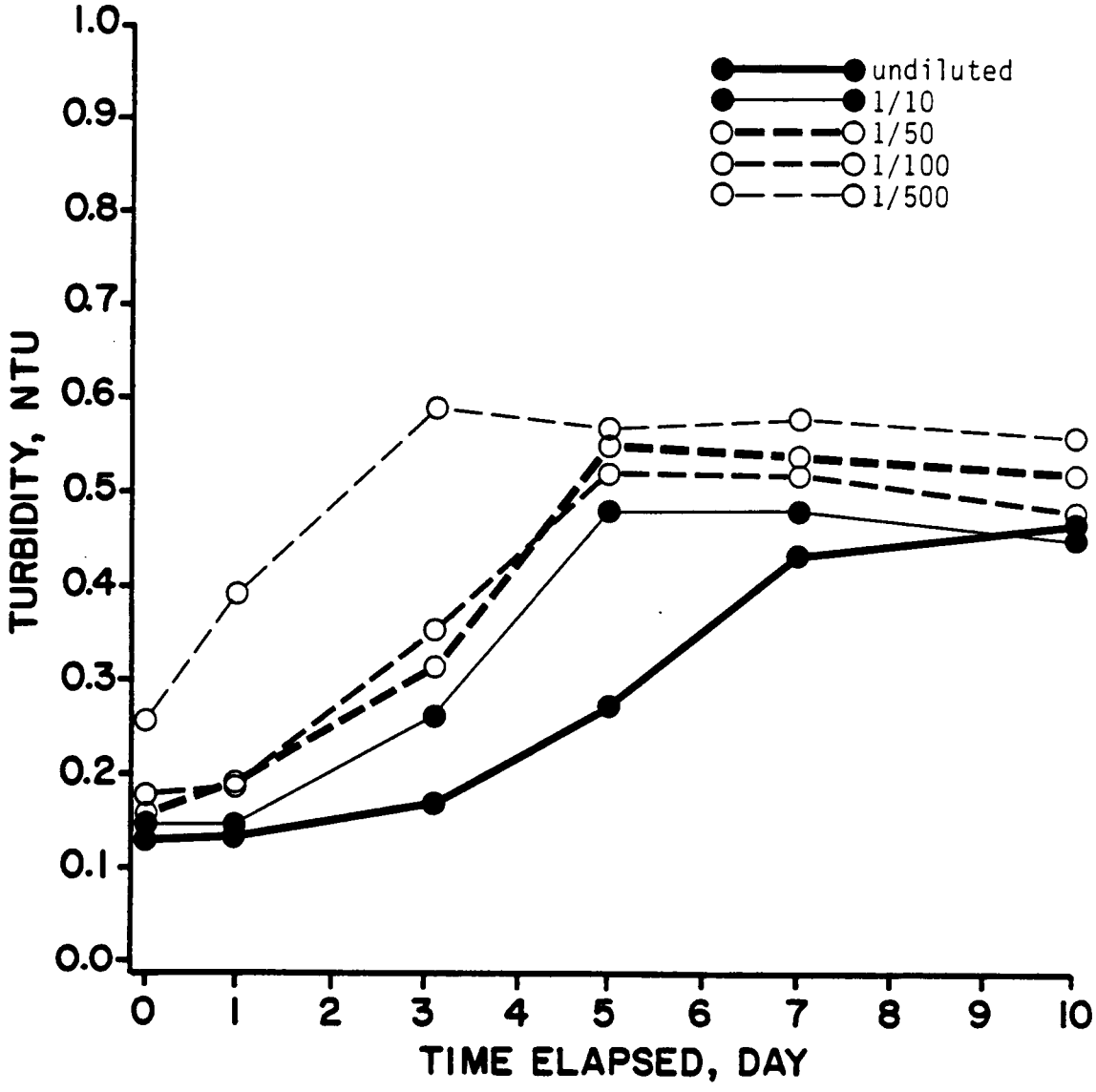


Figure 34. Dilution Effects for 2.5 Ratio Sodium Silicate at 13-14 mg SiO_2/L--pH Controlled: Turbidity.

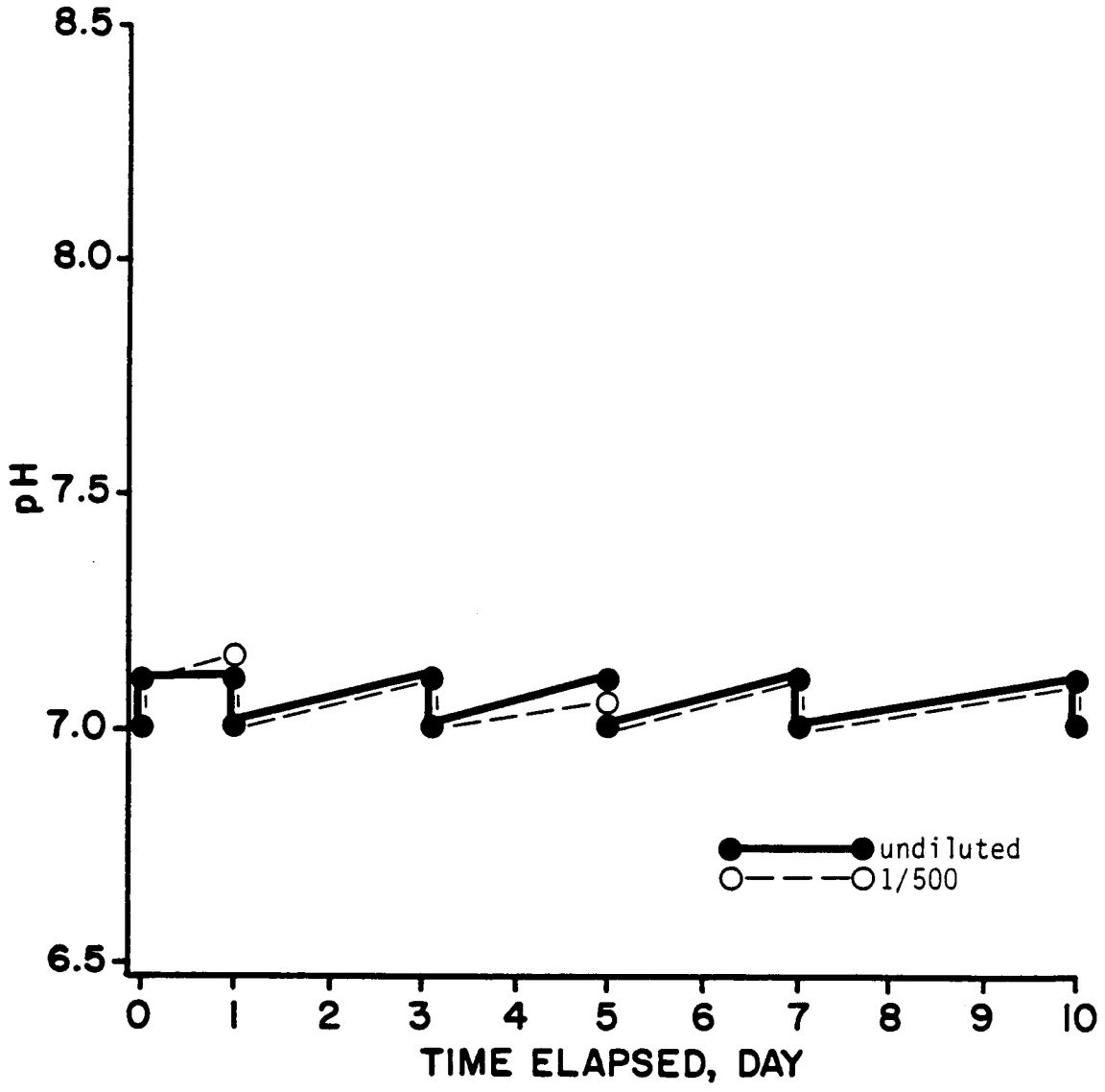


Figure 35. Dilution Effects for 2.5 Ratio Sodium Silicate at 13-14 mg SiO_2/L--pH Controlled: pH.

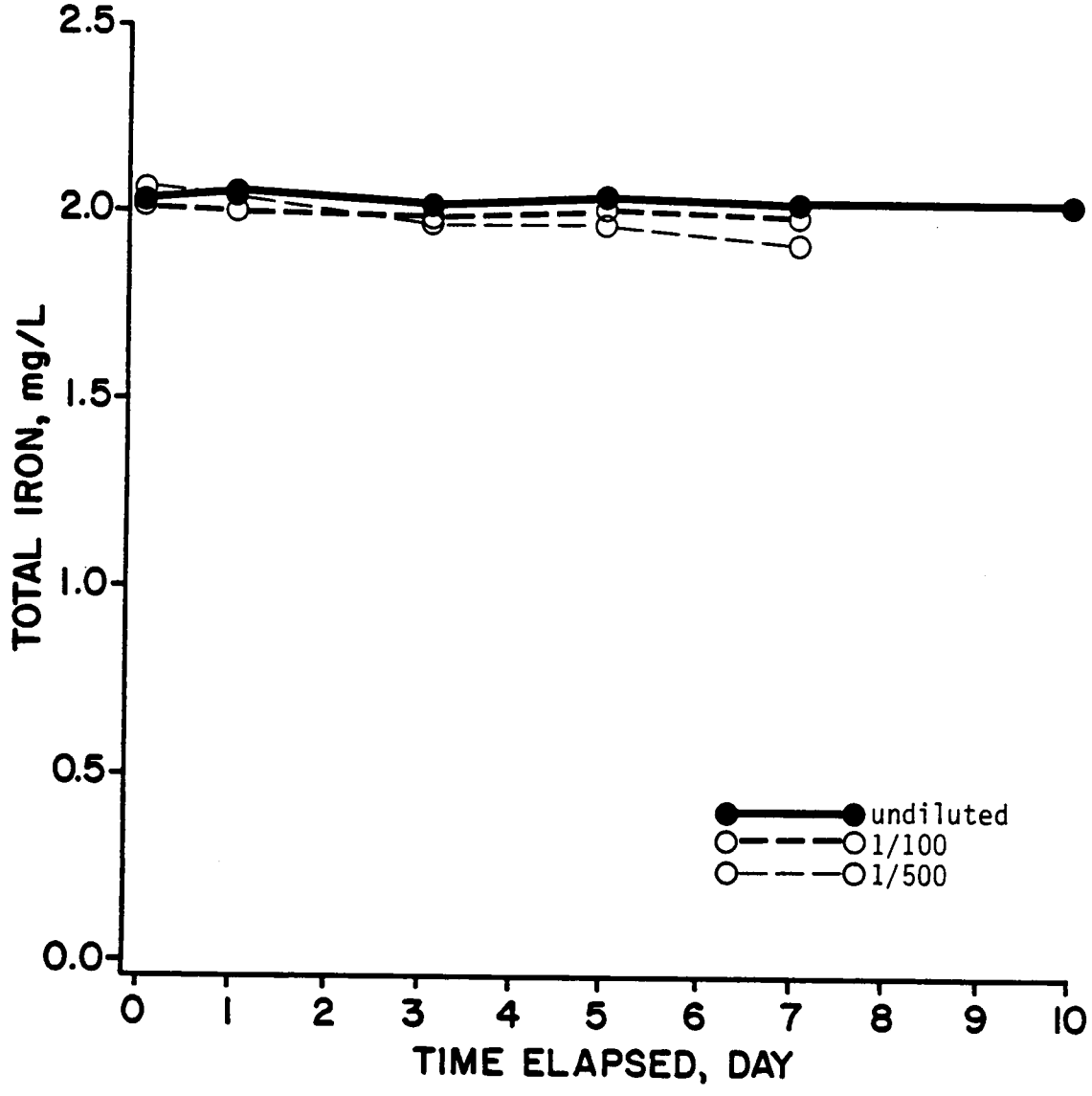


Figure 36. Dilution Effects for 2.5 Ratio Sodium Silicate at 13-14 mg SiO_2/L--pH Controlled: Total Iron.

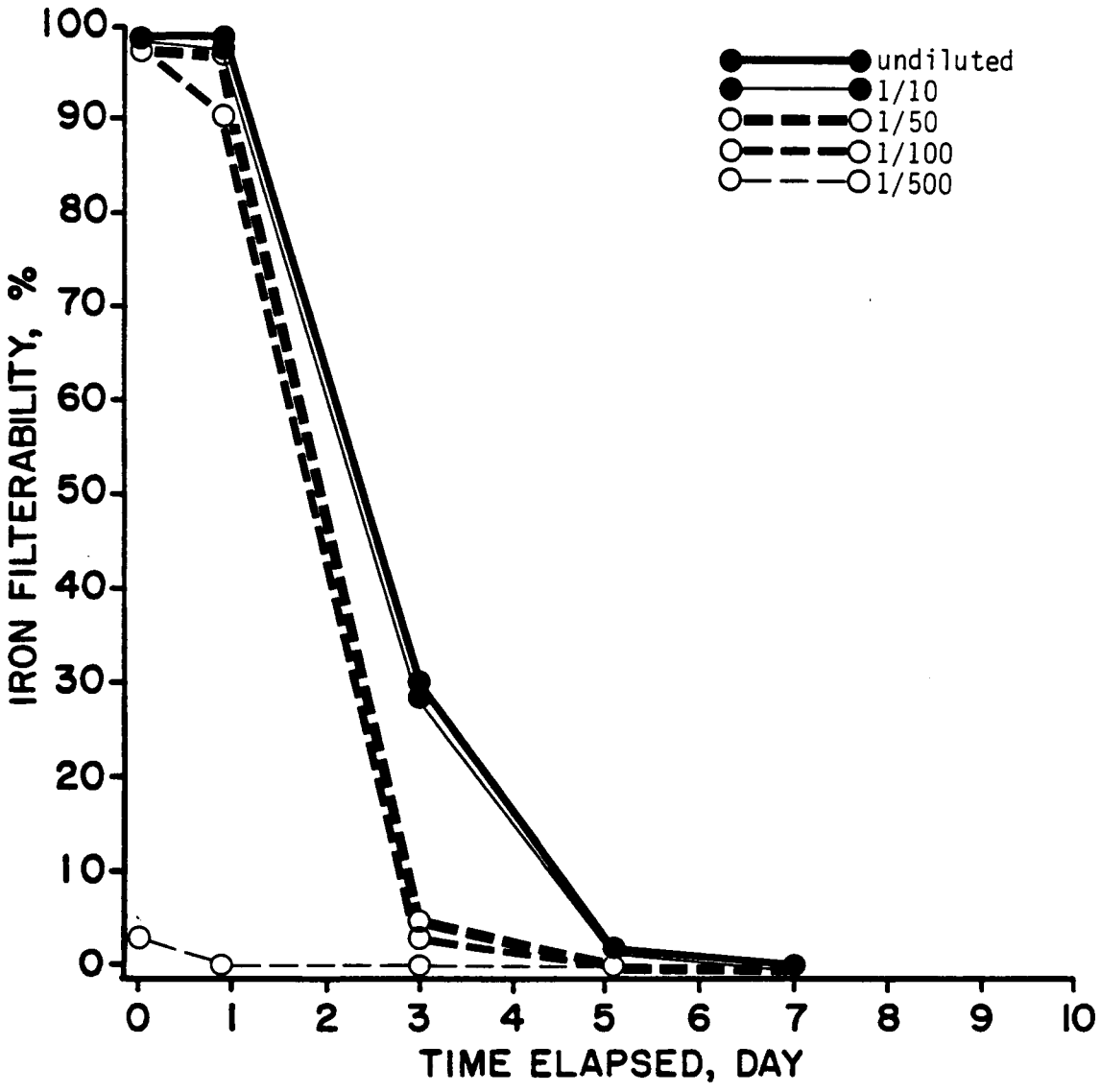


Figure 37. Dilution Effects for 1.8 Ratio Sodium Silicate at 13-15 mg SiO_2/L--pH Controlled: Iron Filterability

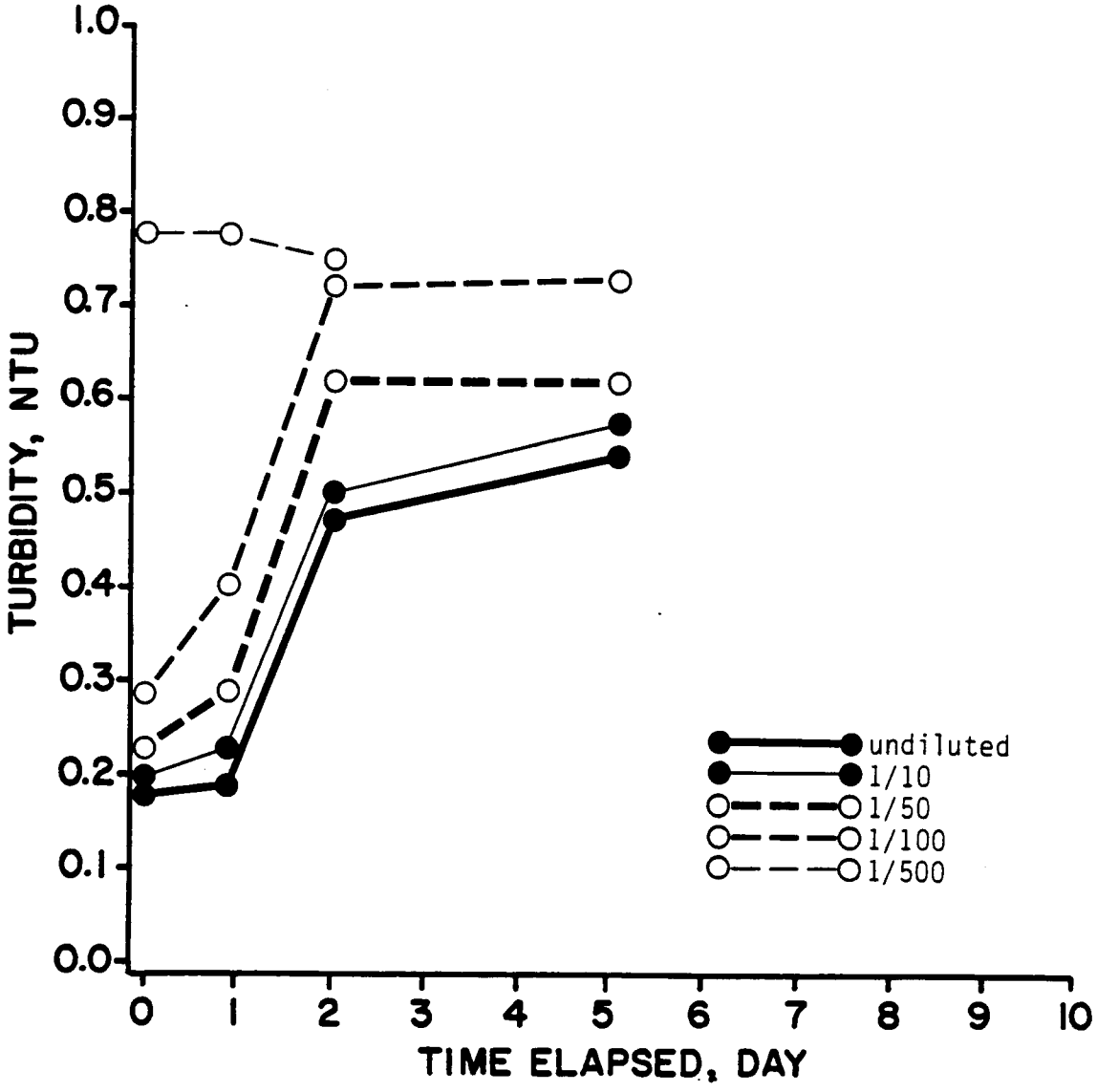


Figure 38. Dilution Effects for 1.8 Ratio Sodium Silicate at 13-15 mg SiO_2/L--pH Controlled: Turbidity.

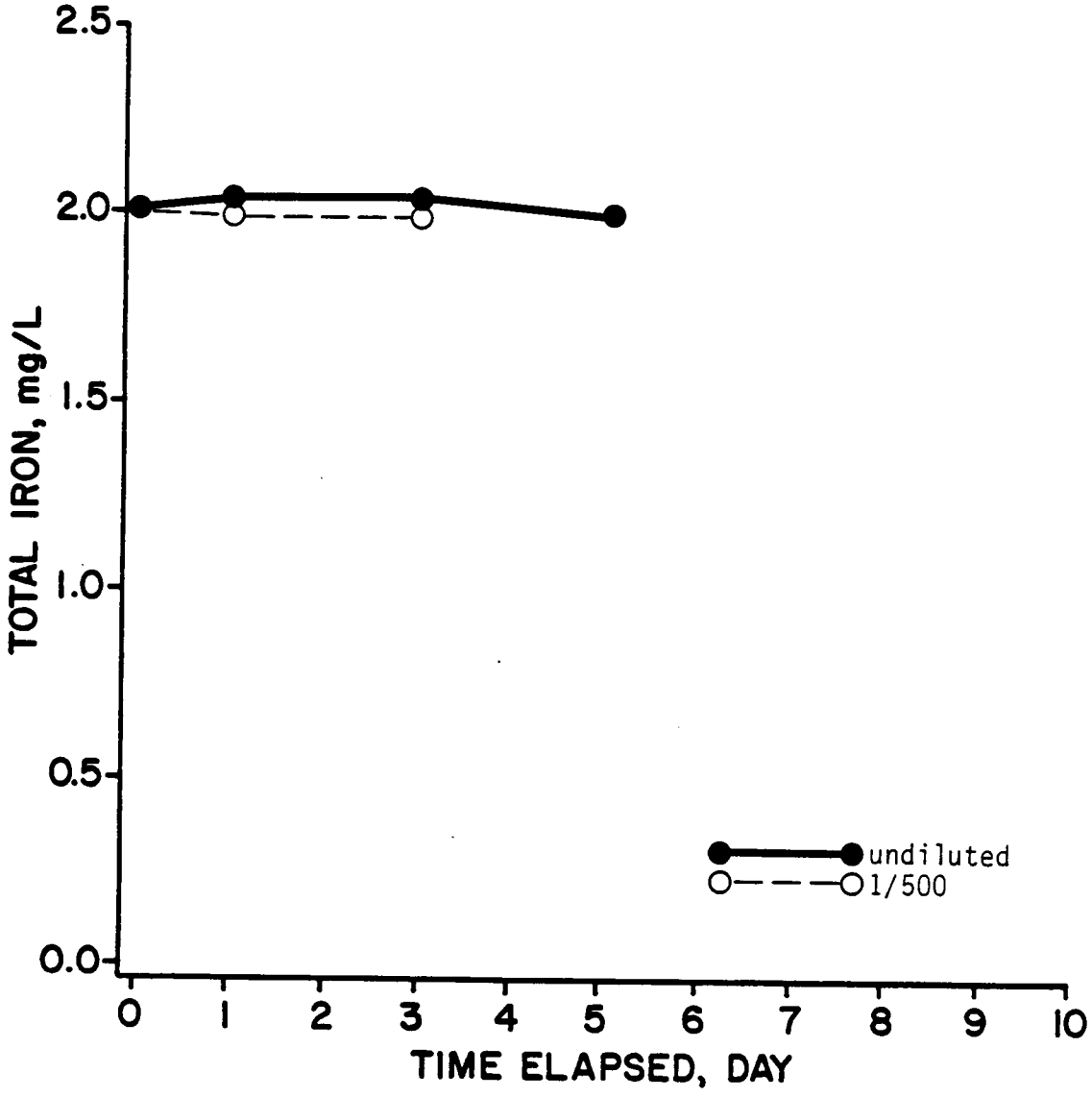


Figure 39. Dilution Effects for 1.8 Ratio Sodium Silicate at 13-15 mg SiO_2/L--pH Controlled: Total Iron.

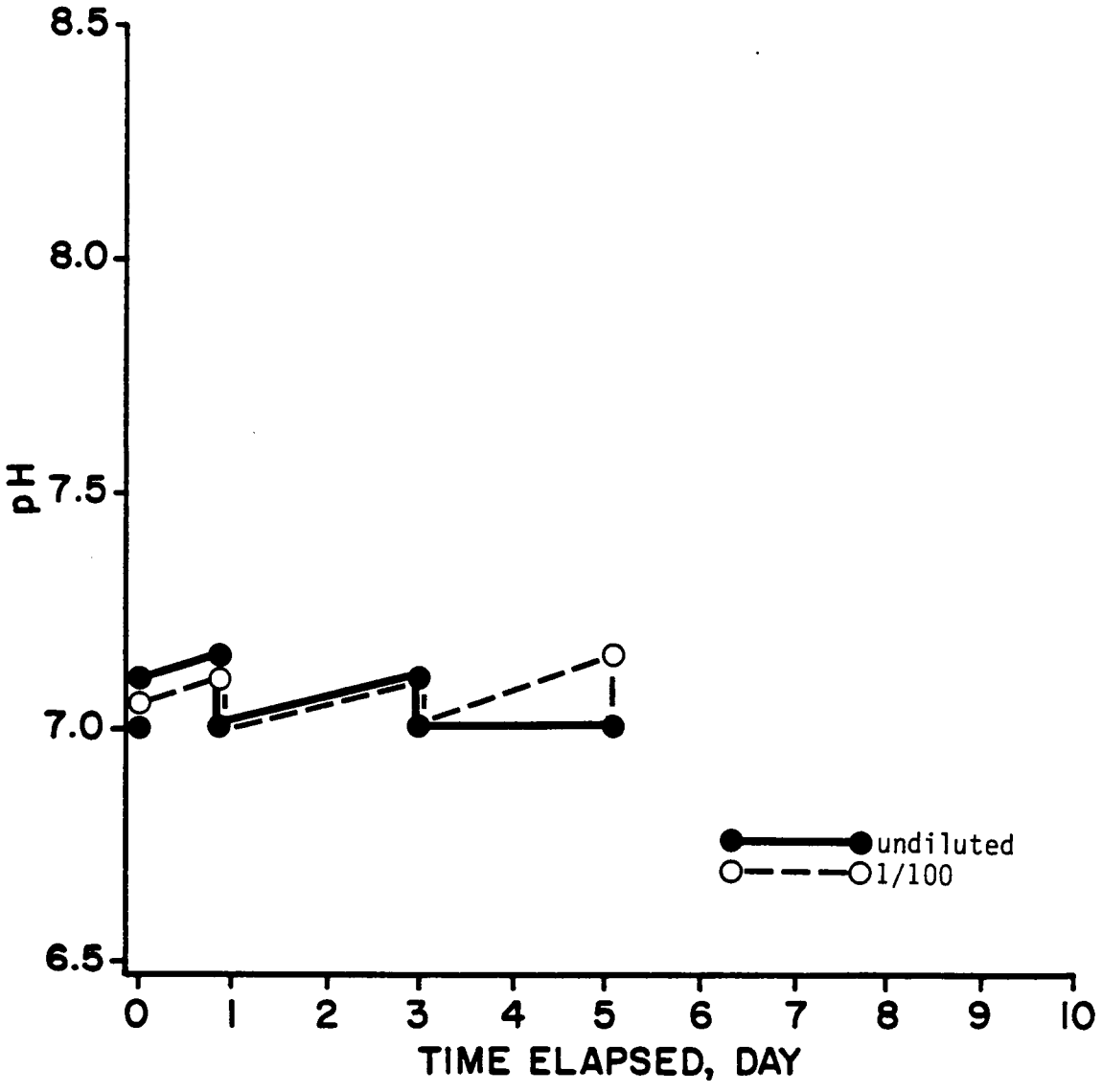


Figure 40. Dilution Effects for 1.8 Ratio Sodium Silicate at 13-15 mg SiO_2/L--pH Controlled: pH.

Table 12. Data on Dilution Effects for 1.8 and 2.5 Ratio Sodium Silicates at 13-15 mg SiO_2/L with pH Controlled

Jar No.	Silicate SiO_2/Na_2O Ratio	Dose[a]	Dilution	Day 0 Turb[b]	0 Tot Fe[c]	0 Filt[d]	0 pH	0.9 Turb	0.9 Tot Fe	0.9 Filt	0.9 pH	3.0 Turb	3.0 Tot Fe	3.0 Filt	3.0 pH	5.1 Turb	5.1 Tot Fe	5.1 Filt	5.1 pH	7.0 Turb	7.0 Tot Fe	7.0 Filt	7.0 pH	9.7 Turb	9.7 Tot Fe	9.7 Filt	9.7 pH
1[f]	1.80	13.0	Undil.	0.18	2.01	99	7.1	0.19	2.04	99	7.15	0.47	2.04	30	7.1	0.54	2.00	2	7.0	-	-	0	-	-	-	0	-
2[f]	1.80	14.3	1/10	0.20	2.01	99.5	7.1	0.23	2.05	98	7.15	0.50	2.03	28	7.1	0.575	2.00	2	7.0	-	-	0	-	-	-	0	-
3[f]	1.80	14.6	1/50	0.23	2.02	97.5	7.1-	0.29	2.04	97	7.1	0.62	2.05	5	7.1	0.62	2.00	2.5	7.05	-	-	0	-	-	-	0	-
5[f]	1.80	1.46	1/100	0.29	2.01	98	7.05	0.40	2.04	90	7.1+	0.72	2.03	3	7.1	0.73	2.02	2	7.1-	-	-	0	-	-	-	0	-
7[f]	1.80	13.2	1/500	0.78	2.01	3	7.05	0.775	1.99	0	7.1	0.75	1.99	0	7.1-	-	-	0	-	-	-	0	-	-	-	0	-
8	2.50	13.7	Undil.	0.22	2.03	97.5	7.05	0.25	2.05	98	7.05+	0.28	2.04	97.5	7.05	0.42	1.99	75	7.05	0.54			7.1	0.53			7.0
9	2.50	14.3	1/50	0.25	2.03	98.5	7.1	0.27	2.05	97	7.1	0.32	2.05	96	7.1-	0.43	2.02	81	7.1	0.56			7.1	0.6			7.05
17	2.50	15.1	1/100	0.275	2.04	98	7.1	0.29	2.05	97	7.1	0.36	2.01	97	7.05-	0.65	2.02	3.5	6.9	0.68			7.0	0.62			7.05

a. Reported as mg SiO_2/L

b. Turbidity, NTU

c. Total iron, mg Fe/L

d. Iron filterability, %

e. Measurement made before any readjustment to pH 7

f. Plotted in Figure 37

probably due, in part, to the variability in dosages--undiluted at 13 mg SiO_2/L and 1/10 at 14.6 mg SiO_2/L, and to the limits of resolution between the 1/50 and 1/100 system traces produced by the two-day sampling interval at that "point". In contrast to the others, the 1/500 dilution never demonstrated any ability to sequester iron even on day zero. Thus, the 1.8 ratio silicate showed the same trends in filterability as related to dilution of the feed solutions as demonstrated for the other test silicates--3.75, 3.22, and 2.5. Notably, none of the 1.8 ratio silicate solutions were especially effective at maintaining iron filterability as compared with the higher ratio silicate systems.

A comparison of the relative effectiveness of the various silicate types and dilutions was facilitated by the summary data presented in Table 13. Here, effectiveness was measured by the time taken for the iron filterability to fall to 50%, t_{50}, for each treatment. The 50% filterability was selected as the level for differentiation because, in general, it occurred within the zone of most rapid decrease in iron filterability with time for each treatment and thus allowed the clearest distinction among treatment performances. Examination of the data in Table 13 readily confirmed the trends discussed previously for dilution of each silicate type, and additional ones with regard to differences among the various types, as a group. Thus, except for the t_{50} values for the 3.22 ratio undiluted and 1/10 dilution values which seem to be reversed, in general, for each ratio silicate there was a decrease in t_{50} value with increasing dilution in each silicate stock solution for a given silica dose. A decrease in t_{50} values indicated a reduced effectiveness at maintaining iron filterability. This result agreed

Table 13. Comparative Effectiveness of Various Dilutions of Selected Sodium Silicates at Maintaining Iron Filterability[a]

Dilution	Time elapsed to 50% filterability for silicate with m-ratio of			
	3.75	3.22	2.5	1.8
	Days			
undiluted	9.8	6.7	5.8	2.4
1/10	8.7	7.6	4.1	2.4
1/50	6.2	5.9	4.0	2.0
1/100	5.5	4.2	3.8	1.9
1/500	2.1	1.0	1.1	0

a. at 13-15 mg SiO_2/L

with the findings of Dart and Foley (6) that undiluted was the most effective dilution of 3.22 ratio silicate at sequestering aqueous iron. Moreover, comparison of t_{50} values among silicate types by dilution demonstrated a general trend of increased effectiveness with increase in m-ratio value. Thus, for the undiluted treatments, the t_{50} values were 2.4, 5.8, 6.7, and 9.8 days, for the 1.8, 2.5, 3.22, and 3.75 ratio silicates, respectively. This trend was consistent with increased effectiveness being associated with those silicates having higher levels of silica polymerization.

As discussed earlier in the section on silicate characterization K_1 and P_0 values for the silicate solutions were quantitative indicators of the state of polymerizaton of silicates. Accordingly, simple regression analysis of filterability and silicate reactivity data provided good statistical support regarding the role of silica polymerization in maintaining iron filterability. Simple regression equations for the relationship between the t_{50} values for the undiluted silicates (Table 13) and the corresponding K_1 and P_0 values (Table 3) individually were:

$$t_{50} = 8.71 - 49.1\ K_1 \qquad 42$$

and

$$t_{50} = -60.2 + 0.793\ P_0 \qquad 43$$

In both instances n, the number of statistical samples, was 4. For equation 42, the correlation coefficient, r = -0.908 and was significant at greater than the 95% probability level. For equation 43, r = +0.834, which was significant at greater than the 90% probability level. Because of the small number of samples no attempt was made to

do any multiple regression analysis on these data using K_1 and P_0 together as independent variables. Nonetheless, these correlation equations (numbers 42 and 43) showed that, for the undiluted silicates, the effectiveness of the treatment was directly and inversely related to the K_1 and P_0 characteristics, respectively, of the silicate solutions.

Statistical Analysis

In order to establish objectively the relative importance of the measured variables in the determination of the iron filterability, more extensive statistical analyses were conducted. For this purpose, multiple linear regression was the method of choice. By this technique, a selected dependent variable is expressed as a function of the measured independent variables, based on the data fed into the system. The resultant multiple regression equations were analyzed by a general linear models GLM procedure (50) and had the following general form:

$$Y_i = B_0 + B_1 Xi_2 + B_2 Xi_2 + \text{---} + B_{p-1} X_{i(p-1)} + Ei \qquad 44$$

where

Y_i = response of the dependent variable on the ith observation,

$X_{i1}, X_{i2}, \text{---}$ = values of the independent variables on the ith observation.

$B_0, B_1, \text{---}$ = coefficients derived from the regression process

i = observation number

E_i = mean of the error distribution of Y.

Multiple linear regression analysis was conducted on three sets of iron filterability-silicate reactivity data as determined by the nature of the data available, and by the desired relationship. For the two major sets, the primary independent variables included time, silica dose, percent polymer (P_0) of silicate solution, and the reactivity coefficient (K_1) of the silicate solution, with the % iron filterability as the dependent variable. For the third data set, the dependent variable was the time taken for the % iron filterability to decrease to 50% (t_{50}), whereas the independent variables included only silica (SiO_2) dose, K_1, and P_0. The t_{50} values were considered to be a coarse assessment of treatment effectiveness with higher t_{50}'s being associated with better effectiveness.

The regression models applied to the third data group are presented in Table 14 along with the corresponding values for the various tests of significance as applied to each model as a whole. The third group included only data from experiments with the various dilutions of N silicate (Tables 8, 9, 10). Results in Table 14 showed the best models, as indicated by R^2 values, to be numbers 1 and 3, which included three independent variables involving SiO_2 dose, P_0 and K_1. A comparison of models 1 and 2 showed that although dropping K_1 as a variable reduced the predictability of t_{50} based on R^2 values, nevertheless, the significance of the level of predictability remained comparable, based on PR>F values. Table 15 gives the results regarding the significance of the contributions of individual independent variables to model predictability. A survey of these results (Table 15) showed P_0 by itself, squared, or combined with K_1, to be the most

Table 14. Statistical Models Applied to Dilutions of 3.22 Ratio Sodium Silicate with t_{50}, the Time to 50% Filterability, as Dependent Variable

	Model[a]	R^2[b]	F[c]	PR>F[c]	C.V.[d]
1.	$t_{50} = -15.5 + 0.083\ P_0 + 1.03\ SiO_2 + 77.3\ K_1$	0.724	7.87	0.0069	31.1
2.	$t_{50} = -16.6 + 0.079\ P_0 + 1.26\ SiO_2$	0.625	8.32	0.0074	34.4
3.	$t_{50} = -7.40 + 0.00075\ P_0^2 + 0.0456\ (SiO_2)^2 + 1774\ K_1^2$	0.715	7.52	0.0080	31.6
4.	$t_{50} = -2.95 + 1.89\ P_0 * K_1 + 0.404\ SiO_2$	0.556	6.26	0.0173	37.4

a. SiO_2 in mg/L; P_0 in %, and K_1 in min^{-1} measured at 21°C.

b. R^2 is a measure of how much variation in the dependent variable can be accounted for by the model.

c. F is the ratio of the mean square of the model divided by the mean square of the error. If the significance probability, PR>F, is small then the model accounts for the dependent variable well.

d. C.V. = coefficient of variation = standard deviation of the dependent variable divided by the mean, times 100, and describes the amount of variation in the population.

Table 15. Probability Significance of Individual Independent Variables in Models Applied to Dilutions of 3.22 Ratio Sodium Silicate with t_{50}, the Time Elapsed to 50% Filterability, as Dependent Variable

Model[a] No.	PR>/T/[b]						
	P_0	SiO_2	K_1	P_0^2	$(SiO_2)^2$	K_1^2	P_0*K_1
1[c]	0.0027	0.0127	0.1056	---	---	---	---
2	0.0051	0.0040	---	---	---	---	---
3	---	---	---	0.0038	0.0150	0.0786	---
4	---	0.2054	---	---	---	---	0.0126

a. SiO_2 in mg/L; P_0 in %, and K_1 in min^{-1} measured at 21°C.

b. If the significance probability, PR>/T/, is small then variation in the independent variable contributes signficantly to the variation in the dependent variable.

c. Model numbers are the same as those in Table 14.

significant, except when included with SiO_2 dose in model 2. K_1 was consistently the least significant except when multiplied by with P_0 in model 4.

The major variables controlling treatment effectiveness, based on by the above analysis, were P_0--the percent polymer, and the silica dose, both of which were positively related to t_{50}.

Regression models applied to iron filterability and variables for treatments involving only undiluted solutions of the four silicate types are presented in Table 16, along with their statistical tests of significance. Based on R^2 values the variables in model number 4 accounted for the highest proportion (0.586) of the variability in % iron filterability, followed closely by model number 1 -- the addition of each variable raised to unit power. Nevertheless, the low values for PR>F indicated that all of the tested models accounted for the observed variability of the % iron filterability well. The significance of the contributions by the individual independent variables are shown in Table 17. Time, as represented by the variable DAY, either alone or combined with K_1, was consistently the most significant independent variable. In model 1, which includes individually each of the four independent variables used, the order of significance was $DAY>SiO_2>K_1>P_0$. Furthermore, when P_0 was dropped from model number 1 to produce model number 2, the decrease in R^2 value (Table 16) was minimal. Where P_0 was not included, K_1 was more significant than SiO_2 dose.

Notably, as shown by model number 1 in which each variable is included individually, the variables DAY and K_1 were inversely proportional, and P_0 and SiO_2 directly proportional to % iron filterability.

Table 16. Statistical Models Applied to Undiluted 3.75, 3.22, 2.5, and 1.8 Ratio Sodium Silicates with % Iron Filterability as Dependent Variable

	Model[a]	R^2[b]	F[c]	PR>F[c]	C.V.[d]
1.	% FILT = -232 - 8.20 DAY + 2.83 P_0 - 244 K_1 + 8.23 SiO_2	0.553	20.43	0.0001	34.8
2.	% FILT = 19.7 - 8.16 DAY - 401 K_1 + 7.78 SiO_2	0.542	26.44	0.0001	34.9
3.	% FILT = 50.9 - 0.815 DAY^2 - 2606 K_1^2 + 0.307 $(SiO_2)^2$	0.504	22.72	0.0001	36.3
4.	% FILT = 97.3 - 4.23 DAY^2 - 17.4 DAY^2 * K_1 + 0.293 DAY^2 * SiO_2	0.586	31.65	0.0001	33.2
5.	% FILT = 114 - 7.55 DAY - 25.2 K_1 * SiO_2	0.463	29.3	0.0001	37.6

a. SiO_2 in mg/L; DAY in days; P_0 in %, and K_1 in min^{-1} at 25°C.

b. R^2 is a measure of how much variation in the dependent variable can be accounted for by the model.

c. F is the ratio of the mean square of the model divided by the mean square of the error. If the significance probability, PR>F, is small then the model accounts for the dependent variable well.

d. C.V. = coefficient of variation = standard deviation of the dependent variable divided by the mean, times 100, and describes the amount of variation in the population.

Table 17. Probability Significance of Individual Independent Variables in Models Applied to Undiluted 3.75, 3.22, 2.5, and 1.8 Ratio Sodium Silicates with % Iron Filterability as Dependent Variable

Model[a] No.	PR > /T/[b]									
	Day	P_0	K_1	SiO_2	Day^2	K_1^2	$(SiO_2)^2$	Day^2*K_1	Day^2*SiO_2	K_1*SiO_2
1[c]	0.0001	0.2045	0.1316	0.0011	---	---	---	---	---	---
2	0.0001	---	0.0002	0.0019	---	---	---	---	---	---
3	---	---	---	---	0.0001	0.0008	0.0041	---	---	---
4	---	---	---	---	0.0002	---	---	0.0001	0.0007	---
5	0.0001	---	---	---	---	---	---	---	---	0.0033

a. SiO_2 in mg/L; DAY in days; P_0 in %, and K_1 in min^{-1} at 25°C

b. If the significance probability, PR >/T/, is small then variation in the independent variable contributes significantly to the variation in the dependent variable.

c. Model numbers are the same as those in Table 16.

Regression models applied to iron filterability and variables for treatments involving the range of dilutions for the 3.22 ratio silicate alone are presented in Table 18, along with their statistical tests of significance. Based on R^2 values the variable in models 1 and 2 accounted for the highest proportion (0.595) of the variability in % iron filterability. However, the low values for PR>F showed that all of the tested models accounted well for the observed variability in % iron filterability. The significance of the contributions by the individual independent variables are provided in Table 19. A comparison of the values for models 1 and 2 showed the variables DAY, P_0, and SiO_2 to be significant, and more so than K_1. In fact, omitting K_1 from model number 1 produced no measurable reduction in predictability of % iron filterability. In general, the variables DAY, P_0, and SiO_2 were significant contributors whatever the form in which they were included. As observed for the earlier models for % iron filterability, this variable was again inversely related to DAY and K_1, and directly related to SiO_2 and P_0.

The insignificance of P_0, for the models involving the iron filterability of undiluted silicates (Tables 16 and 17), and K_1, for the models involving the iron filterability of the various dilutions of the 3.22 ratio silicates (Tables 18 and 19), provide an apparent contradiction which is readily explained. For the undiluted silicates, the variable P_0 showed a narrow range of values (Table 3) as well as almost identical values for two different ratio silicates (2.5 and 1.8). These factors contributed to the observed weak relationship between % iron filterability and P_0 values (Tables 16 and 17). For the various

Table 18. Statistical Models Applied to Dilutions of 3.22 Ratio Sodium Silicate with % Iron Filterability as Dependent Variable

	Model[a]	R^2[b]	F[c]	PR>F[c]	C.V.[d]
1.	% FILT = -66.2 - 8.93 DAY + 0.654 P_0 - 28.9 K_1 + 10.1 SiO_2	0.595	39.23	0.0001	38.4
2.	% FILT = -65.7 - 8.93 DAY + 0.653 P_0 + 9.98 SiO_2	0.595	52.78	0.0001	38.2
3.	% FILT = 5.17 - 0.845 DAY^2 - 0.0049 P_0^2 + 0.376 $(SiO_2)^2$	0.514	38.04	0.0001	41.9
4.	% FILT = 90.2 - 8.27 DAY^2 + 0.0169 DAY^2 * P_0 + 0.476 DAY^2 * SiO_2	0.576	48.98	0.0001	39.1
5.	% FILT = 14.1 + 0.291 $(SiO_2)^2$ - 0.44 DAY * $(SiO_2)^2$ + 0.0035 P_0 * $(SiO_2)^2$	0.516	38.42	0.0001	41.8
6.	% FILT = 12.6 + 5.78 SiO_2 - 8.62 DAY + 12.6 P_0 * K_1	0.519	38.78	0.0001	41.7

a. SiO_2 in mg/L; DAY in days; P_0 in %, and K_1 in min^{-1} at 21°C

b. R^2 is a measure of how much variation in the dependent variable can be accounted for by the model.

c. F is the ratio of the mean square of the model divided by the mean square of the error. If the significance probability, PR > F, is small then the model accounts for the dependent variable well.

d. C.V. = coefficient of variation = standard deviation of the dependent variable divided by the mean, times 100, and describes the amount of variation in the population.

Table 19. Probability Significance of Individual Independent Variables in Models Applied to Dilutions of 3.22 Ratio Sodium Silicate with % Iron Filterability as Dependent Variable

	PR > /T/[b]											
Model[a] No.	Day	P_0	K_1	SiO_2	Day^2	P_0^2	$(SiO_2)^2$	Day^2*P_0	Day^2*SiO_2	$Day*(SiO_2)^2$	$P_0*(SiO_2)^2$	P_0*K_1
1[c]	0.0001	0.0001	0.9117	0.0001	---	---	---	---	---	---	---	---
2	0.0001	0.0001	---	0.0001	---	---	---	---	---	---	---	---
3	---	---	---	---	0.0001	0.0001	0.0001	---	---	---	---	---
4	---	---	---	---	0.0001	---	---	0.0001	0.0001	---	---	---
5	---	---	---	---	---	---	0.0002	---	---	0.0001	0.0001	---
6	0.0001	---	---	0.0014	---	---	---	---	---	---	---	0.0002

a. SiO_2 in mg/L; DAY in days; P_0 in %, and K_1 in min^{-1} at 21°C

b. If the significance probability, PR >/T/, is small then variation in the independent variable contributes significantly to the variation in the dependent variable.

c. Model numbers are the same as those in Table 18.

dilutions of the 3.22 ratio silicate, the relationship between K_1 and silica concent-ration in the various dilutions (Figure 6) was inconsistent. This irregularity was attributed to the inability of the selected computer program, from which K_1 values were derived, to fit the observed data for the more dilute silicate solutions which showed zones of sharp curvature. These inconsistencies contributed to the observed weak relationship between % iron filterability and K_1 values (Tables 18 and 19).

The relative magnitudes of the R^2 values are useful in making comparisons among the various models and instrictive in suggesting or explaining mechanisms. However, none of the R^2 values are high enough to allow the models to be used for engineering design purposes.

Ultrafiltration

In order to provide a more detailed understanding of the changes in particle size distribution of iron particulates with time, filterability was examined further by applying ultrafiltration, in addition to 0.1 μm-filtration, to selected silicate treatments. The resultant iron filterabilities and associated data for treatments with 3.75 ratio and 3.22 ratio silicates, each as undiluted and 1/100-dilution solutions, are presented in Figures 41 to 47, and Table 20.

The general trends for standard (<0.1 μm) iron filterability were the same as before for these dilutions--essentially complete or substantial filterability being maintained through day 5 for all treatments. Also, while the high filterability continued through day 7 for

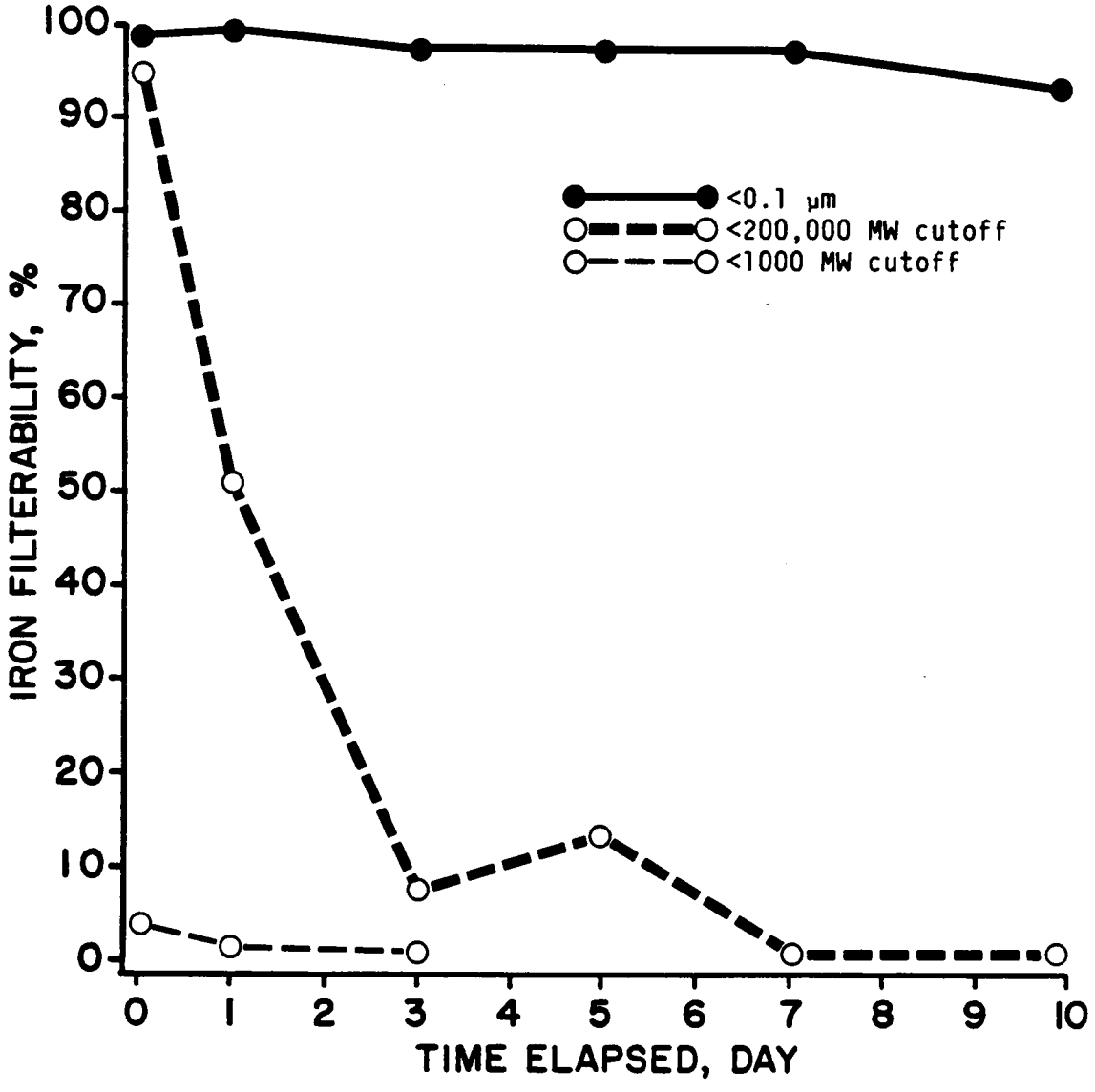


Figure 41. Iron Filterability for an Undiluted 3.75 Ratio Sodium Silicate System at 12.5 mg SiO_2/L under Controlled pH Using Standard Filtration and Ultrafiltration.

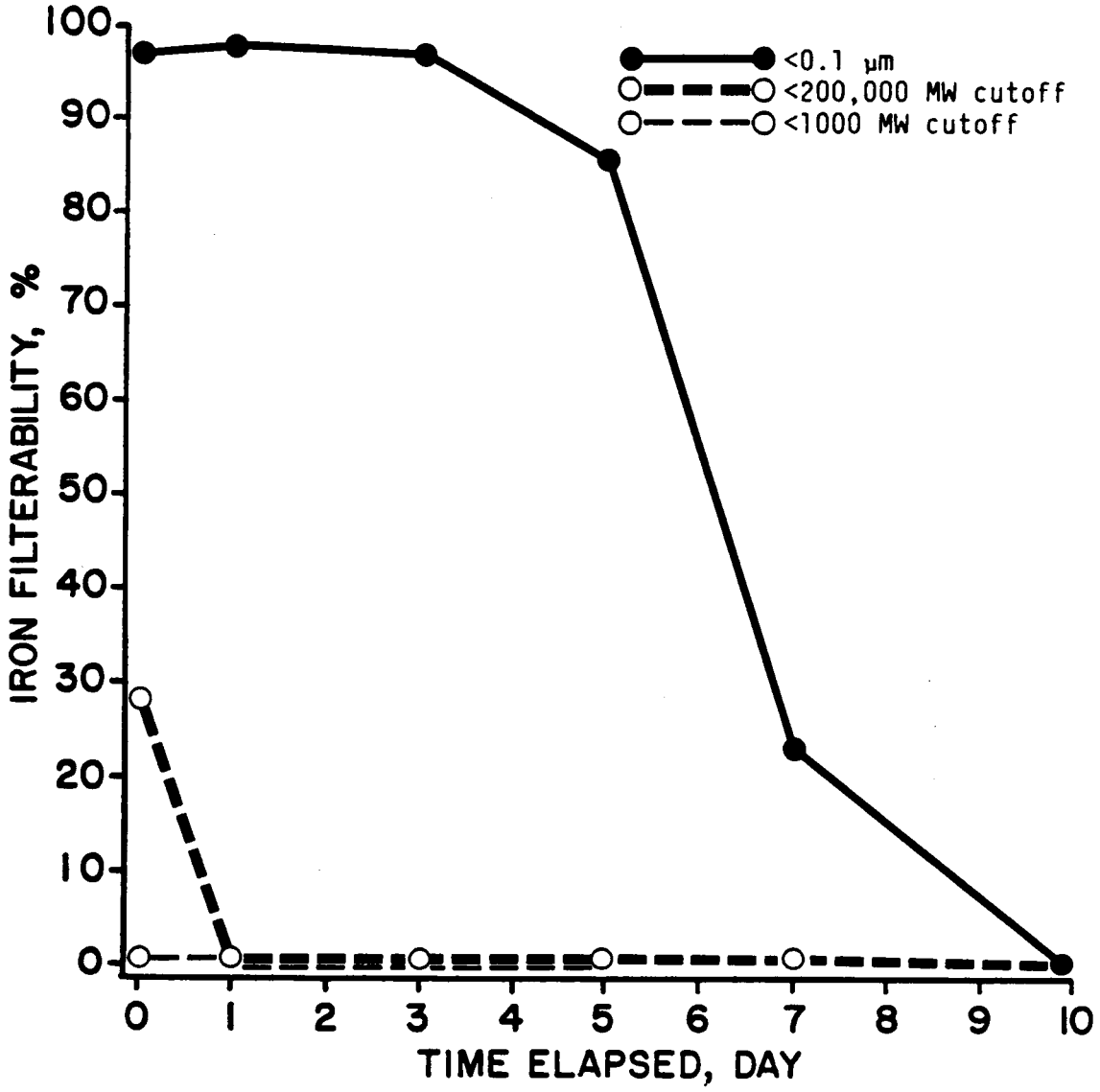


Figure 42. Iron Filterability for a 1/100 Dilution of 3.75 Ratio Sodium Silicate System at 14.1 mg SiO_2/L under Controlled pH Using Standard Filtration and Ultrafiltration.

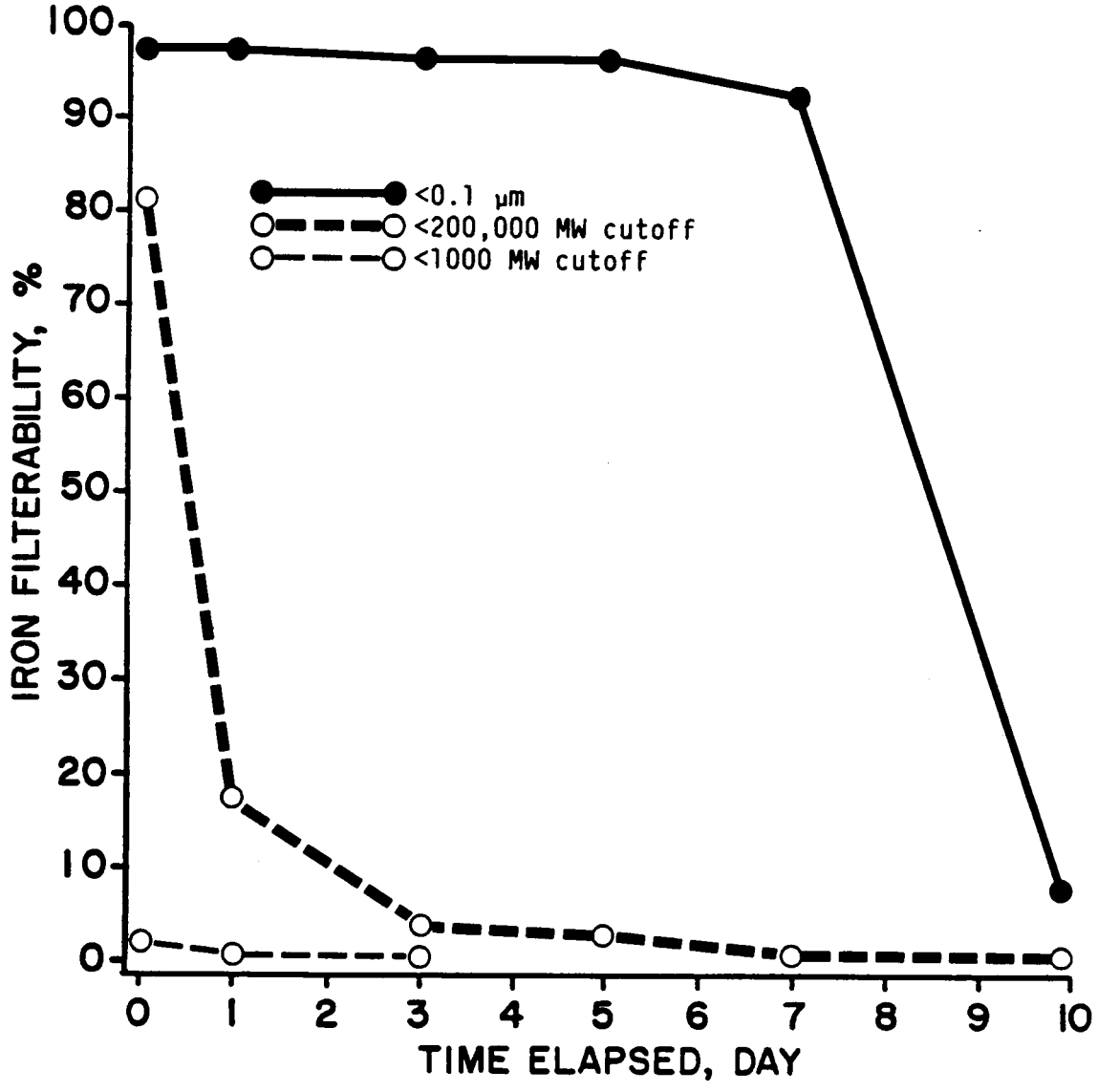


Figure 43. Iron Filterability for an Undiluted 3.22 Ratio Sodium Silicate System at 13.9 mg SiO_2/L under Controlled pH Using Standard Filtration and Ultrafiltration.

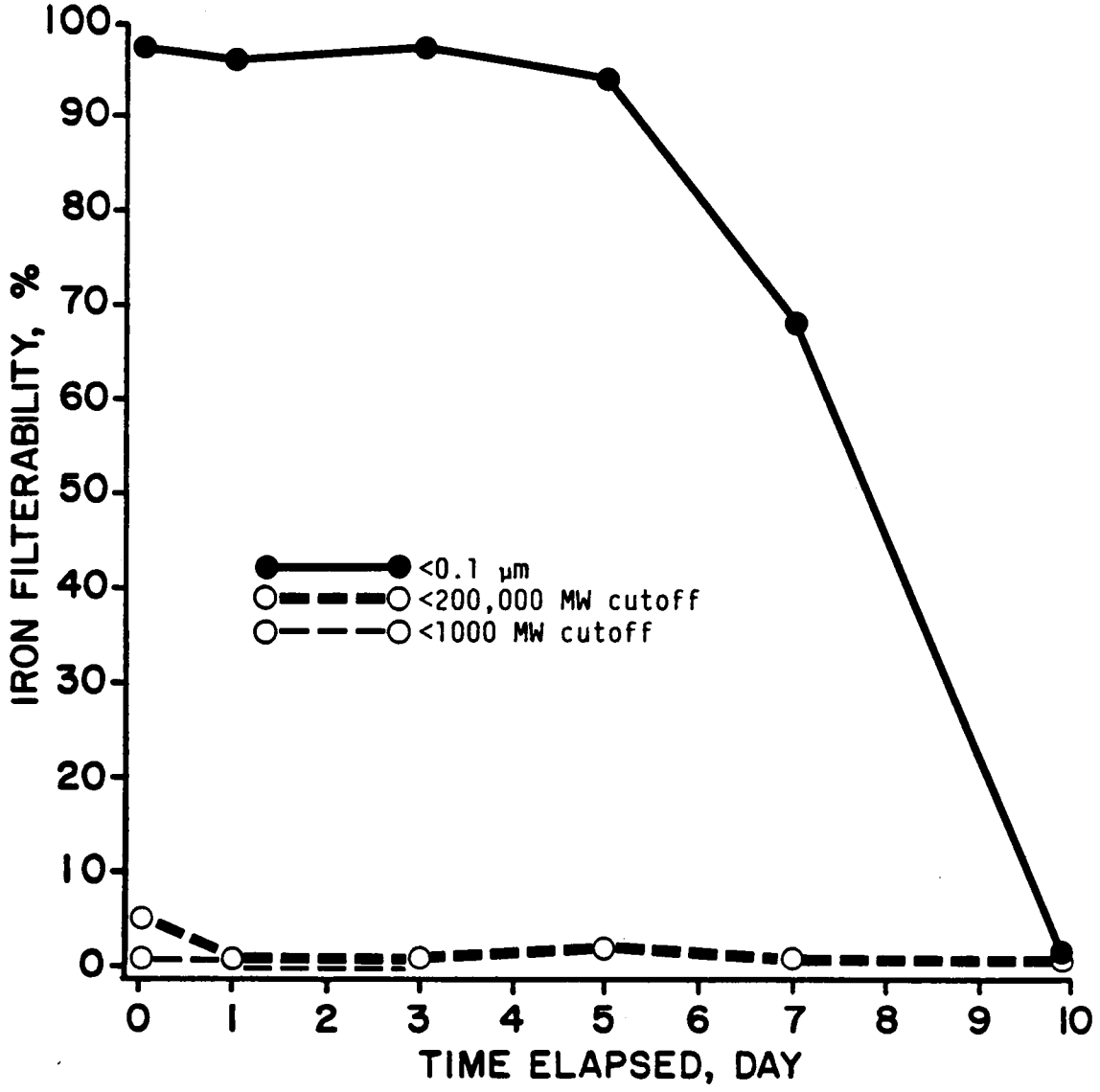


Figure 44. Iron Filterability for a 1/100 Dilution of 3.22 Ratio Sodium Silicate System at 13.8 mg SiO_2/L Under Controlled pH Using Standard Filtration and Ultrafiltration.

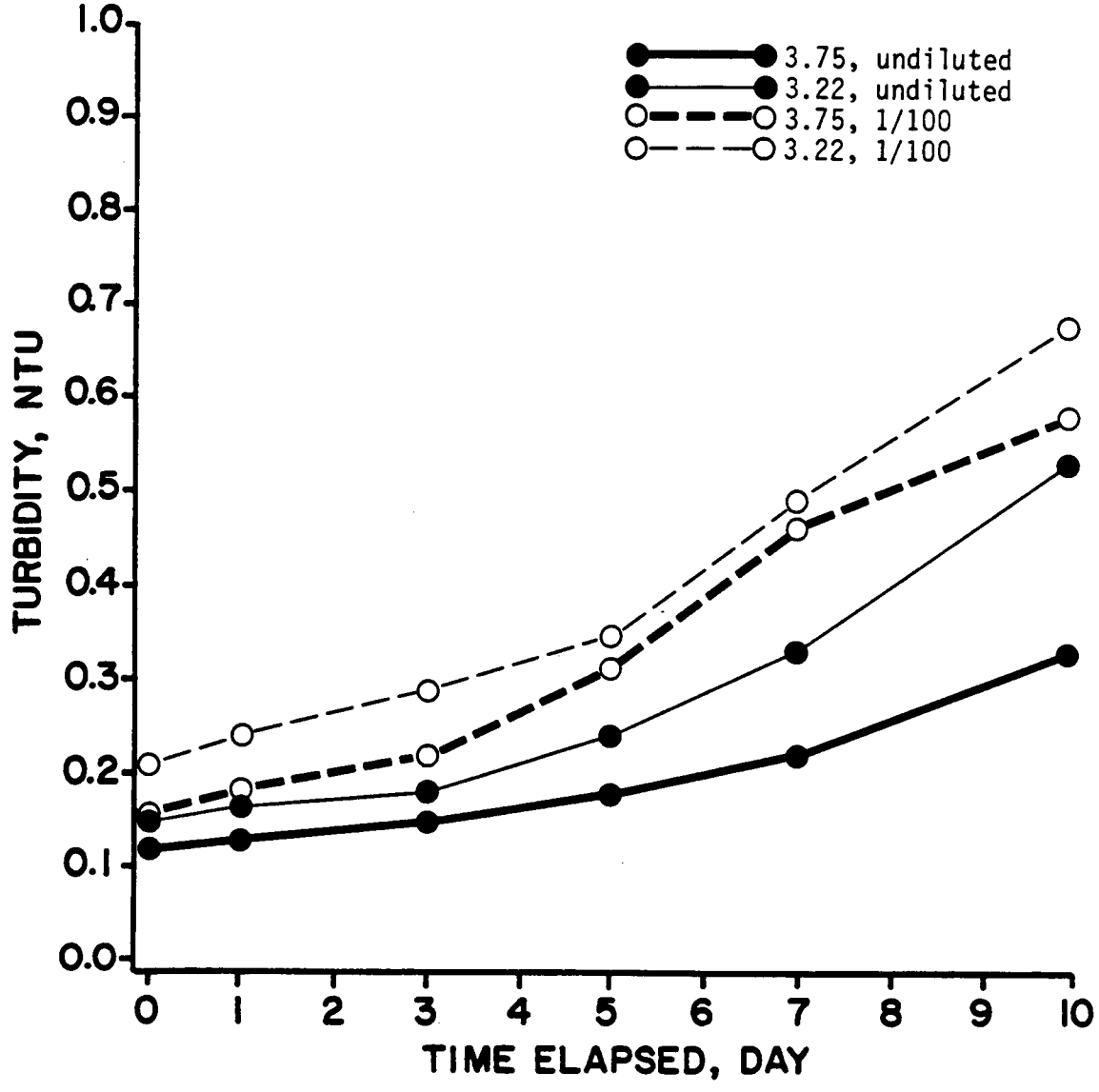


Figure 45. Dilution Effects for 3.22 and 3.75 Ratio Sodium Silicates at 12-14 mg SiO_2/L--pH Controlled: Turbidity.

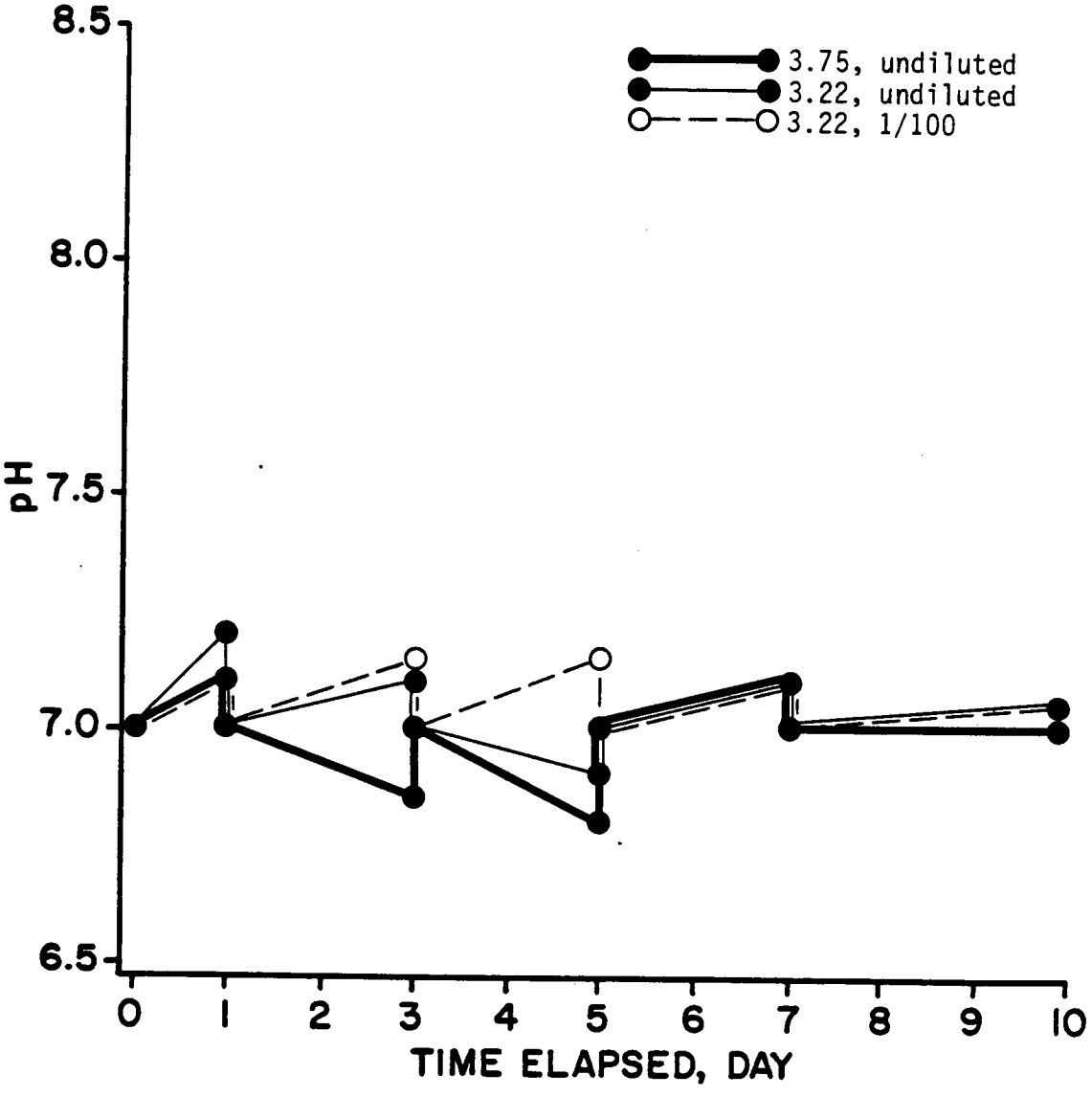


Figure 46. Dilution Effects for 3.22 and 3.75 Ratio Sodium Silicates at 12-14 mg SiO_2/L--pH Controlled: pH.

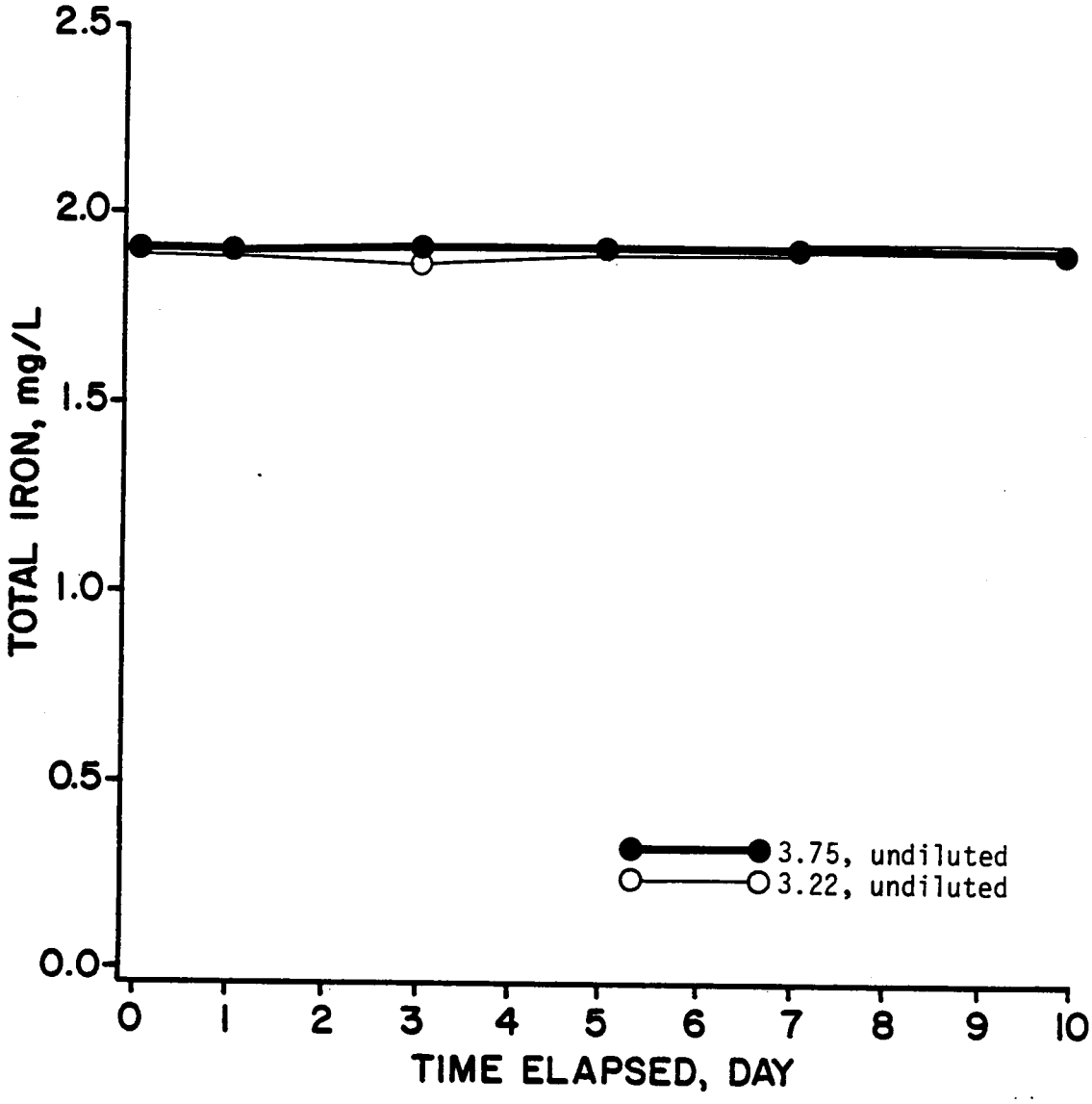


Figure 47. Dilution Effects for 3.22 and 3.75 Ratio Sodium Silicates at 12-14 mg SiO_2/L--pH Controlled: Total Iron.

Table 20. Data on Dilution Effects for 3.22 and 3.75 Ratio Sodium Silicates at 12-14 mg SiO_2/L with pH Controlled and Detail on Filterability by Ultrafiltration

	Silicate			Day																							
				0				1.0				3.0				5.0				7.0				9.9			
Jar No.	SiO_2/Na_2O Ratio	Dose[a]	Dilution	Turb[b]	Tot Fe[c]	Filt[d]	pH	Turb	Tot Fe	Filt	pH	Turb	Tot Fe	Filt	pH	Turb	Tot Fe	Filt	pH	Turb	Tot Fe	Filt	pH	Turb	Tot Fe	Filt	pH
13	3.75	12.5	Undil.	0.12	1.91	99 95 4	7.0	0.13	1.90	99.5 51 1.5	7.1	0.15	1.92	98 7 1	6.85	0.175	1.92	98 13 -	6.8	0.22	1.92	98 1 -	7.1	0.33	1.91	93 1 -	7.0
15	3.75	14.1	1/100	0.16	1.90	97 28 1	7.0	0.19	1.88	98 1 1	7.1	0.22	1.91	97 1 1	7.1	0.31	1.91	86 1 -	7.0	0.46	1.91	23 1 -	7.1	0.58	1.87	<1 1 -	6.9
16	3.22	13.9	Undil.	0.15	1.90	98 81 2	7.0	0.165	1.90	98 17 1	7.2	0.18	1.87	97 4 1	7.1	0.24	1.91	97 3 -	6.9	0.33	1.92	93 1 -	7.1	0.53	1.92	7 1 -	7.05
17	3.22	13.8	1/100	0.21	1.90	97 5 1	7.0	0.24	1.90	96 1 1	7.1	0.29	1.88	97 1 1	7.15	0.345	1.90	94 2 -	7.15	0.49	1.90	68 1 -	7.1	0.68	1.91	3 1 -	7.05

a. Reported as mg SiO_2/L

b. Turbidity, NTU

c. Total iron, mg Fe/L

d. Iron filterability, %; for a given jar the values are consecutively from the top down-- <0.1 μm, <200,000 MW cut off, <1000 MW cutoff

e. Measurement made before any readjustment to pH 7

both of the undiluted silicates, for the 1/100 dilutions the filterability had decreased significantly by that point, but more so for the 3.75 than for the 3.22 ratio material. The undiluted-silicate treatments provided better continued filterability than the 1/100 dilution treatments. As is consistent with the results of the earlier experiments, for similar silica doses, the 3.75 ratio silicates provided better treatment (higher filterability) than the 3.22 ratio silicates for the undiluted treatments. However, surprisingly, the 3.22 ratio silicate produced a more extended filterability than the 3.75 ratio silicate at the 1/100 dilution. This result was inconsistent with the previous experimental results. This apparent anomaly can be explained by the inability of the analytical methods used to establish real differences in silica doses at the necessary desired level of accuracy.

The use of ultrafiltration allowed a more complete understanding of the change in iron filterability with time and of the effect of filter pore-size selection on the observed apparent filterability. The 1,000 and 200,000 molecular weight (MW) cutoff ultrafilters correspond to approximate pore-sizes of 12 and 74Å, respectively. On day 0, the iron filterability was essentially identical for all of the four treatments, based on the 0.1 μm cutoff. However, closer examination based on ultrafiltration (Figure 41-44) revealed that, in fact, even on day 0 the undiluted treatments provided higher iron filterabilities than did the 1/100 dilutions for both the 3.22 and 3.75 ratio silicates. However, these differences were more readily observed for the <200,000 MW cutoff than for the <1,000 MW cutoff iron filterabilities. For the 1/100 dilution treatments, by day 0 for the <1,000 MW cutoff and by day 1 for

the <200,000 MW cutoff data, the iron filterabilities were reduced to ~1% or less. In contrast, for the undiluted silicate treatments, the <200,000 MW cutoff iron filterability was substantial on day 0 (95 and 81% for the 3.75 and 3.22 ratio silicates, respectively), and significantly greater than 1% through day 5. The iron filterabilities based on the <1,000 MW cutoff filter were all very low even on day 0, for all treatments. However, what little differences there were, occurred on day 0, with values of 4 and 2% for the undiluted 3.75 and 3.22 ratio silicates, respectively, and 1% for the rest.

These ultrafiltrability results support the notion that in effecting the sequestration of aqueous ferric iron the role of the silicates is to control the growth of ferric iron particulates. At comparable silica doses, the undiluted silicates limited particulate growth more so than the 1/100 dilutions. These differences were apparent from the earliest stages of interaction and at the smallest particle sizes.

Characterization of Iron Particulates

Assuming that the role of the silicate is in fact to retard the growth of iron particulates, the question arose as to the nature of these iron particulates. As a result, in conjunction with the ultrafiltration studies discussed above, unfiltered samples were taken periodically from each treatment, appropriately prepared, and examined by transmission electron microscopy (TEM). Particles deposited on the grids were analyzed by bright field (BF) and selected area electron diffraction (SAD) techniques. The former allowed determination of particle size and morphology whereas the latter technique provided

information for the identification of any mineral phases present. Upon application of SAD to a particle, the absence of well defined diffraction lines indicated an amorphous character whereas distinct diffraction lines indicated the presence of crystalline materials, the definition of the lines being the criterion for crystallinity. Diffraction patterns are fingerprints for mineral phases. Comparisons of these patterns for unknown samples with those for known minerals with regard to interplanar(d-) spacings and intensity can be used to identify the unknowns.

TEM was applied to samples taken from four treatments, viz., undiluted and 1/100 dilutions of the 3.22 and 3.75 ratio silicates dosed at approximately 13.5 mg SiO_2/L. The TEM analysis did not reveal any consistent trends with regard to the development of particle crystallinity with time, or silicate dilution. Some crystallinity was observed with samples taken from as early as day 0, and amorphous material as late as day 10. Well defined particles tended to be most often plates and sometimes scrolls. A picture of one such plate is shown in Figure 48. The SAD pattern for a plate derived from the 1/100 dilution of the 3.22 ratio silicate treatment on day 10 (sample A10) is presented in Figure 49. This is an example of a clearly crystalline particulate. The d-spacings of the crystalline particles were calculated based the measured positions of the different rings in the diffraction patterns such as these. Table 21 gives the d-spacings of the rings observed for sample A10, together with qualitative estimations of their intensities. A computer search of the Joint Committee on Powder Diffraction Standards (JCPDS) files was conducted with the stipulation that the elements Fe, O, and H be present and other elements such as Na, and Si be optional.

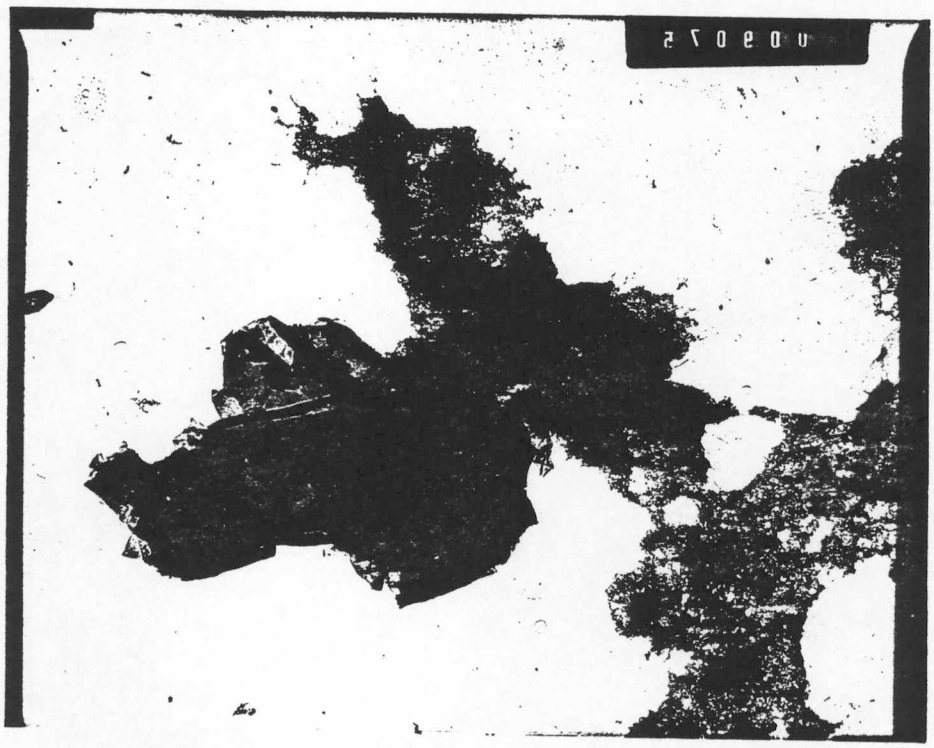


Figure 48. Iron Particulate--Plate

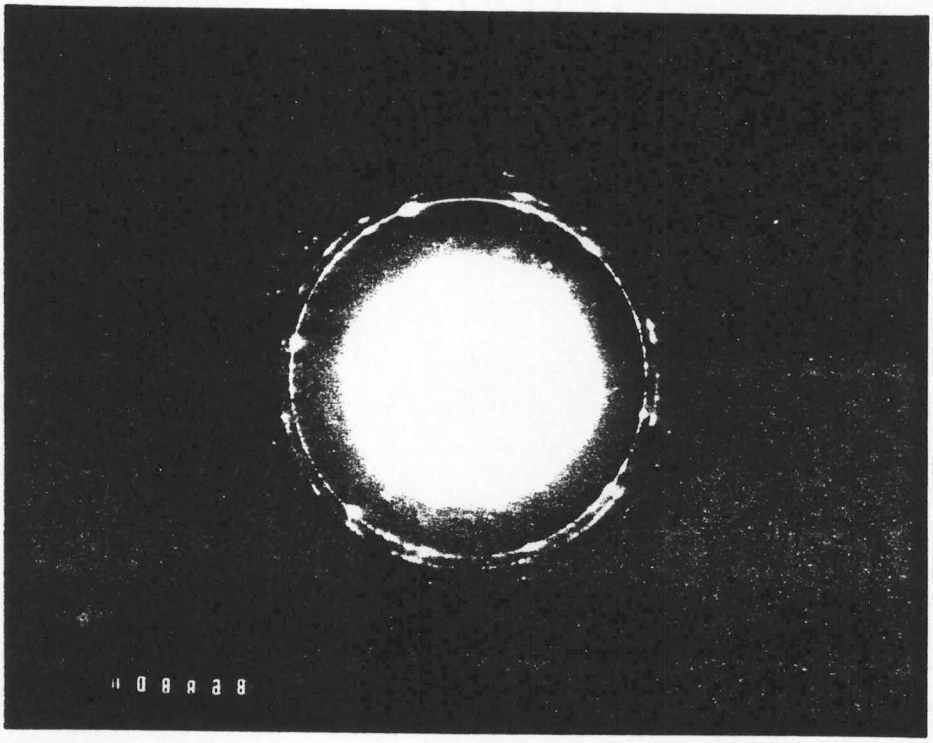


Figure 49. Selected Area Diffraction Pattern--Sample A10.

Table 21. Selected Area Diffraction Data for Particulate from the 1/100 Dilution of the 3.22 Ratio Sodium Silicate--Day 10 (Sample A-10)

Line no.	Diffraction Ring Radius mm	Diffraction Spacing Å	Intensity[a]
1	7.5	3.476[b]	VW
2	8.75	2.980[b]	VW
3	9.9	2.634[b]	VW
4	11.9	2.191[b]	MS
5	12.4	2.103[b]	S
6	17.3	1.507[b]	VW
7	20.5	1.272[b]	VS
8	21.75	1.199[b]	S
9	23.75	1.098[b]	W
10	25.5	1.023[b]	W
11	31.1	0.838	W
12	33.5	0.778	W
13	35.75	0.729	VW
14	40.5	0.644	VW
15	42.5	0.613	VW

a. VW = Very Weak; W = Weak; S = Strong; MS = Medium Strong; VS = Very Srong.

b. Matches a line for iron oxide hydroxide.

The best agreement, albeit still poor, between lines from the unknown sample (A10) and from a reference sample was obtained for an unnamed iron oxide hydroxide (Fe O OH). Partial matches in d-spacings were also observed for lepidocrocite and akagenite. Particulates from iron treatment systems have been identified as lepidocrocite (18). No matches were seen for mineral phases including Si. Work by Robinson et al. (18) at different iron and silicate concentrations suggested that, above a certain threshold value, metasilicate favored the formation of amorphous particulates. In this investigation, the inclusion of silicate in particulates may have favored amorphous characteristics, but the resultant absence of well defined diffraction rings prevented identification. Large particles (5-10μm) were observed on day 10 for some of treatments. However, because concentration of particulates by centrifugation was part of sample preparation, the size of these late experiment samples which were absent from initial samples imply nothing more than general particle growth with time.

V. GENERAL DISCUSSION

The objective of the silicate-hypochlorite procedure for the treatment of iron in groundwaters is to oxidize the ferrous iron under conditions that allow the resultant ferric iron to remain sequestered or stabilized, such that the iron will not settle out either in the treatment plant or in the water distribution system. Because at pH levels near or above neutrality hypochlorite oxidizes ferrous iron almost instantaneously (54), it can be assumed that upon addition of excess hypochlorite under the other experimental conditions of this investigation, the iron present initially as ferrous would be converted rapidly and completely to ferric iron. In neutral or alkaline water the ferric ion produced would be hydrolyzed rapidly to hydrous ferric oxide or some similar compound (10). Because of the very limited solubility of this material, ferric ion concentrations in excess of a fraction of a mg/L would favor its precipitation (10). It has been proposed that the primary role of silicate in iron treatment is to limit the growth of particulate ferric iron species (44, 46). This aspect of the mechanism has been verified indirectly by the results of ultrafiltration studies presented earlier in the text. It was shown that differences in the effectiveness among various silicate treatments occurred not only in the <0.1 μm fraction but also in the <126Å, and <74Å fractions. The pattern of filterability with time showed a gradual growth of particle size, with the more successful treatments growing more slowly. The predominance of iron particulates, as indicated by low values for the <12Å fraction, on day 0, also implies a

minimal contribution in terms of quantity (proportion), from iron-silicate complexes (which are soluble).

If the function of the silicate is to limit the growth of ferric iron particulates, then it is likely that this is best accomplished if the silicate is already present in the system when the ferric iron is generated. By and large, experimental findings have been in agreement with this concept. Thus, Dart and Foley (6) obtained best treatment with approximately simultaneous application of silicate and oxidant (chlorine or hypochlorite) or with the silicate just ahead of oxidant. Data presented here earlier conformed to these ideas, and in fact showed that the application of the oxidant two minutes ahead of the silicate achieved no treatment at all. Nevertheless, some caution is advised with regard to generalization, since Henry (46) observed better treatment applying chlorine ahead silicate. Evidently, there were some unknown factors prevailing which allowed results that would seem to be unexpected.

The results presented and discussed earlier also provided ample evidence that the level of silica polymerization in the dosed silicate is a critical factor in the success of the treatment. The role of silica polymerization was addressed by using treatments that varied this parameter by two different methods, viz. (a) by varying the SiO_2/Na_2O ratio of the silicate, and (b) by varying the dilution (and thus the silica concentration) of the dosed silicate. Earlier investigations by Iler (21) had indicated that increases in the SiO_2/Na_2O ratios of soluble silicates above 2 were accompanied by an increase in

the complexity of the predominant silica polymer form. Also, O'Connor (31) had examined the effect of dilution on a 3.3 ratio silicate regarding the nature of polymerization. O'Connor's method was based on the analysis of the rate of reaction of the silicate with molybdic acid as monitored by measurement of absorbance at 400 nm, and yielded two coefficients, K_1 and P_0, which were considered to represent, respectively, the level of complexity and the fraction of silicate provided by the major silica polymer present. Furthermore, Dart and Foley (6) obtained better treatment with undiluted rather than diluted silicate, and Holden (48), in preliminary tests, had also observed progressively better treatment with lesser dilution of the dosed silicate solution.

Application of O'Connor's technique for the characterization of silicates to the silicates used in the various treatments, in combination with the effects on iron filterability represents a major contribution of this investigation. Visual examination of the appropriate figures, as presented earlier, showed clearly that (1) for a given ratio silicate at a given silica dose, the treatment was more effective, i.e., the level of iron filterability remained higher for longer, as the dosed silicate was less dilute, undiluted being the most effective, and (2) for a given dose and dilution, the higher ratio silicates were more effective at maintaining iron filterability. These tendencies were more generally substantiated by the statistical application of multiple linear regression models to the data grouped in accordance with measured variables. Accordingly, for treatments involving undiluted silicates of varying ratios, for the models tested, the variables controlling % iron filterability in order of significance were

DAY(time) >SiO_2 dose >K_1>P_0. In fact, P_0, because it did not vary much among undiluted silicates proved to be relatively insignificant as a predictor. Also, for the treatments involving the various dilutions of the 3.22 ratio silicate, for the models tested, the variables controlling % iron filterability in order of significance were DAY = SiO_2 dose = P_0 > K_1. K_1 was a poor predictor of % iron filterability, in this instance, because of poor values for this variable, for the more dilute silicate solutions. Importantly, the % iron filterability was inversely correlated with time (DAY) and K_1, and directly correlated with SiO_2 dose and P_0. Because higher values of K_1 indicate more rapid reaction with molybdic acid and thus a lower silicate complexity (31), and higher P_0 values correspond to having more silicate in the polymer form, the above results were consistent with the conclusion that more complex silica and higher proportions of polymeric silica in the dosed silicate favor iron stabilization.

Hazel (42) working with sodium silicate of m-ratios ranging from 1/1 to 4/1, examined the ability of sodium silicate solutions to convert the surfaces of aged iron oxide sols from positively to negatively charged, a process favoring dispersion of these colloids. It was observed that for silicate added at a given pH, the higher ratio silicates were more effective at discharging (or changing charge to negative) oxide surfaces, a result that agrees well with the findings of this investigation. He also found that decreasing the initial silicate pH shifted recharging concentrations to higher values. This result is analogous to the finding in this investigation that allowing the system

pH to drift upward lowered the silica dose needed for effective treatment.

Any proposed mechanisms to explain the observed effects of the various silicates on iron filterability dispersion must account for (1) the superior performance of the higher ratio silicates and lesser dilutions, (2) the reduction in silica dose requirement with an increase in system pH, (3) the increased silica dose requirement for Ca^{2+} over equivalent concentrations of Na^{+}, (4) progressively lower filterabilities with smaller filter pore sizes, and (5), rather fast transition from high filterability to low filterability after a period of time. The mechanisms proposed will address only the first four requirements at this time.

A plausible mechanism is one based on the concepts of point of zero charge (PZC), double layer theory, and equilbrium silicate species distribution characteristics. The pH_{pzc} of a colloidal particle is the pH at which the net charge on the particle is zero (10). At higher and lower pH values the net charge on the particle would be negative or positive, respectively. For metal oxides in constant ionic strength solutions, coagulation occurs at pH values in the neighborhood of the pH_{pzc}, as was observed by Hazel (42). When the silicate treatment is applied, the iron particles (hydrous ferric oxide for the sake of argument) are associated with polymeric silica, initially. The pH_{pzc} of the combination particle is the weighted average of the pH_{pzc}'s of the individual particles (10). The pH_{pzc} of the hydrous ferric oxide is ~8.5(10). The pK_a of monomeric silica is ~9.8, the pH_{pzc} of silica

gel is ~2.0, and as implied by Falcone (30) the pH_{pzc} of other polymeric silica lies in between these end points with the more complex silica having the lower pH_{pzc} values. Thus, the more complex the silicate polymer the lower will be the pH_{pzc} of the iron-silica particle. For the experiments conducted at pH = 7, and the ones where the pH is uncontrolled and drifts higher, these combination particles should be overwhelmingly negatively charged, a condition favoring dispersion of these particles.

There are at least two alternative explanations, which are not necessarily mutually exclusive, accounting for the reversal of dispersion, or flocculation, following treatment. These are based on charge reduction or on simple collision theory. If the overwhelming majority of the post treatment iron is in the particulate form (as implied by the pH-solubility requirements for Fe^{3+} (10)), then particle growth, as indicated by decreasing iron filterability, must be achieved by the joining or agglomeration of particles. In a constant ionic strength system, because opposite charges attract and like charges repel each other, a change in particle surface charges favoring reduction in repulsion would favor the coalescence of particles, and perforce, particle growth also. However, this may not be a necessary requirement for the occurrence of agglomeration, since hydrophobic colloidal systems, such as these treatment systems, are not thermodynamically stable and will eventually flocculate (55), because of particle collisions.

A simple scenario accounting for charge reduction with time is as follows. Because the monomeric form of silica is the equilibrium

species at the concentrations (<15 mg SiO_2/l) used in this investigation (Figure 2), with time, the silica moieties of the iron-silica particles depolymerize. With silica depolymerization the pH_{pzc} of the combination particle gradually increases, eventually making the prevailing pH appropriate for the coagulation of particles. By the same mechanism, it is clear that at a higher pH the particles are likely to be more negatively charged, favoring dispersion of particles and higher iron filterability.

The validity of charge reduction via is silicate depolymerization as a relevant mechanism is challenged in the treatment system (Figure 16) for which, at a pH of 8 to 8.5, the % iron filterability remained elevated for 161 days until the pH was lowered to 7 at which time the filterability decreased rapidly. The question arises as to why a change in pH would allow a silicate not to depolymerize for such a long time, and logically, is charge reduction then a necessary mechanism. The explanation is simple. The depolymerization of the silica is incomplete. The work of Robinson (16) and Robinson et al. (18), in which iron particulates were increasingly amorphous in the presence of increasing levels of metasilicate during the oxidation of ferrous iron, implies that silicate is being incorporated into the cell structure of the iron particulates, causing disruption. In this investigation, it is likely that some of the silica associated with the iron is surficial, while the remainder is incorporated more deeply. As a result, the depolymerization occurs only or mainly at the particle surface and is incomplete in terms of the entire particle. At the elevated pH in the uncontrolled pH system (8 to 8.5) (Figure 16), which is already in

the neighborhood of the pH_{pzc} of the iron particle by itself, the charge contribution from the entrapped silica moiety need not be much in order to favor dispersion. More than likely, in the actual treatment system, charge reduction and collision work together to bring about coagulation.

Dart and Foley (6) and Holden (48) observed that the presence of Ca^{2+} ions (hardness) in the system increased the silica dosage needed for effective treatment. Dart and Foley (6), observed that a five-fold increase in silica was required to stabilize iron when hardness was increased from 0 to 1,000 mg/L as $CaCO_3$. Holden (48), in one of his experiments, found that a silica dose of 16 mg SiO_2/L stabilized 2 mg Fe/L through day 10 in the absence of $CaCl_2$, whereas this same silica dose stabilized the iron for less than five days in the presence of 25 mg/L $CaCl_2$ as $CaCO_3$. In a follow up experiment, about 25 mg SiO_2/L was required to stabilize the iron through day 10 in the presence of 25 mg/L $CaCl_2$ as $CaCO_3$. The $CaCl_2$ at 25 mg/L as $CaCO_3$ increased the required dose by a factor of ~1.6. Based on free energy calculations Holden showed that under the prevailing treatment conditions, mineral phases such as wollastonite ($CaSiO_3$) should not precipitate, nor should species such as $CaOSi(OH)_3^+$ and $(Ca[OSi(OH)_3]_2)^\circ$ represent significant sinks for added silicate. Furthermore, the Ca^{2+} effect could not be reproduced by substitution of Na^+ at comparable ionic strengths. The Ca^{2+} effect was thus left basically unexplained.

However, this Ca^{2+} effect is readily explained within the mechanism proposed by this author in this discussion, to which standard

double layer (DLVO) theory is applicable. By applying the Schultze-Hardy Valency rule to double layer theory with some simplifying assumptions it has been shown that the critical coagulation concentration of mono- and divalent ions are in the ratio $(1/Z)^6$ or 100 : 1.6, where Z is the ion valency (10). Applying this concept to the current investigation, it is likely that under the conditions of iron treatment the coagulating effect of Ca^{2+} is substantially greater than for Na^+ necessitating a marked increase in silica dosage to counteract the valency effect. Yet another contributor to the "silica demand" of Ca^{2+} is the effect of specific adsorption of Ca^{2+} by iron oxide type surfaces (43). Specific adsorption of the divalent cation Ca^{2+} would raise the pH_{pzc} of the hydrous ferric oxide present. This then increased the silica dose required to lower the pH_{pzc} of the Fe-Si combination particle such that at pH 7 or above it is substantially negatively charged, favoring dispersion and thus filterability.

Efforts in this investigation to identify the particulate iron phase during the duration of the experiments met with moderate success. When a crystalline mineral phase could be identified it turned out to be an unnamed iron oxide hydroxide (FeOOH) with some similarities to lepidocrocite and akagenite. Lepidocrocite has been identified as a common particulate phase produced by the oxidation of model groundwaters (18, 19). Robinson et al. (18) observed that increasing the silica to iron ratio in the aerated system favored the production of amorphous iron. In this investigation amorphous material was obtained,

but silica dose was not a variable. Surprisingly, no correlation could be made between occurrence of crystalline phases and time into the experiment.

VI. CONCLUSIONS

1. Silicate solutions could not be universally well characterized in terms of reactivity parameters, K_1 and P_0, based on mathematical analysis of the rate of reaction of the solution with molybdic acid. The model, which is based on the equation (number 27) from O'Connor's work (31), in its present form and as exploited by our nonlinear analysis system was inadequate for dilute (<0.3% SiO_2) silicate solutions. These solutions reacted with molybdic acid to yield "log unreacted silica vs. time" curves each with two distinct phases of markedly differing slopes, a conformation not well reproduced by the model as it is. However, while statistical models based on the reactivity parameters were not good enough for engineering design purposes, they were nonetheless useful for the elucidation of mechanisms involved in the treatment of iron by sodium silicates.

2. For successful iron treatment, the optimal sequence of chemical application was sodium silicate applied, with mixing, 15 to 150 seconds ahead of the oxidant, sodium hypochlorite.

3. At higher pH levels, such as those produced when the pH was controlled by atmospheric CO_2 (8 to 8.5), significantly lower silica doses were required to obtain the desired iron stabilization than where the pH was controlled at ~7.0.

4. Under conditions of controlled pH, for a given ratio silicate (1.8,2.5,3.22,3.75) at a given dose (13-15 mg SiO_2/L), the more concentrated feed solutions were progressively more effective than the more dilute solutions at producing the desired iron stabilization.

5. Under conditions of controlled pH, among silicate solutions of differing m-ratios, at a given silica dose, the level of observed iron stabilization improved progressively with increasing m-ratios. This trend should hold for any given dilution, such as 1/10, 1/50 or undiluted, although differences become obscured when dealing with the more dilute solutions.

6. Statistical analysis of the relationship between treatment success, and silicate m-ratio and dilution, verified the importance of silica polymerization, as represented by K_1 and P_0, in controlling the effectiveness of silicate solutions at stabilizing aqueous ferric iron. The critical roles of time and silica dose were also substantiated.

7. Detailed analysis by ultrafiltration of particle size distribution for various treatments supported the premise that the role of silicate in effecting iron stabilization was to disperse the iron particulates, limiting their coalescence, growth, and subsequent sedimentation.

8. The role of silica polymerization in determining the effectiveness of the silicate treatment was readily explained in terms of classical double layer theory as applied to treatment-generated colloids that were a combination of iron and silicate particulates. Essentially, the more complex silica was more effective at lowering the pH_{pzc} of the combination particulates, which in turn helped certify that the colloidal surface charge would be negative at the prevailing pH (7.0). This surface charge condition favored dispersion.

9. The examination by transmission electron microscopy of particulates generated in treatment did not provide any consistent trends

regarding the development of crystallinity with time or dilution. Where tentative mineral identification was possible, the best characterization indicated the particle to be an unnamed iron oxide hydroxide.

VII. RECOMMENDATIONS FOR FURTHER WORK

1. Modification of the O'Connor model for the characterization of silicate solutions in terms of reactivity with molybdic acid, to make it fully applicable to dilute silicate solutions.
2. Use of model developed in item 1 above to complete examination of the connection between silicate solution reactivity characteristics and treatment effectiveness for the range of dilutions and each of silicates used in this investigation.
3. Quantitative examination of the effect of Ca^{2+} on the silicate dose required for effective treatment.
4. Development of a generalized dosage formula for iron treatment by the silicate technique.
5. Examination of the role of zeta potentials in the flocculation and iron filterability patterns of treatment systems.
6. More quantitative analysis regarding the size, morphology, and identity of iron/silica particulates produced during treatment.
7. Examination of silica filterability along with iron filterability to assist in establishing the role of silicate depolymerization in the loss of iron filterability with time.

BIBLIOGRAPHY

BIBLIOGRAPHY

1. Viessman, W., Jr., and M.J. Hammer. 1985 Water Supply and Pollution Control. Fourth Edition. Harper and Row, Publishers, New York, 797 pp.

2. U.S. Environmental Protection Agency. 1977. National secondary drinking water regulations. Fed. Regis. 42: 17144-17147.

3. Stiles, J.F., III. 1978. Survey of the iron and manganese problems in the USA. In Proceedings AWWA 1978 Annual Conference Part II, Paper 20-4b., The American Water Works Association, Denver, Co.

4. Zurawski, A. 1978. Summary Appraisals of the Nation's Ground Water Resources. USGS Prof. Paper 813-L. U.S. Government Printing Office, Washington, D.C.

5. Dart, F.J., and P.D. Foley. 1970. Preventing iron deposition with sodium silicate. J. Amer. Water Wks. Assoc. 62(10): 663-668.

6. Dart, F.J., and P.D. Foley. 1972. Silicate as Fe, Mn deposition preventative in distribution systems. J. Amer. Water Wks. Assoc. 64(4): 244-249.

7. Stumm, W., and G.F. Lee. 1961. Oxygenation of ferrous iron. Ind. Eng. Chem. 53(2): 143-146.

8. Singer, P.C., and W. Stumm. 1970. Oxygenation of ferrous iron. Science 167: 3921-3923.

9. Ghosh, M.M., J.T. O'Connor, and R.S. Englebrecht. 1966. Precipitation of iron in aerated ground water. J. Sanit. Engr. Div., ASCE. 92: 199-213.

10. Stumm, W., and J.J. Morgan. 1981. Aquatic Chemistry. John Wiley & Sons, New York. 780 pp.

11. Tamura, H., K. Goto, and M. Nagayama. 1976. The effect of ferric hydroxide on the oxygenation of ferrous ions in neutral solutions. Corrosion Sci. 16: 197-297.

12. Schenk, J.E., and W.J. Weber, Jr. 1968. Chemical interactions of dissolved silica with iron (II) and (III). J. Amer. Water Wks. Assoc. 60: 199-212.

13. Huffman, R.E., and N. Davidson. 1956. Kinetics of the ferrous iron-oxygen reaction in sulfuric acid solution. J. Amer. Chem. Soc. 78: 4836-4842.

14. Cher, M., and N. Davidson. 1955. The kinetics of the oxygenation of ferrous iron in phosphoric acid solution. J. Amer. Chem. Soc. 77: 793-798.

15. Crabtree, J.H., and W.P. Schaefer. 1966. The oxidation of iron (II) by chlorine. Inorg. Chem. 5(8): 1348-1351.

16. Robinson, R.B. 1979. The iron precipitate in groundwater supplies. Ph.D. Dissertation unpublished. Iowa State University, Ames, IA.

17. Schwertman, U., and R.M. Taylor. 1972. The transformation of lepidocrocite to goethite. Clays Clay Min. 20: 151-158.

18. Robinson, R.B., T. Demirel, and E.R. Baumann. 1981. The identity and character of iron precipitates. J. Environ. Engr. Div., Proc. Amer. Soc. Civ. Engr. 107(EE6): 1211-1227.

19. Schwertman, U., and H. Thalman. 1976. The influence of Fe(II), Si, and pH on the formation of lepidocrocite and ferrihydrite during oxidation of aqueous $FeCl_2$ solutions. Clay Min. 11: 189-200.

20. Iler, R.K. 1955. The Colloid Chemistry of Silica and Silicates. Cornell University Press, Ithaca, New York. 324 pp.

21. Iler, R.K. 1979. The Chemistry of Silica. John Wiley & Sons, New York. 866 pp.

22. Iler, R.K. 1980. Isolation and characterization of particle nuclei during the polymerization of silicic acid to colloidal silica. J. Coll. Interfac. Sci. 75:138-148.

23. Andersson, K.R., L.S. Dent Glasser, and D.N. Smith. 1982. Polymerization and colloid formation in silicate solutions. pp. 115-131 In J.S. Falcone, Jr.(Ed). Soluble Silicates. ACS Symposium Series 194, American Chemical Society, Washington, D.C.

24. Roy, C.J. 1945. Silica in natural waters. Amer. J. Sci. 243(7): 393-403.

25. Alexander, G.B., W.M. Hester, and R.K. Iler. 1954. The solubility of amorphous silica in water. J. Phys. Chem. 58: 453-455.

26. The PQ Corporation. 1979. Sodium Silicates: Liquids/solids. Bull. 17-103. The PQ Corporation, Valley Forge, PA. 17 pp.

27. Pearce, C.A. 1972. Silicon Chemistry and Applications. The Chemical Society Monograph for Teachers No. 20. Billing & Sons Limited, Guildford and London, U.K. 74 pp.

28. Katsanis, E.P., W.B. Esmonde, and R.W. Spencer. 1985. Soluble silicates as corrosion inhibitors in water systems. pp. 369/1-369/15. Corrosion 85, The International Corrosion Forum, March 25-29, 1985, Boston, MA.

29. Iler, R.K. 1982. Colloidal components in solutions of sodium silicate. pp. 95-114. In J.S. Falcone, Jr.(Ed.) Soluble Silicates. ACS Symposium Series 194, American Chemical Society, Washington, D.C.

30. Falcone, J.S., Jr. 1982. The effect of degree of polymerization of silicates on their interactions with cations in solution. pp. 134-148. In J.S. Falcone, Jr.(Ed.). Soluble Silicates. ACS Symposium Series 194. American Chemical Society, Washington, D.C.

31. O'Connor, T.L. 1961. The reaction rates of polysilicic acids with molybdic acid. J. Phys. Chem. 65: 1-5.

32. McGarry, M.A. and J.F. Hazel. 1965. Electron microscopy of labile alkali silicate solutions. J. Colloid Sci. 20: 72-80.

33. Hazel, J.F. 1962. Lability of aqueous solutions of potassium silicate. J. Colloid Sci. 19: 162-168.

34. Lehrman, L., and H.L. Shuldener. 1951. The role of sodium silicate in inhibiting corrosion by film formation on water piping. J. Amer. Water Wks. Assoc. 43(3): 175-188.

35. Alexander, G. 1953. The reaction of low molecular weight silicic acids with molybdic acid. J. Amer. Chem. Soc. 75: 5655-5657.

36. Garrett, H.E., and A.J. Walker. 1964. The spectrophotometric determination of silicic acid in dilute solution. Analyst 89: 642-650.

37. Marsmann, H.C., and M. Vongehr. 1982. Silicon NMR studies on dissolved silicates. pp. 73-78 In J.S. Falcone, Jr.(Ed.) Soluble Silicates. ACS Symposium Series 194, American Chemical Society, Washington, D.C.

38. Debye, P., and R.V. Nauman. 1961. The slow change in turbidity of sodium silicate solutions. J. Phys. Chem. 65: 5-7.

39. Hazel, J.F., R.U. Schock Jr., and M. Gordon. 1949. Interaction of ferric ions with silicic acid. J. Amer. Chem. Soc. 71(6): 2256-2257.

40. Weber, W.J., and W. Stumm. 1965. Formation of a silicato-iron(III) complex in dilute aqueous solution. J. Inorg. Nuclear Chem. 27:237-239.

41. Olson, L.L. and C.R. O'Melia. 1973. The interactions of Fe(III) with $Si(OH)_4$. J. Inorg. Nuclear Chem. 35: 1977-1985.

42. Hazel, F. 1945. The effect of sodium silicates on iron oxide surfaces. J. Phys. Chem. 49: 520-537.

43. Kinniburgh, D.G., and M.L. Jackson. 1981. Cation adsorption by hydrous metal oxides and clay. pp. 91-160. In M.A. Anderson and A.J. Rubin (Eds), Adsorption of Inorganics at Solid Liquid Interfaces, Ann Arbor Science Publishers, Inc., Ann Arbor, MI.

44. Cameron, A.J., and P.S. Liss. 1984. The stabilization of "dissolved" iron in freshwaters. Water Res. 18(2): 179-185.

45. Hazel, J.F., W.M. McNabb, and P.E. Machemer. 1952. A potentiometric study of the interaction of zinc ions with sodium silicates. J. Electrochem. Soc. 99(7): 301-307.

46. Henry, C.R. 1950. Prevention of the settlement of iron. J. Amer. Water Wks. Assoc. 42(9): 886-896.

47. Dart, F.J. 1983. Recent developments in iron and manganese control. Annual Conference Seminar on Control of Inorganic Contaminants. pp. 1-20.

48. Holden, J.M. 1985. Treatment of iron bearing groundwaters by the simultaneous addition of sodium silicate and sodium hypochlorite. MS. Thesis, unpublished, The University of Tennessee, Knoxville, TN. 197 pp.

49. Strickland, J.D.H. 1952. The preparation and properties of silicomolybdic acid. I. The properties of alpha silicomolybdic acid. J. Amer. Chem. Soc. 74(4): 862-867.

50. SAS Institute. 1979. SAS User's Guide. SAS Institute, Cary, N.C.

51. American Public Health Association, American Water Works Association, Water Pollution Control Federation. 1981. Standard Methods for the Analysis of Water and Wastewater, 15th Edition, American Public Health Association, Washington, D.C.

52. Hach. 1983. Test Instructions. Free and Total Chlorine Test Kit. Model CN-70. Cat. No. 14542-00. Hach Company, Loveland, CO.

53. USEPA. 1979. Methods for Chemical Analysis of Water and Wastes. EPA-600/4-79-020 March 1979. Office of Research and Development, USEPA, Cincinnati, OH.

54. Snoeyink, V.L., and D. Jenkins. 1980. Water Chemistry. John Wiley and Sons, New York.

55. Weber, W.J. 1972. Physiochemical Processes for Water Quality Control. John Wiley and Sons, New York.

APPENDIX

Table A1. Raw and Converted Optical Density Data for the Reaction of Undiluted 3.75 Ratio Sodium Silicate with Molybdic Acid with Time at 400 nm and 25-26°C[a]

Time min	OD_t	Unreacted SiO_2 %	Time min	OD_t	Unreacted SiO_2 %
3.0	0.063	90.2	70.0	0.402	37.5
4.0	0.078	87.9	80.0	0.424	34.1
5.0	0.090	86.0	90.0	0.440	31.6
6.0	0.102	84.1	100.0	0.455	29.2
7.0	0.114	82.3	110.0	0.467	27.4
8.0	0.124	80.7	120.0	0.479	25.5
9.0	0.133	79.3	130.0	0.488	24.1
10.0	0.142	77.9	140.0	0.496	22.9
11.0	0.151	76.5	150.0	0.503	21.8
12.0	0.159	75.3	160.0	0.509	20.8
13.0	0.167	74.0	170.0	0.514	20.1
14.0	0.175	72.8	180.0	0.518	19.4
15.0	0.182	71.7	190.0	0.522	18.8
20.0	0.216	66.4	200.0	0.526	18.2
25.0	0.245	61.9	210.0	0.528	17.9
30.0	0.271	57.9	220.0	0.530	17.6
35.0	0.294	54.3	230.0	0.532	17.3
40.0	0.315	51.0	240.0	0.534	17.1
45.0	0.334	48.1	250.0	0.534	17.0
50.0	0.350	45.6	260.0	0.535	16.8
55.0	0.365	43.2	270.0	0.535	-
60.0	0.379	41.1	280.0	0.535	-

a. OD_t = optical density at time t; OD_T = maximum optical density for total silica as β-silicomolybdate; % unreacted SiO_2=100 $(OD_T-OD_t)/OD_T$;

OD_T = 0.643; total silica ≃ 17 mg SiO_2/L.

Table A2. Raw and Converted Optical Density Data for the Reaction of Undiluted 3.22 Ratio Sodium Silicate with Molybdic Acid with Time at 400 nm and 25-26°C[a]

Time min	OD_t	Unreacted SiO_2 %	Time min	OD_t	Unreacted SiO_2 %
3.5	0.106	86.3	70.0	0.548	29.0
4.0	0.117	84.8	80.0	0.571	26.0
5.0	0.135	82.5	90.0	0.589	23.7
6.0	0.151	80.4	100.0	0.604	21.8
7.0	0.168	78.2	110.0	0.616	20.2
8.0	0.183	76.3	120.0	0.625	19.0
9.0	0.195	74.7	130.0	0.634	17.9
10.0	0.210	72.8	140.0	0.639	17.2
11.0	0.222	71.2	150.0	0.645	16.5
12.0	0.233	69.8	160.0	0.649	15.9
13.0	0.245	68.3	170.0	0.654	15.3
14.0	0.256	66.8	180.0	0.655	15.2
15.0	0.266	65.5	190.0	0.658	14.8
20.0	0.313	59.5	200	0.659	14.6
25.0	0.349	54.8	210	0.660	14.5
30.0	0.387	49.9	220	0.660	14.5
35.0	0.416	46.1			
40.0	0.442	42.8			
45.0	0.465	39.8			
50.0	0.486	37.1			
55.0	0.504	34.7			
60.0	0.520	32.6			

a. OD_t = optical density at time t; OD_T = maximum optical density for total silica as β-silicomolybdate; % unreacted SiO_2=100 $(OD_T-OD_t)/OD_T$;

OD_T = 0.772; total SiO_2 ≃ 20 mg/L.

Table A3. Raw and Converted Optical Density Data for the Reaction of Undiluted 2.5 Ratio Sodium Silicate with Molybdic Acid with Time at 400 nm and 25-26°C[a]

Time min	OD_t	Unreacted SiO_2 %	Time min	OD_t	Unreacted SiO_2 %
2.0	0.152	79.2			
3.0	0.195	73.2			
4.0	0.233	68.0			
5.0	0.265	63.6			
10.0	0.376	48.4			
11.5	0.401	45.0			
15.0	0.449	38.4			
17.5	0.477	34.6			
20.0	0.502	31.1			
25.0	0.541	25.8			
30.0	0.572	21.5			
35.0	0.596	18.2			
40.0	0.613	15.9			
45.0	0.627	14.0			
50.0	0.637	12.6			
55.0	0.645	11.5			
60.0	0.650	10.8			
65.0	0.655	10.2			
70.0	0.658	9.7			
80.0	0.660	9.5			
90.0	0.661	9.3			

a. OD_t = optical density at time t; OD_T = maximum optical density for total silica as β-silicomolybdate; % unreacted SiO_2=100 $(OD_T-OD_t)/OD_T$;

OD_T = 0.729; total silica ≃ 19 mg SiO_2/L.

Table A4. Raw and Converted Optical Density Data for the Reaction of Undiluted 1.80 Ratio Sodium Silicate with Molybdic Acid with Time at 400 nm and 25-26°C[a]

Time min	OD_t	Unreacted SiO_2. %	Time min	OD_t	Unreacted SiO2 %
2.5	0.257	62.3			
3.0	0.296	56.6			
4.0	0.362	46.9			
5.0	0.414	39.3			
6.0	0.452	33.7			
7.0	0.480	29.6			
8.0	0.503	26.3			
9.0	0.521	23.6			
10.0	0.537	21.3			
11.0	0.550	19.4			
12.0	0.562	17.6			
13.0	0.573	16.0			
14.0	0.580	15.0			
15.0	0.589	13.6			
20.0	0.616	9.7			
25.0	0.630	7.6			
30.0	0.639	6.3			
35.0	0.644	5.6			
40.0	0.645	5.4			
45.0	0.646	5.3			
50.0	0.645	5.4			

a. OD_t = optical density at time t; OD_T = maximum optical density for total silica as β-silicomolybdate; % unreacted SiO_2=100 $(OD_T-OD_t)/OD_T$;

OD_T = 0.682; total silica ≃ 17 mg SiO_2/L.

Table A5. Raw and Converted Optical Density Data for the Reaction of Undiluted 2.50 Ratio Sodium Silicate with Molybdic Acid with Time at 400 nm and 20-21°C[a]

Time min	OD_t	Unreacted SiO_2 %	Time min	OD_t	Unreacted SiO_2 %
3.0	0.122	83.1	70.0	0.614	15.1
4.0	0.156	78.4	80.0	0.627	13.3
5.0	0.188	74.0	90.0	0.638	11.8
6.0	0.214	70.4	100.0	0.645	10.8
7.0	0.237	67.2	110.0	0.652	9.8
8.0	0.259	64.2	120.0	0.656	9.3
9.0	0.278	61.6	130.0	0.659	8.9
10.0	0.295	59.2	140.0	0.661	8.6
11.0	0.311	57.0	150.0	0.663	8.3
12.0	0.326	54.9	160.0	0.664	8.2
13.0	0.340	53.0			
14.0	0.353	51.2			
15.0	0.365	49.5			
20.0	0.417	42.3			
25.0	0.458	36.7			
30.0	0.490	32.2			
35.0	0.515	28.8			
40.0	0.537	25.7			
45.0	0.555	23.2			
50.0	0.570	21.2			
55.0	0.584	19.2			
60.0	0.595	17.7			

a. OD_t = optical density at time t; OD_T = maximum optical density for total silica as β-silicomolybdate; % unreacted SiO_2=100 $(OD_T-OD_t)/OD_T$;

OD_T = 0.723; total silica ≃ 19 mg SiO_2/L.

Table A6. Raw and Converted Optical Density Data for the Reaction of Undiluted 3.22 Ratio Sodium Silicate with Molybdic Acid with Time at 400 nm and 20-21°C[a]

Time min	OD_t	Unreacted SiO_2 %	Time min	OD_t	Unreacted SiO_2 %
3.03	0.056	89.3	65.0	0.325	37.7
3.17	0.059	88.7	70.0	0.334	36.0
3.5	0.063	87.9	80.0	0.351	32.8
4.0	0.070	86.6	90.0	0.366	29.9
4.5	0.075	85.6	100.0	0.379	27.5
5.0	0.081	84.5	110.0	0.390	25.3
6.0	0.091	82.6	120.0	0.400	23.4
7.0	0.100	80.8	130.0	0.408	21.8
8.0	0.109	79.1	140.0	0.416	20.3
9.0	0.117	77.6	150.0	0.424	18.9
10.0	0.125	76.1	165.0	0.433	17.0
11.0	0.132	74.7	180.0	0.440	15.7
12.0	0.139	73.4	195.0	0.446	14.6
13.0	0.145	72.2	210.0	0.453	13.2
14.0	0.152	71.0	225.0	0.457	12.5
15.0	0.158	69.7	240.0	0.461	11.7
20.0	0.185	64.6	260.0	0.465	10.9
25.0	0.209	60.0	280.0	0.469	10.15
30.0	0.229	56.1	300.0	0.471	9.8
35.0	0.247	52.7	320.0	0.473	9.4
40.0	0.264	49.5	340.0	0.474	9.2
45.0	0.278	46.7	360.0	0.475	9.0
50.0	0.291	44.3	380.0	0.476	8.9
55.0	0.303	42.0	400.0	0.475	9.0
60.0	0.314	39.8			

a. OD_t = optical density at time t; OD_T = maximum optical density for total silica as β-silicomolybdate; % unreacted SiO_2=100 $(OD_T-OD_t)/OD_T$;

OD_T = 0.522; total silica ≃ 14 mg SiO_2/L.

Table A7. Raw and Converted Optical Density Data for the Reaction of 1/10 Dilution of 3.22 Ratio Sodium Silicate with Molybdic Acid with Time at 400 nm and 20-21°C[a]

Time min	OD_t	Unreacted SiO_2 %	Time min	OD_t	Unreacted SiO_2 %
3.25	0.125	76.1	18.0	0.318	39.1
3.67	0.135	74.2	19.0	0.325	37.8
4.0	0.144	72.4	20.0	0.332	36.5
4.5	0.156	70.1	21.0	0.338	35.3
5.0	0.166	68.2	22.0	0.345	34.1
5.5	0.176	66.3	23.0	0.350	33.0
6.0	0.183	65.0	24.0	0.356	31.9
6.5	0.194	62.9	25.0	0.362	30.8
7.0	0.202	61.3	30.0	0.385	26.3
7.5	0.211	59.6	35.0	0.403	22.9
8.0	0.217	58.5	40.0	0.418	20.0
8.5	0.225	56.9	45.0	0.431	17.5
9.0	0.231	55.8	50.0	0.442	15.4
9.5	0.238	54.4	55.0	0.451	13.8
10.0	0.244	53.3	60.0	0.458	12.4
11.0	0.257	50.8	70.0	0.468	10.4
12.0	0.268	48.8	80.0	0.476	8.9
13.17	0.279	46.6	90.0	0.481	7.9
14.0	0.287	45.1	100.0	0.486	7.1
15.0	0.295	43.5	110.0	0.489	6.4
16.0	0.304	41.9	120.0	0.491	6.1
17.0	0.312	40.3	130.0	0.492	5.8
			140.0	0.493	5.7
			150.0	0.492	5.8

a. OD_t = optical density at time t; OD_T = maximum optical density for total silica as β-silicomolybdate; % unreacted SiO_2=100 $(OD_T-OD_t)/OD_T$;

OD_T = 0.5225; total silica ≃ 14 mg SiO_2/L.

Table A8. Raw and Converted Optical Density Data for the Reaction of 1/50 Dilution of 3.22 Ratio Sodium Silicate with Molybdic Acid with Time at 400 nm and 20-21°C[a]

Time min	OD_t	Unreacted SiO_2 %	Time min	OD_t	Unreacted SiO_2 %
3.25	0.222	59.8	18.0	0.395	28.5
3.5	0.229	58.5	19.0	0.399	27.7
4.0	0.243	56.0	20.0	0.404	26.8
4.5	0.254	54.0	21.0	0.409	25.9
5.0	0.264	52.2	22.0	0.413	25.2
5.5	0.275	50.2	23.0	0.416	24.6
6.0	0.284	48.6	24.0	0.421	23.8
6.5	0.292	47.1	25.0	0.425	23.0
7.0	0.299	45.8	30.0	0.441	20.1
7.5	0.306	44.6	35.0	0.453	17.9
8.0	0.313	43.3	40.0	0.462	16.3
8.5	0.319	42.2	45.0	0.469	15.0
9.0	0.325	41.1	50.0	0.475	13.9
9.5	0.331	40.0	55.0	0.480	13.0
10.0	0.336	39.1	60.0	0.484	12.3
11.0	0.346	37.3	70.0	0.490	11.2
12.0	0.355	35.7	80.0	0.494	10.5
13.0	0.362	34.5	90.0	0.497	10.0
14.0	0.369	33.2	100.0	0.498	9.8
15.0	0.376	31.9	110.0	0.499	9.6
16.0	0.383	30.6	120.0	0.499	9.6
17.0	0.388	29.7	130.0	0.499	9.6

a. OD_t = optical density at time t; OD_T = maximum optical density for total silica as β-silicomolybdate; % unreacted SiO_2=100 $(OD_T-OD_t)/OD_T$;

OD_T = 0.522; total silica ≃ 14 mg SiO_2/L.

Table A9. Raw and Converted Optical Density Data for the Reaction of 1/100 Dilution of 3.22 Ratio Sodium Silicate with Molybdic Acid with Time at 400 nm and 20-21°C[a]

Time min	OD_t	Unreacted SiO_2 %	Time min	OD_t	Unreacted SiO_2 %
3.0	0.269	48.2	30.0	0.391	24.7
3.5	0.283	45.5	35.0	0.394	24.2
4.0	0.294	43.4	40.0	0.396	23.8
4.5	0.303	41.7	45.0	0.397	23.6
5.0	0.311	40.1	50.0	0.399	23.3
5.5	0.318	38.8	55.0	0.400	23.0
6.0	0.323	37.8	60.0	0.400	23.0
6.5	0.329	36.7	65.0	0.400	23.0
7.0	0.333	35.9	70.0	0.400	23.0
7.5	0.337	35.1			
8.0	0.341	34.6			
8.5	0.344	33.8			
9.0	0.347	33.2			
9.5	0.350	32.6			
10.0	0.353	32.1			
11.0	0.358	31.1			
12.0	0.362	30.3			
13.0	0.365	29.7			
14.0	0.368	29.2			
15.0	0.370	28.8			
20.0	0.380	26.9			
25.0	0.387	25.5			

a. OD_t = optical density at time t; OD_T = maximum optical density for total silica as β-silicomolybdate; % unreacted SiO_2=100 $(OD_T-OD_t)/OD_T$;

OD_T = 0.5195; total silica ≃ 14 mg SiO_2/L.

Table A10. Raw and Converted Optical Density Data for the Reaction of 1/500 Dilution of 3.22 Ratio Sodium Silicate with Molybdic Acid with Time at 400 nm and 20-21°C[a]

Time min	OD_t	Unreacted SiO_2 %	Time min	OD_t	Unreacted SiO_2 %
3.5	0.381	13.4			
4.0	0.384	12.7			
5.0	0.388	11.8			
6.0	0.391	11.1			
7.0	0.393	10.7			
8.0	0.394	10.6			
9.0	0.3945	10.3			
10.0	0.3945	10.3			
11.0	0.3945	10.3			
12.0	0.3950	10.2			
13.0	0.3950	10.2			
14.0	0.3950	10.2			

a. OD_t = optical density at time t; OD_T = maximum optical density for total silica as β-silicomolybdate; % unreacted SiO_2=100 $(OD_T-OD_t)/OD_T$;

OD_T = 0.440; total silica ≃ 12 mg SiO_2/L.

VITA

Michael Gordon Browman was born on November 20, 1943 in Georgetown, British Guiana (now Guyana). He attended Queen's College (High School) in Georgetown from 1954 to 1962. In September 1962, he enrolled at Cornell University, New York and graduated in January 1966 with a B.S. in Soil Science. At this time he changed locations and enrolled in The Graduate School at The University of Wisconsin in Madison, Wisconsin. He received a Ph.D. degree in Soil Science with a Distributed Minor in Analytical and Water Chemistry in January 1971 having already obtained an M.S. degree in Soil Science in January 1968 also from The University of Wisconsin. Since receiving his doctorate in 1971, he has held a variety of positions including Postdoctoral Fellow, Lecturer, Visiting Lecturer, Temporary Assistant Professor and Research Associate at different institutions primarily in the midwestern and southeastern USA. In September 1982, he returned to school as a student enrolling in the Environmental Engineering Program in the Civil Engineering Department at The University of Tennessee-Knoxville. He received the M.S. in Environmental Engineering in August 1986.

The author is a member of Sigma Xi, the American Society of Civil Engineers, the American Society of Agronomy, and the Soil Science Society of America. Mr. Browman will be employed by the Tennessee Valley Authority after graduation.